# The Role of Human RECQ5 helicase in the Maintenance of Genomic Stability Revealed by Protein-Protein Interaction Study

Dissertation

zur

Erlangung der naturwissenschaftlichen Doktorwürde

(Dr. sc. nat.)

vorgelegt der

Mathematisch-naturwissenschaftlichen Fakultät

der

Universität Zürich

von

Lu Zheng

aus

CHINA

Promotionskomitee

Prof. Dr. Josef Jiricny (Vorsitz)

Prof. Dr. Ulrich Hübscher

Dr. Pavel Janscak (Leitung der Dissertation)

Zürich, 2008

# TABLE OF CONTENTS

# ACKNOWLEDGEMENT

I would like to express my sincere gratitude to all who made this thesis possible.

I am deeply indebted to my supervisor Dr. Pavel Janscak for the possibility to join his group to finish my PhD study. Thanks for his concern, guidance and patience in the course of my experiments and writing of this thesis.

I would like to thank Prof. Josef Jiricny for being friendly and supportive all the time, for making IMCR such a paradise to study and work, for many nice conversations and stimulating suggestions.

Thank all the lab members in Pavel's group, Kanagaraj Radhakrishnan, Nurten Saydam, Daniela Hühn, Sybille Schwendener, Javier Pena Diaz, Patric L Garcia, Boris Mihaljevic for their friendship, help and nice atmosphere in the lab.

Thank Prof. Igor Stagljar for his instruction and help with the yeast two hybrid experiements, and Dr. Thorsten Kleffman for his help with the Mass spectrometry experiment.

Thank all the old friends in IMCR, Elisabetta Pani, Elda Cannavo, Petr Cejka, Lovorka Stojic, Nina Mojas, Mahmud El Shemerly, Giancarlo Marra, Stefano Ferrari, Anne Anstett, Franziska Fischer, Kai Neelsen and Emilja Veljkovic.

Many thanks to Marianne Koepfler, Christine Hemmerle, Ippa Haider,

Margaret Faesi, Helga Pletscher, Christoph Moser, Malika Salah, Najat Maanaoui-Salah and Farah M'Hamedi-Baccouche for their excellent technical assistance.

Thank Jing Song, Tao Bai, Jian Chen, and Fubo Liang for being life long friends and sharing their great moments with me.

A very special thank to my parents for their love and care; to Xiaoqiang for his patience, love and being a man I could always rely on.

I would like to dedicate this thesis to my little Isa. Her smile is the most wonderful gift I have and she makes my life complete.

# SUMMARY

All living cells possess efficient mechanisms to protect their genomes from deleterious effects of DNA damage. RecQ DNA helicases that are highly conserved from bacteria to men play important roles in these processes. In humans, five RecQ homologues have been identified: RECQ1, BLM, WRN, RECQ4 and RECQ5. Defects in the genes encoding for BLM, WRN and RECQ4 have been found to cause Bloom syndrome, Werner syndrome and Rothmund-Thomson syndrome, respectively. These distinct autosomal recessive disorders are characterized by genomic instability and predisposition to cancer, highlighting the fundamental role of RecQ helicases in maintenance of genomic stability. Although no human disease has been linked to defects in the RECQ5 gene, RecQ5 knockout mice were found to be highly prone to various types of cancer (Hu, Raynard et al. 2007), suggesting a role of RECQ5 on the DNA transactions in the cell.

The goal of this thesis is to advance our understanding of the role of RECQ5 in the maintenance of genomic stability. In the first part of the project, we used yeast-two-hybrid screening and immunoprecipitation / mass spectrometry approach to search for proteins that interact with RECQ5 in the cell. In total we identified 91 proteins as novel interaction partners of RECQ5. In the second part of the project, we explored the functional significance of the interactions between RECQ5 and PCNA, RAD51 and the MRE11/RAD50/NBS1 (MRN) complex.

Using pull-down assays with recombinant proteins, we confirmed that the interaction between RECQ5 and PCNA is dependent on the PCNA interaction motif located at the C-terminus of RECQ5. Indirect immunofluorescence imaging of RECQ5 and PCNA *in vivo* showed that RECQ5 is localized in the DNA replication factories in S phase nuclei and persists at the sites of stalled replication forks. We also found that RECQ5

promotes strand exchange on synthetic forked DNA structures that resemble a stalled replication fork. Together, these findings suggested that RECQ5 could mediate regression of stalled replication forks *in vivo* to facilitate DNA damage bypass by template switching.

As for the interaction between RECQ5 and the RAD51 recombinase, we could demonstrate that RECQ5 inhibits RAD51-mediated D-loop formation *in vitro*. Moreover, by biochemical means and electron microscopy, RECQ5 was shown to be able to displace RAD51 from single-stranded DNA. At the cellular level, RECQ5 deficiency was found to result in accumulation of RAD51 foci and elevated levels of homologous recombination. Together, our results suggested that RECQ5 suppresses tumorigenesis by preventing inappropriate homologous recmobination events via RAD51 presynaptic filament disruption.

Using recombinant proteins, we showed that the RECQ5/MRN complex is formed by direct binding of RECQ5 to MRE11 and NBS1. Biochemical analysis revealed that RECQ5 strongly inhibits the 3'-5' exonuclease activity associated with the MRE11 protein. Immunofluorescence studies indicated that RECQ5 and MRN colocalized at stalled replication forks and DNA double-strand breaks. Further experiments with MRE11-deficient cells showed that the MRN complex was required for the recruitment of RECQ5 to the sites of DNA damage. Taken together, our data revealed a functional relationship between RECQ5 and the MRN complex in the cellular response to DNA damage.

# ZUSAMMENFASSUNG

Alle Zellen besitzen Mechanismen, um ihr Genom vor DNA Schäden zu schützen. RecQ DNA Helikasen sind vom Bakterium zum Menschen hoch konserviert und spielen eine wichtige Rolle in diesen Prozessen. Im Menschen wurden fünf RecQ Homologe identifiziert: RECQ1, BLM, WRN, RECQ4 und RECQ5. Mutationen in den Genen, die für BLM, WRN und RECQ4 kodieren, verursachen das Bloom-, das Werner- bzw. das Rothmund-Thomson Syndrom. Diese autosomal-rezessiv vererbten Krankheiten sind durch genomische Instabilität und eine Prädisposition zu Krebs charakterisiert, wodurch eine fundamentale Rolle der RecQ Helikasen für die Integrität des Genoms deutlich wird. Obwohl noch keine menschliche Erkrankung mit Defekten im RECQ5 Gen in Verbindung gebracht werden konnte, neigen RecQ5 Knockout-Mäuse zu verschieden Krebsarten (Hu, Raynard et al. 2007).

Das Ziel dieser Doktorarbeit ist es, die Rolle von RECQ5 in der Erhaltung der Stabilität des Genoms zu verstehen. Im ersten Teil des Projekts wurde mittels Hefe-Zwei-Hybrid-System und Immunpräzipitation mit anschließender Massenspektrometrie nach Proteinen gesucht, die mit RECQ5 interagieren. Insgesamt konnten wir 91 Proteine als neue Interaktionspartner von RECQ5 identifizieren. Im zweiten Teil des Projekts wurde die funktionelle Bedeutung der Interaktionen zwischen RECQ5 und PCNA, RAD51 and dem MRE11/RAD50/NBS1 (MRN) Komplex untersucht.

In Pulldown-Experimenten mit rekombinanten Proteinen konnten wir bestätigen, dass die Interaktion zwischen RECQ5 und PCNA von dem PCNA-Interaktionsmotif am C-Terminus von RECQ5 abhängt. Die indirekte Immunfluoreszenz von RECQ5 und PCNA in vivo zeigte, dass RECQ5 in DNA-Replikationseinheiten von S-Phasen Zellkernen und an arretierten Replikationsgabeln lokalisiert ist. Weiterhin konnten wir zeigen, dass RECQ5 den Strangaustausch an synthetischen gabelförmigen DNA-Strukturen

katalysiert, die arretierten Replikationsgabeln ähneln. Zusammen deuten diese Ergebnisse darauf hin, dass RECQ5 die Regression arretierter Replikationsgabeln in vivo vermittelt um einen DNA-Schaden durch einen Wechsel des Templatstrangs zu umgehen.

Für die Interaktion zwischen RECQ5 und der RAD51 Rekombinase konnten wir demonstrieren, dass RECQ5 die von RAD51-vermittelte Bildung von so genannten D-Schleifen in vitro verhindert. Darüber hinaus wurde durch biochemische Analysen und Elektronenmikroskopie gezeigt, dass RECQ5 an einzelsträngige DNA gebundenes RAD51 verdrängen kann. Auf zellulärer Ebene wurde beobachtet, dass das Fehlen von RECQ5 zur Akkumulation von RAD51-Foci und einem erhöhten Level an homologer Rekombination führt. Zusammenfassend deuten diese Ergebnisse darauf hin, dass RECQ5 die Tumorgenese unterdrückt, indem es die Bildung präsynaptischer RAD51-Filamente inhibiert und somit exzessive homologe Rekombination verhindert.

Unter Verwendung rekombinanter Proteine konnten wir zeigen, dass der RECQ5/MRN-Komplex durch die direkte Bindung von RECQ5 an MRE11 gebildet wird. Biochemische Untersuchungen ergaben eine deutliche Inhibition der 3′-5′ Exonukleaseaktivität von MRE11 durch RECQ5. Immunfluoreszenzstudien deuten auf eine Co-Lokalisierung von RECQ5 und MRE11 an arretierten Replikationsgabeln und DNA-Doppelstrangbrüchen hin. Weitere Experimente mit MRE11-defizienten Zellen zeigten, dass der MRN-Komplex unentbehrlich für die Rekrutierung von RECQ5 zu Bereichen mit DNA-Schäden. Zusammengefasst beweisen unsere Daten eine funktionelle Beziehung zwischen RECQ5 and dem MRN-Komplex in der zellulären Reaktion auf Schädigungen der DNA.

## 1 Introduction

DNA damage is a frequent event in the life of every cell. It can stem from numerous sources: by-products of natural aerobic respiration, environmental chemicals, ultraviolet (UV) light or ionizing radiation (IR). For example, oxidation, alkylation, deamination, depurination and depyrimidation of DNA create $<10^4$ mutagenic DNA base lesions per day in each human cell (Lindahl 1993). DNA damage can hence result in genetic alterations and induce tumorigenesis. To counteract the potentially deleterious effects of DNA damage, all living cells have evolved an efficient defence mechanism, termed DNA damage response (Figure 1.1).

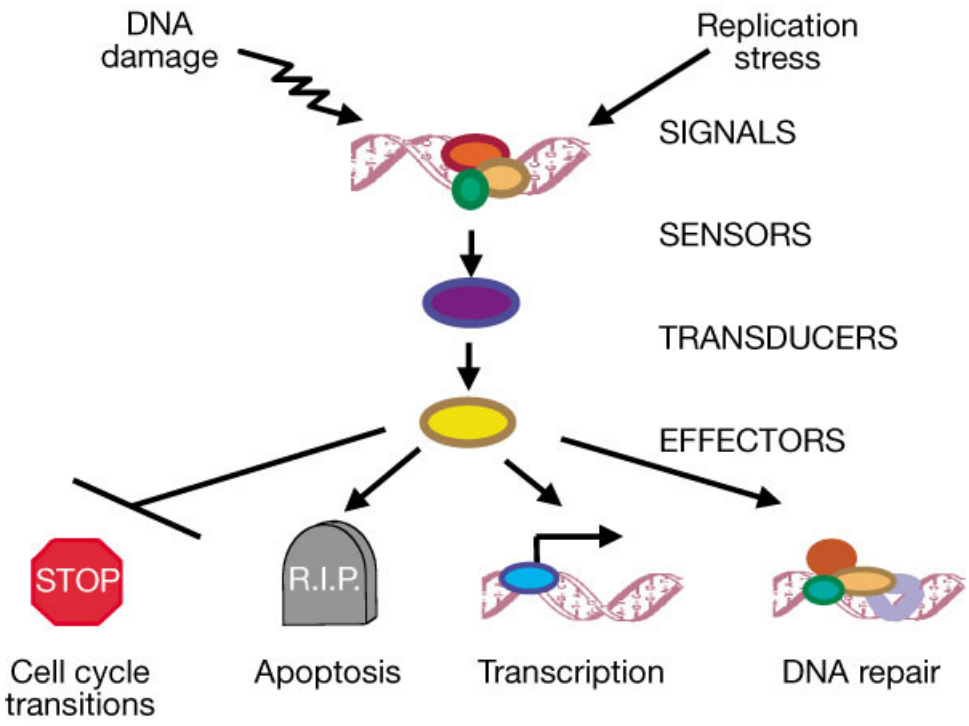


Figure 1.1 DNA damage response. For the purpose of simplicity, the network of interacting pathways is depicted as a linear pathway consisting of signals, sensors, transducers and effectors. Adapted from (Zhou and Elledge 2000).

Upon sensing DNA damage or stalls in replication, damage signals will be transduced to effectors that enable the cell either to eliminate or cope with the damage or to activate a programmed cell death process. These DNA damage response reactions include:

(A) Activation of DNA-repair pathways, which remove DNA damages and restore the continuity of the DNA duplex.

(B) Activation of a DNA damage checkpoint, which arrests cell cycle progression so as to allow for repair and prevention of the transmission of damaged or incompletely replicated chromosomes.

(C) Induction of transcriptional programs, which causes changes in the beneficial transcription profile.

(D) Initiation of apoptosis, which eliminates heavily damaged or seriously deregulated cells.

All of these processes are carefully coordinated so that the genetic material is faithfully maintained, duplicated, and segregated within the cell.

## 1.1 DNA damage and repair

### 1.1.1 Structure of DNA

A DNA strand is a long polymer built from nucleotides. Each nucleotide contains three parts: a phosphate group, the sugar deoxyribose, and one of four nitrogen bases (Adenine, Guanine, Thymine and Cytosine). In the Watson-Crick model of DNA, two complementary polynucleotide strands are held together by hydrogen

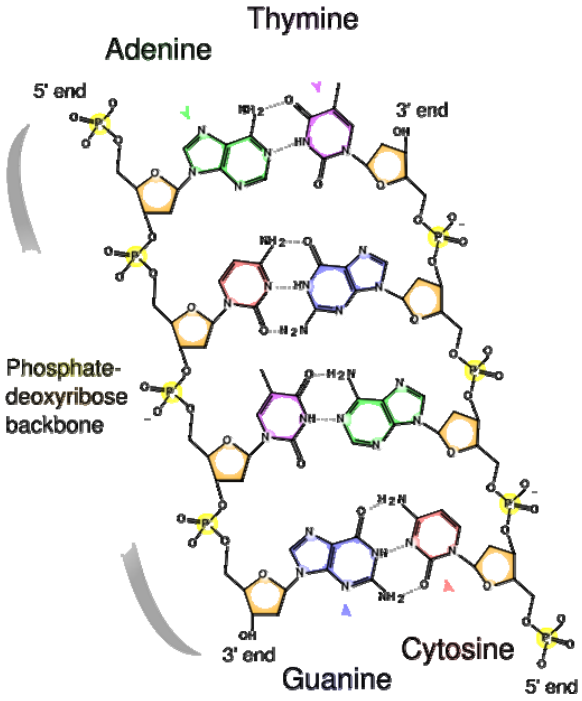


**Figure 1.2** The chemical structure of DNA. Hydrogen bonds are shown as dotted lines. Adapted from (MolecularStation 2007).

bonds formed between the bases A and T and between G and C. As a direct consequence of this base-pairing mechanism, it becomes evident that genetic information is stored in the linear sequence of bases. DNA can thus be viewed as a linear quaternary code, much like a computer code (which is binary). A sequence of 100 nucleotides can have $4^{100}$ forms, or 1,00000048,576, if all possible sequences are considered.

### 1.1.2 Types of DNA damage

DNA is continuously subjected to the threat of damage by a wide variety of external agents as well as spontaneous endogenous processes (Friedberg 1995). DNA molecules, like all other biomolecules, can be damaged in numerous ways. Spontaneous damage due to replication errors, deamination, depurination and oxidation is compounded in the real world by the additional effects of radiation and environmental chemicals. The number of ways that DNA molecules can be damaged is very large as shown in Table1.1. Since repair systems must be capable of recognizing and dealing with each type of damage, it is not surprising that there is a large number of different types of repair mechanisms (Sancar, Lindsey-Boltz et al. 2004).

| Type of damage | Description | Picture |
|---|---|---|
| **Base loss** | The glycosyl bond linking DNA bases with deoxyribose is labile under physiological conditions. Loss of a purine or pyrimidine base creates an apurinic/ apyrimidinic (AP) site (also called an abasic site). | 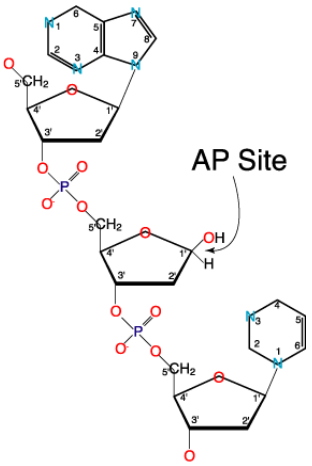 |
| **Base modification** | **Deamination** happens when the primary amino groups of nucleic acid bases are converted to keto groups. | 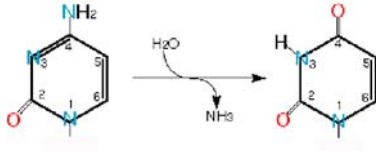 |

| | | |
|---|---|---|
| | **Oxidation:** Several types of hyper-reactive oxygen (singlet oxygen, peroxide radicals, hydrogen peroxide and hydroxyl radicals) are generated as byproducts during normal oxidative metabolism and also by ionizing radiation (X-rays, gamma rays). | 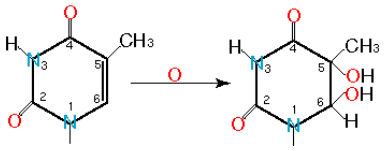 <br>Thymine Thymine glycol |
| | **Alkylation(usually methylation):** Many chemicals can also modify DNA bases, frequently by addition of a methyl or other alkyl group. | 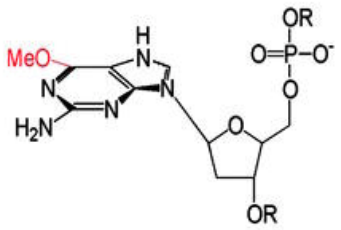 <br>$O^6$-methyldeoxyguanosine |
| **Photodamage** | **Pyrimidine dimer:** The most frequent photoproducts are the consequences of bond formation between adjacent pyrimidines within one strand, and, of these, the most frequent are cyclobutane pyrimidine dimers (CPDs). T-T CPDs are formed most readily, followed by T-C or C-T; C-C dimers are least abundant. | 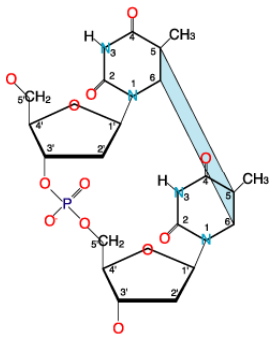 <br>T-T CPD |

| | | |
|---|---|---|
| | **Pyrimidine (6-4) pyrimidone photoproducts:** Dimers can also be produced by formation of a single covalent bond between the 6 position of one pyrimidine and the 4 position of the adjacent pyrimidine on the 3' side. Although only one bond attaches the adjacent pyrimidines, there is nevertheless extensive distortion of the normal DNA structure. | 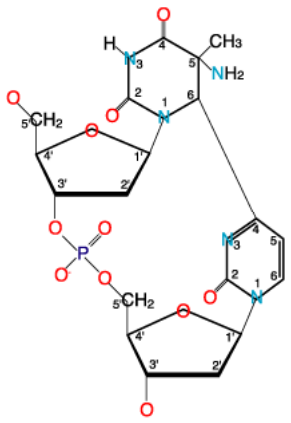 <br>6-4PP |
| **Inter-strand crosslinks** | By attaching to bases on both strands, bifunctional alkylating agents such as the psoralens, and Cisplatin(Cis-Pt) can cross-link both strands.<br>Cross-links can also be generated by UV and ionizing radiation. | 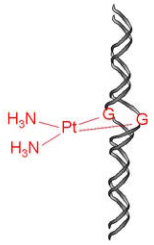 <br>Cis-Pt G-G interstrand cross-link |
| **DNA-protein crosslinks** | DNA oxidation can also lead to the formation of covalent adducts to bases, and the lysine-rich motifs that bind DNA provide abundant nucleophiles for cross-linking. Bifunctional alkylating agents and radiation can also create crosslinks between DNA and protein molecules. | 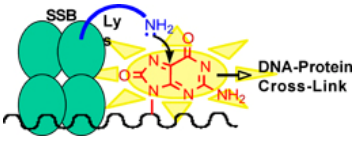 |

| | | |
|---|---|---|
| **Strand breaks** | Single-strand and double-strand breaks are produced at low frequency during normal DNA metabolism by topoisomerases, nucleases, replication fork "collapse", and repair processes. Breaks are also produced by ionizing radiation. | 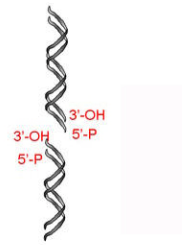 Double-strand break |
| **Replication errors** | Another major source of potential alterations in DNA is the generation of mismatches or small insertions or deletions during DNA replication. | |

**Table 1.1** Types of DNA damage. Adapted from (Brown 2002; Sancar, Lindsey-Boltz et al. 2004).

### 1.1.3 DNA repair pathways

Upon sensing damages on DNA or stalled DNA replication forks, one or more DNA repair pathways will be activated based on the type of damage. Direct reversal is the simplest DNA repair pathway, which involves a single enzyme to remove a damage on DNA (i.e. photolyase removes photo-adducts from UV damaged DNA; DNA methyl transferase removes alkylation lesion from DNA; AlKB reverses oxidative methylation; DNA ligase seals a set of nicks having 5'-phosphates and 3'-hydroxyls). For the other types of damages, more complicated repair pathway are applied as shown in Figure 1.3 and described in the next few sections.

.

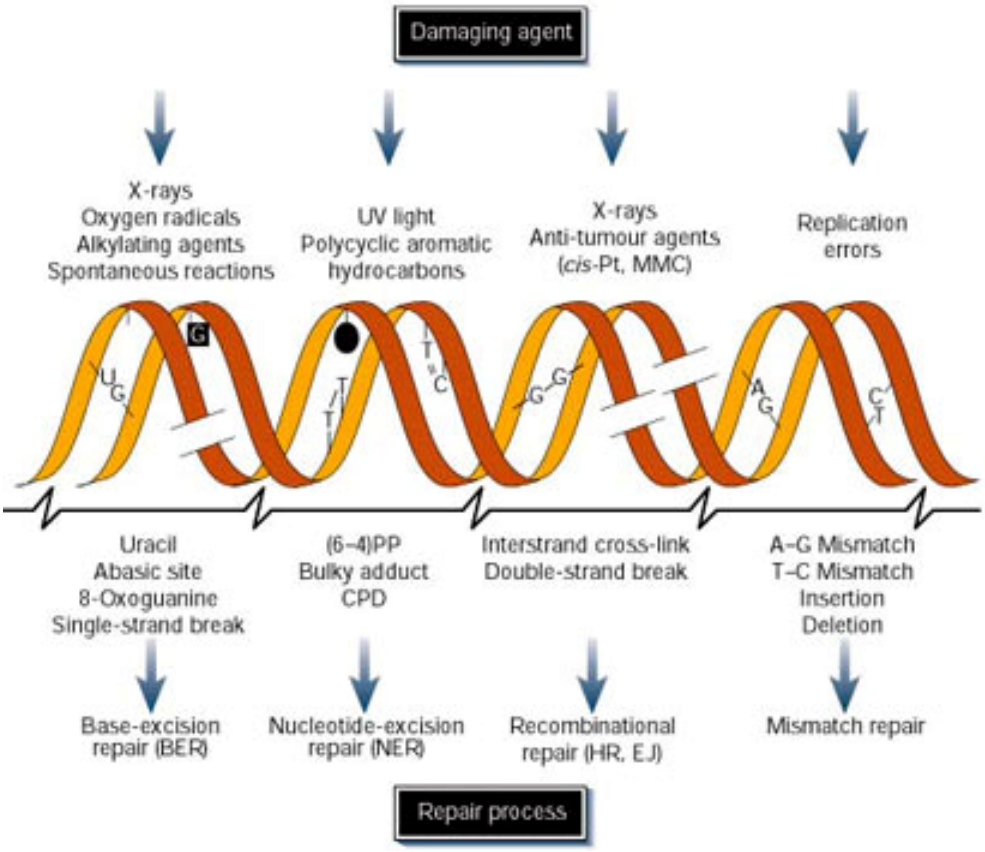


**Figure 1.3** A simplified scheme of the most important DNA repair pathways. Adapted from (Hoeijmakers 2001).

### 1.1.3.1 Base excision repair (BER)

BER is a multi-step process that corrects non-bulky damage to bases resulting from oxidation, methylation, deamination, or spontaneous loss of the DNA base itself. These alterations, although simple in nature, are highly mutagenic and therefore represent a significant threat to genome fidelity and stability (Pinto, Silva et al. 2003). BER is essential to protect DNA from various types of lesions, such as uracil, hydroxymethyluracil, methylcytosine, hypoxanthine, G-T mispairs, 3-methyladenine, 7-methylguanine, 3-methylguanine, formamidopyrimidine, 8-hydroxyguanine, and 5,6-hydrated thymine (Friedberg 1995). Each of these modifications is recognized by a specific DNA glycosylase, which is followed by excision of the damaged base and DNA resynthesis (Figure 1.4).

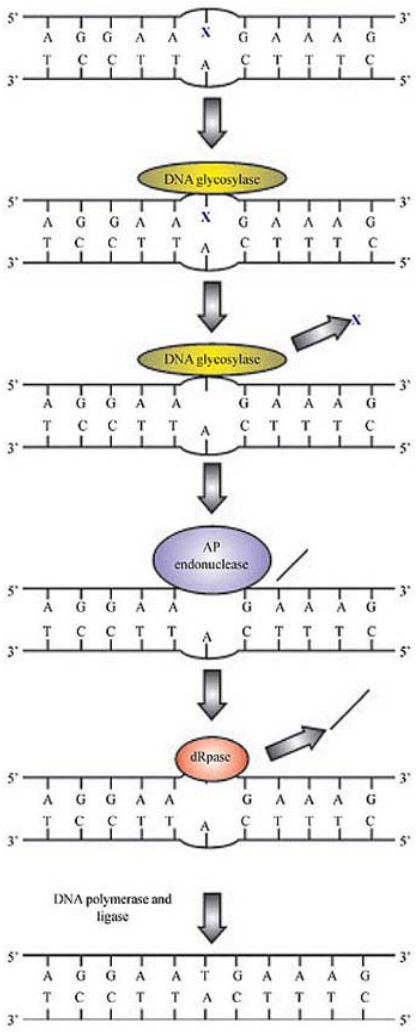


**Figure 1.4** Schematic representaion of base excision repair. Adapted from (Pinto, Silva et al. 2003). The BER pathways can be considered to consist of four steps:

1. Removal of the incorrect base by an appropriate DNA N-glycosylase to create an AP site.
2. Nicking of the damaged DNA strand by AP endonuclease upstream of the AP site, thus creating a 3'-OH terminus adjacent to the AP site.
3. Extension of the 3'-OH terminus by a DNA polymerase, accompanied by excision of the AP site.
4. DNA re-synthesis and ligation.

### 1.1.3.2 Nucleotide excision repair (NER)

NER is perhaps the most flexible of the DNA repair pathways considering the diversity of DNA lesions it acts upon (Wood 1997). The NER substrates include bulky DNA adducts such as pyrimidine dimers (CPDs and 6-4 PPs), large chemical adducts, DNA intrastrand crosslinks or some forms of oxidative damage. In humans, mutation in any of the seven XP genes, called XPA through XPG, causes a photosensitivity syndrome called Xeroderma pigmentosum (XP), which is characterized by a very high incidence of light-induced skin cancer (Christmann, Tomicic et al. 2003; Costa, Chigancas et al. 2003; Sancar, Lindsey-Boltz et al. 2004).

The NER process requires a series of proteins that mediate damage recognition, local opening of the DNA duplex around the lesion, dual incision of the damaged DNA strand, gap repair synthesis, and strand ligation (Sancar 1996; Wood 1997; Friedberg 2001). NER can be subdivided into two distinct subpathways: global genomic repair (GGR), which corrects damage in transcriptionally silent areas of the genome and transcription coupled repair (TCR), which repairs lesions in actively transcribed strands of the DNA, see in Figure 1.5. The GGR and TCR pathways are fundamentally identical except for their mechanism of damage recognition. In GGR, the XPC/HR23B protein complex is responsible for the initial detection of damaged DNA. While TCR is thought to occur when the transcription machinery is stalled at the site of injury, rather than require XPC. The stalled RNA polymerase complex must then be displaced in order to allow the NER proteins access to the damaged DNA. This displacement is aided by the action of the CSA and CSB proteins, as well as other TCR specific factors.

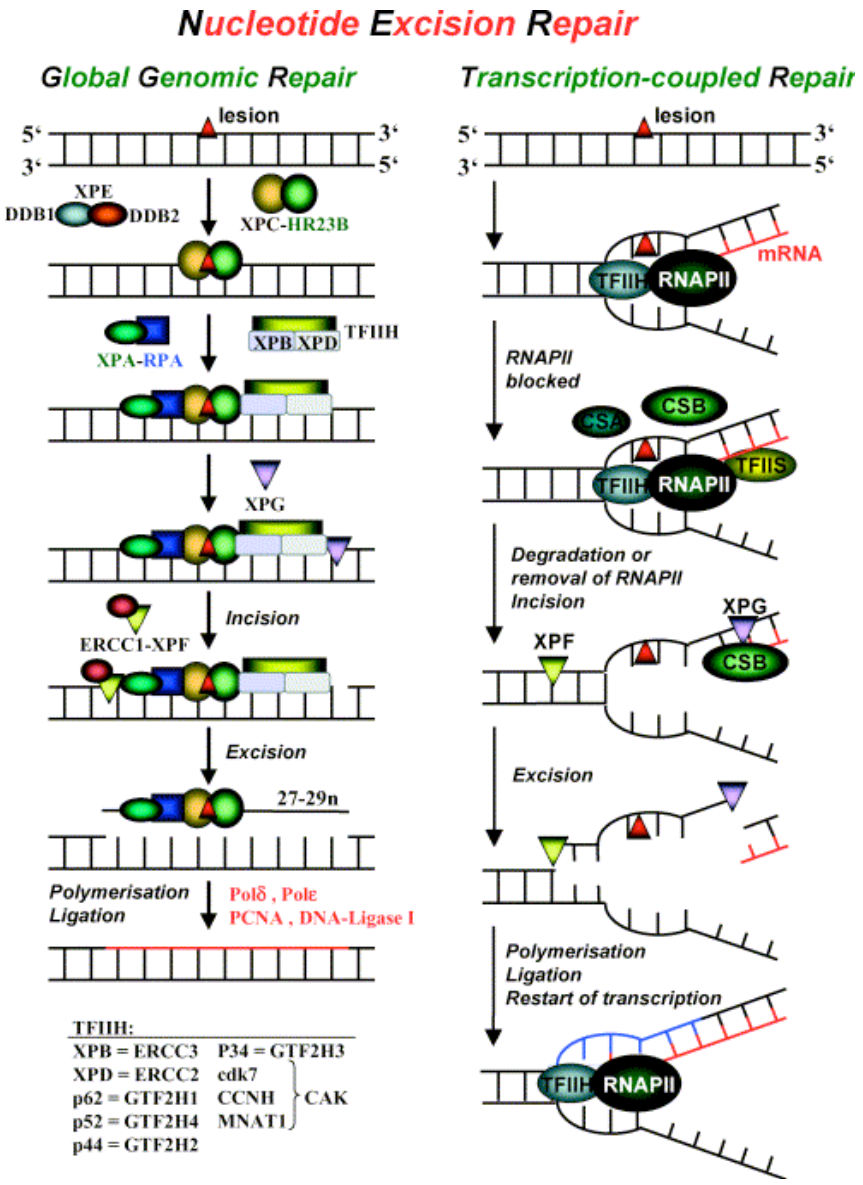


**Figure 1.5** Mechanism of NER. During GGR, recognition of the DNA lesion occurs by XPC–HR23B, RPA–XPA or DDB1–DDB2. DNA unwinding is performed by the transcription factor TFIIH and excision of the lesion-containing nucleotide by XPG and XPF–ERCC1. Finally, resynthesis occurs by Polδ or Polε and ligation by DNA ligase I. During TCR, the lesion blocks RNA-Polymerase II, This leads to assembly of CSA, CSB and/or TFIIS at the site of the lesion, by which RNAPII is removed from the DNA or displaced from the lesion, making it accessible to the exonucleases XPF–ERCC1 and XPG, cleaving the lesion-containing DNA strand. Resynthesis again occurs by Polδ or Polε and ligation by DNA ligase I. Adapted from (Christmann, Tomicic et al. 2003).

### 1.1.3.3 Mismatch Repair (MMR)

MMR pathway plays an essential role in the correction of replication errors such as base-base mismatches and insertion/deletion loops (IDLs) that result from DNA polymerase misincorporation of nucleotides and template slippage, respectively. Mispairs generated by the spontaneous deamination of 5-methylcytosine and heteroduplexes formed following genetic recombination are also corrected by MMR (Kolodner and Marsischky 1999; Christmann, Tomicic et al. 2003; Li 2008). The overall process of MMR is as follows: DNA lesion is recognized, a patch containing the lesion is excised and the strand is corrected by DNA repair synthesis and re-ligation (Kunkel and Erie 2005; Li 2008).

The mammalian MMR pathway is initiated by recognition of mismatches or IDLs. The predominant base-base mismatch and single-base IDL recognition activity in human cells is provided by MutSα (MSH2-MSH6 heterodimer); larger IDLs are usually recognized by MutSβ (MSH2-MSH3 heterodimer) (McCulloch, Gu et al. 2003; Kunkel and Erie 2005). There is, however, some partial overlap in substrate specificity of these two heterodimers. Following lesion identification, MutSα/β binds ATP, undergoes a conformational change and slides along the DNA away from the mismatch until additional MMR proteins are encountered. Higher order protein complexes are formed, including those containing the MLH1-PMS2 herodimer (MutLα), the MLH1-MLH3 heterodimer (MutLβ), and replication factors (Modrich 2006). Excision and resynthesis of the nascent strand (containing the mismatch or IDL) is performed by a number of factors including PCNA, RPA, RFC, exonuclease I (ExoI), DNA polymerases delta and epsilon, endonuclease FEN1, and additional factors. See Table 1.3 for a full list of proteins that participate in the human MMR (Li 2008).

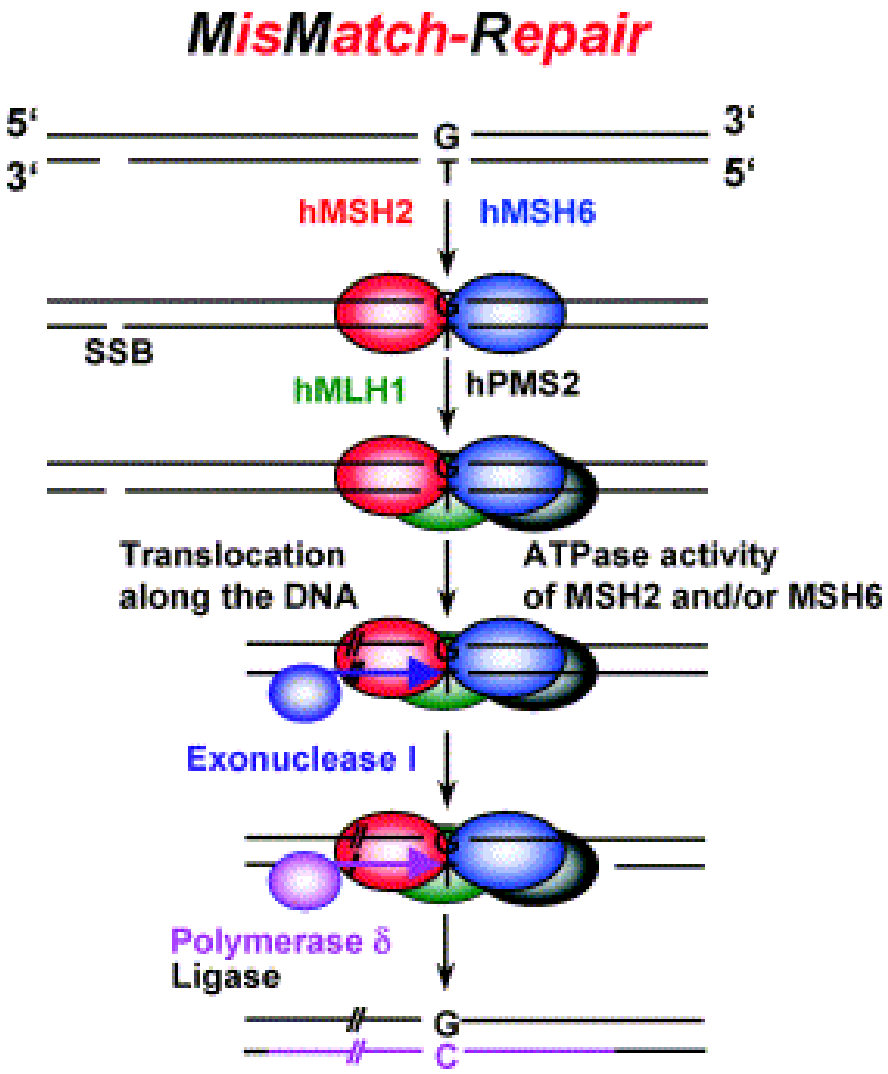


**Figure 1.6** Mechanism of mismatch repair. Recognition of DNA lesions is mediated by MutSα (MSH2–MSH6). According to the molecular switch model, binding of MutSα–ADP triggers ADP→ATP transition, stimulates intrinsic ATPase activity, and provokes the formation of a hydrolysis-independent sliding clamp, followed by binding of the MutLα complex (MLH1–PMS2). According to the hydrolysis-driven translocation model, ATP hydrolysis induces translocation of MutSα along the DNA. After formation of a complex composed of MutSα and MutLα, excision is performed by ExoI and repair synthesis by Polδ. Adapted from (Christmann, Tomicic et al. 2003).

| **Protein name** | **Function** |
|---|---|
| hMutSα (MSH2-MSH6)<br>hMutSβ (MSH2-MSH3) | DNA mismatch/damage recognition |
| hMutLα (MLH1-PMS2)<br>hMutLβ (MLH1-PMS1)<br>MutLγ (MLH1-MLH3) | Molecular matchmaker; endonuclease, termination of mismatch-provoked excision |
| ExoI | DNA excision; mismatch excision |
| Pol δ | DNA re-synthesis |
| PCNA | Initiation of MMR, DNA re-synthesis |
| RPA | ssDNA binding/protection; stimulating mismatch excision; termination of DNA excision; promoting DNA resynthesis |
| HMGB1 | Mismatch-provoked excision |
| RFC | PCNA loading; 3' nick-directed repair; activation of MutLalpha endonuclease |
| DNA ligase I | Nick ligation |

**Table 1.3** MMR components and their functions. Adapted from (Li 2008).

#### 1.1.3.4 DNA double strand break repair

DNA double-strand breaks (DSBs) arise at much lower frequency than other types of DNA damage, yet they are perhaps the most serious form of DNA damage because they pose problems for transcription, replication, and chromosome segregation (Jackson 2002). Because of the threats posed by DSBs, eukaryotic cells have evolved complex and highly conserved systems to rapidly and efficiently detect these lesions, signal their presence and bring about their repair (Hoeijmakers 2001). DNA DSBs are generated when the two complementary stands of the DNA double helix are broken simultaneously at sites that are sufficiently close to one another that base-pairing and chromatin structure are insufficient to keep the two DNA ends juxtaposed. Damage of this type is caused by a variety of sources including reactive oxygen species, ionizing radiation, and chemicals that generate reactive oxygen species. DSBs are also generated during V(D)J recombination and immunoglobulin class-switching processes and occur during replication as a consequence of replication fork arrest and collapse (Jackson 2001; van Gent, Hoeijmakers et al. 2001; D'Amours and Jackson 2002; Rouse and Jackson 2002). DSBs differ from most other types of DNA lesions in that they affect both strands of the DNA duplex and therefore prevent use of the complementary strand as a template for repair (see BER, NER, and MMR) (Christmann, Tomicic et al. 2003). Failure to repair these defects can result in chromosomal instability, leading to deregulated gene expression and carcinogenesis. To counteract the detrimental effects of these potent lesions, DSBs are repaired in eukaryotes by two distinct mechanisms: RAD52-dependent homologous recombination (HR) and Ku-dependent non-homologous end joining (NHEJ). The cellular decision as to which pathway to utilize for DSB repair is unclear, however, it appears to be largely influenced by the stage of the cell cycle at the time of damage acquisition (van Gent, Hoeijmakers et al. 2001; Jackson 2002; Sancar, Lindsey-Boltz et al. 2004).

#### 1.1.3.4.1 Non-homologous end joining (NHEJ)

NHEJ rejoins the two broken ends directly and generally leads to small deletions of DNA sequence. It requires the Ku70/Ku80 heterodimeric protein, which binds to free DNA ends and recruits DNA-dependent protein kinase (DNA-PKcs) (Smith and Jackson 1999). Ku then recruits XRCC4 along with DNA ligase IV, and DNA-PKcs-mediated phosphorylation of XRCC4 may influence its activity. Because the ends of most DSBs generated by genotoxic agents are damaged and unable to be directly ligated, they often have to undergo limited processing by nucleases and/or polymerases before NHEJ can proceed. The nuclease(s) responsible for this processing remains to be determined. Strong candidates for this activity include the MRE11/Rad50/NBS1 complex, FEN-1, and the Artemis protein. The final step in NHEJ repair involves ligation of the DNA ends by Ligase IV in a complex that also includes XRCC4 and Ku. In many cases, NHEJ may also require the actions of DNA polymerases (Critchlow and Jackson 1998; Lieber 1999).

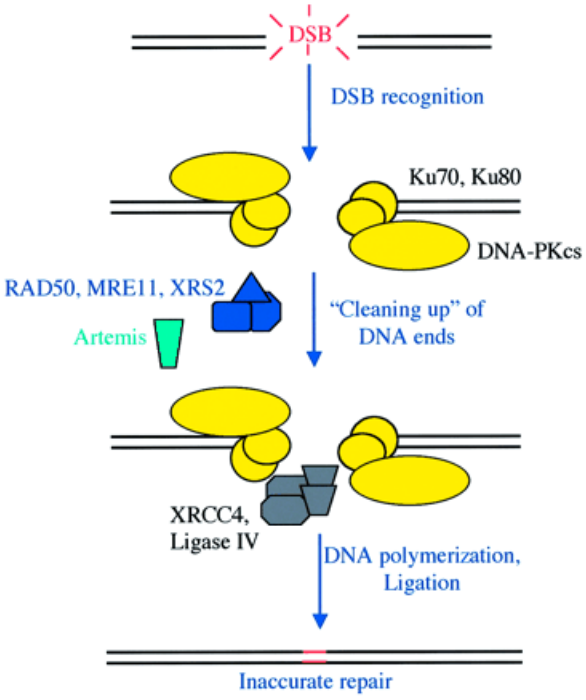


**Figure 1.7** Schematic representation of the NHEJ pathway of DNA DSB repair, indicating the known players in this pathway in vertebrates. Adapted from (Jackson 2002).

#### 1.1.3.4.2 Homologous recombination (HR)

HR can repair DSBs by using the undamaged sister chromatid as a template. Therefore, HR generally results in accurate repair of DSBs (van Gent, Hoeijmakers et al. 2001). The majority of HR-based repair takes place in late S- and G2- phases of the cell cycle when an undamaged sister chromatid is available for use as repair template. In organisms that range from yeasts to mammals, the RAD52 epistasis group of proteins, including RAD50, RAD51, RAD52, RAD54, and MRE11 mediate this process. The RAD52 protein itself is thought to be the initial sensor of the broken DNA ends.

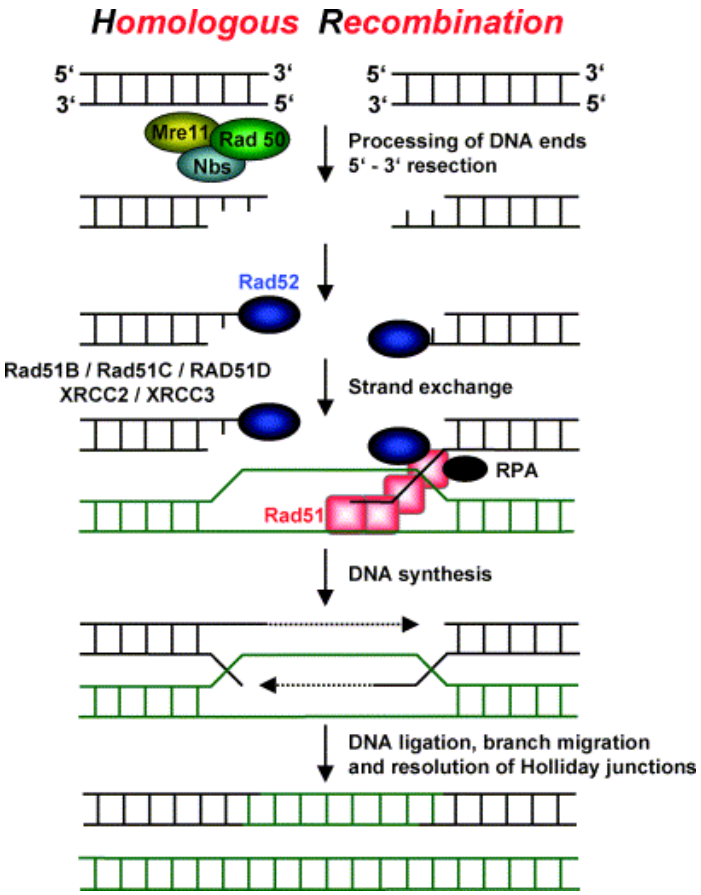


**Figure 1.8** Overview of the main steps of DNA DSB repair by HR. Adapted from (Christmann, Tomicic et al. 2003).

The events of HR are complex and, based on analyses of HR under various biological circumstances and in different organisms, there are various models for precisely how they take place (Cromie, Connelly et al. 2001). Homologous recombination starts with nucleolytic resection of the DSB in the 5′→3′ direction by the MRE11–RAD50–NBS1 complex, resulting in a 3′ single-stranded DNA fragment to which RAD52 binds. RAD52 interacts with RAD51, to form RAD51 nucleoprotein filament. Assembly of the RAD51 nucleoprotein filament is facilitated by different RAD51 paralogues such as RAD51B, RAD51C and RAD51D, XRCC2 and XRCC3. RAD51 filaments mediates strand invasion of a homologous DNA duplex. Polymerase then extends the 3' end of the invading strand and subsequent ligation by DNA ligase I yields a heteroduplexed DNA structure. This recombination intermediate is resolved and the precise, error-free correction of the DSB is complete (Cromie, Connelly et al. 2001).

## 1.2 RECQ family of DNA helicases

DNA helicases are ubiquitous enzymes that are defined by their capacity to catalyze the unwinding of duplex nucleic acids through coupling of ATP hydrolysis to DNA translocation (Ellis 1997; Sharma, Doherty et al. 2006). They participate in multiple cellular processes including DNA replication, repair and recombination. In fact, DNA helicases are involved in almost all aspects of nucleic acid metabolism (Ellis 1997; Kawasaki, Maruyama et al. 2002). The growing number of DNA helicases implicated in human disease implies their important roles in the maintenance of genome stability. In particular, one family of DNA helicases - the RecQ family, has gained extensive attention base on the fact that three human autosomal recessive disorders, namely Bloom syndrome (BS), Werner syndrome (WS) and Rothmund–Thomson syndrome (RTS), have been linked to loss of function of the human RecQ homologs *BLM, WRN* and *RECQ4*, respectively (Karow, Wu et al. 2000; Kawasaki, Maruyama et al. 2002; Sharma, Doherty et al. 2006). The RecQ DNA helicase family derives its name after the *recQ* gene product of *Escherichia coli* and is highly conserved from bacteria to humans (Bachrati and Hickson 2003; Hickson 2003). In bacteria and unicellular eukaryote, only one family member is present, whereas two or more RecQ homologues are expressed in higher eukaryots. Humans have five RecQ homologues, namely RECQ1, BLM, WRN, RECQ4 and RECQ5 (Hickson 2003; Khakhar, Cobb et al. 2003; Wu and Hickson 2006).

A highly conserved helicase domain that includes seven helicase motifs defines the RecQ family as shown in Figure 1.9. Many, but not all, RecQ helicases contain a second feature, the RecQ-Ct (RecQ C-terminal) domain, which is unique to RecQ family members, and a third HRDC domain (helicase and RNaseD C-terminal), which is present in several helicases and in RNaseD enzymes, as its name indicates (Wu and Hickson 2006).

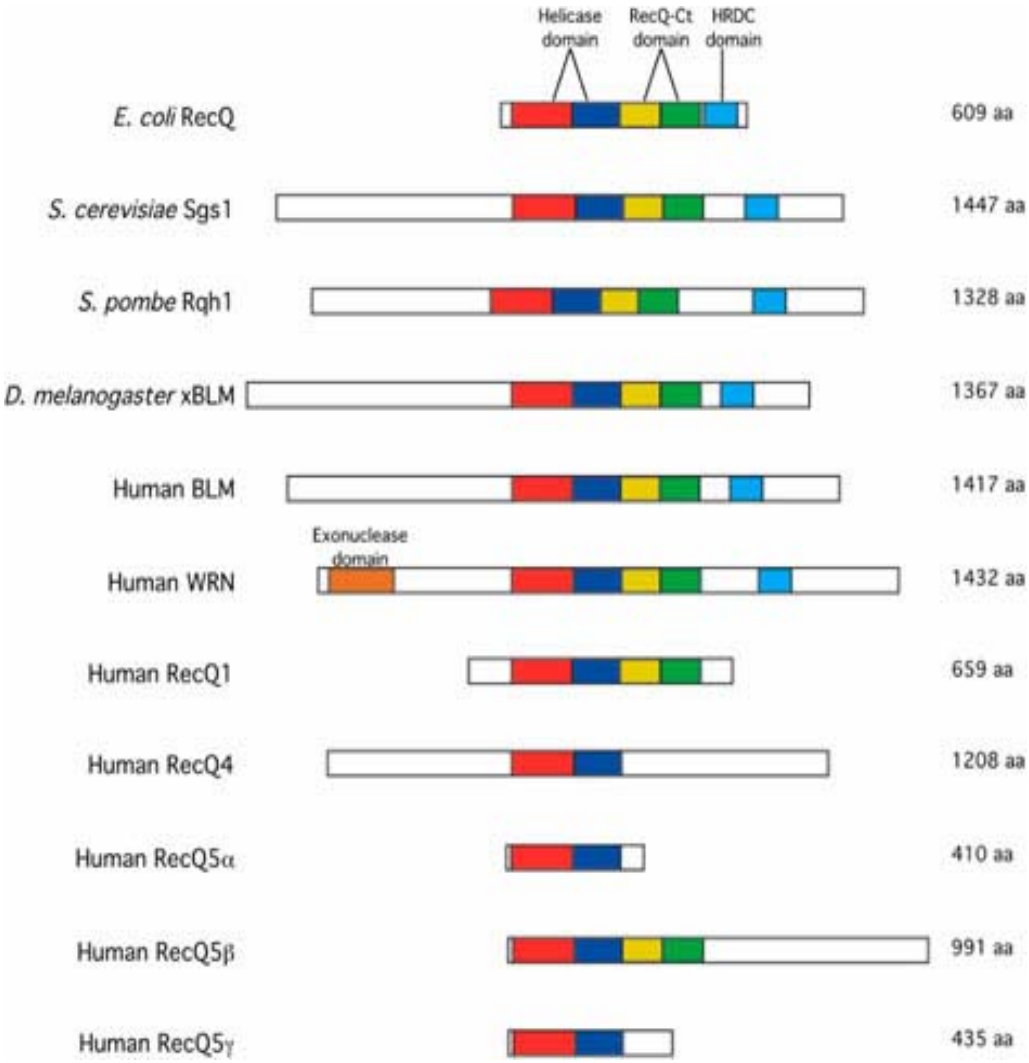


**Figure 1.9** Schematic diagram of selected members of the RecQ family of DNA helicases. Helicase subdomains are shown in red and blue, and the RecQ-Ct domain is composed of a $Zn^{2+}$-binding subdomain (yellow) and a WH domain (green). The HRDC domain is depicted in cyan, and the exonuclease domain of WRN is shown in orange (Bennett and Keck 2004).

### 1.2.1 The *Escherichia coli* RecQ

The founding member of the RecQ helicase family, the *E. coli* RecQ, was first identified in 1984 through isolating an *Escherichia coli* K12 mutants resistant to thymineless death (Nakayama, Nakayama et al. 1984). The *E. coli recQ* gene was shown to encode a DNA helicase bearing DNA-dependent ATPase activity, which functions in the RecF recombination pathway (Nakayama, Nakayama et al. 1984; Nakayama, Irino et al. 1985; Umezu, Nakayama et al. 1990) and repair of UV-induced DNA damage (Kowalczykowski, Dixon et al. 1994).

*E. coli* RecQ shares the three conserved protein regions with other family members referred to as the Helicase, RecQ-Ct and HRDC domains (Morozov, Mushegian et al. 1997).

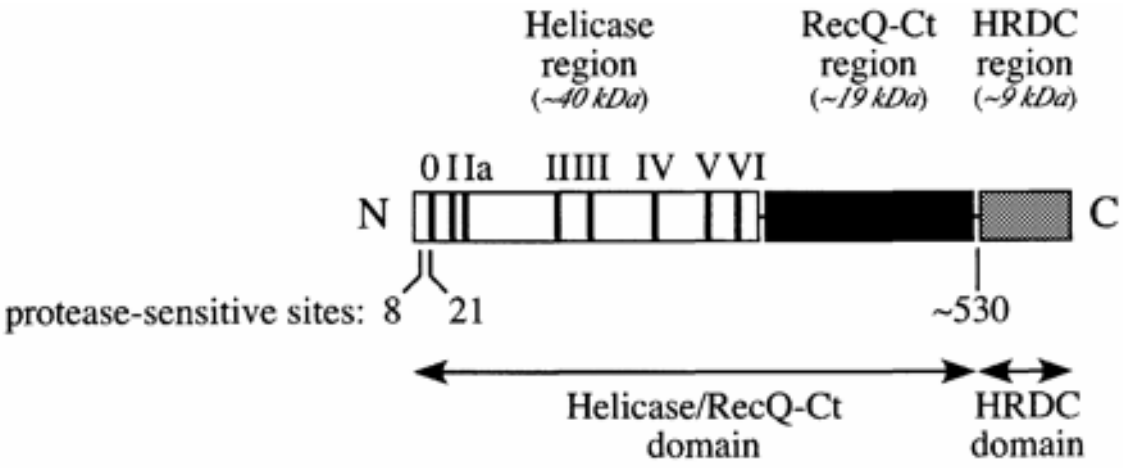


**Figure 1.10** Schematic diagram of *E.coli* RecQ. The conserved regions, helicase (white), RecQ-Ct (black) and HRDC (gray) are shown as boxes. The locations of the conserved helicase motifs (I–VI) are indicated with bars within the Helicase box. The approximate molecular weight of each region is listed. Adapted from (Bernstein and Keck 2003).

The helicase region contains sequence motifs necessary for ATP binding and hydrolysis (Ellis 1997). The RecQ-Ct region is located C-terminal to the

helicase domain in RecQ proteins (Morozov, Mushegian et al. 1997). Previous mutational studies have indicated that RecQ-Ct is important for the enzymatic activity of RecQ (Foucault, Vaury et al. 1997; Ui, Satoh et al. 2001).

Domain mapping experiments with *E.coli* RecQ revealed that a 59 kDa structural domain (RecQΔC) consisting of conserved helicase and RecQ-Ct regions is active as a DNA-dependent ATPase and DNA helicase, suggesting that this domain represents the catalytic core of the enzyme (Bernstein and Keck 2003). Bernstein et al. resolved the crystal structure of this catalytic core of the *E. coli* RecQ protein, as shown in Figure 1.11 (Bernstein, Zittel et al. 2003).

The third conserved region, HRDC domain, was crystallized separately and its structure solved (Bernstein and Keck 2005). The HRDC domain could preferentially binds single-stranded DNA. It was hypothesized that differential evolution of HRDC domains can lead to specialized DNA binding modes in different RecQ proteins (Bernstein and Keck 2005).

Extensive biochemical studies have been focused on *E.coli* RecQ, (Umezu, Nakayama et al. 1990; Harmon and Kowalczykowski 2001). The *E.coli* RecQ helicase showed unwinding activity on blunt-ended duplexes, three-strand junctions, synthetic Holliday junctions and fork structures *in vitro* (Harmon and Kowalczykowski 1998; Harmon, DiGate et al. 1999). In addition, it is also shown to unwind the lagging-strand equivalent in model forks, suggesting a role in the rescue of a stalled replication fork, as shown in Figure 1.12 (Hishida, Han et al. 2004).

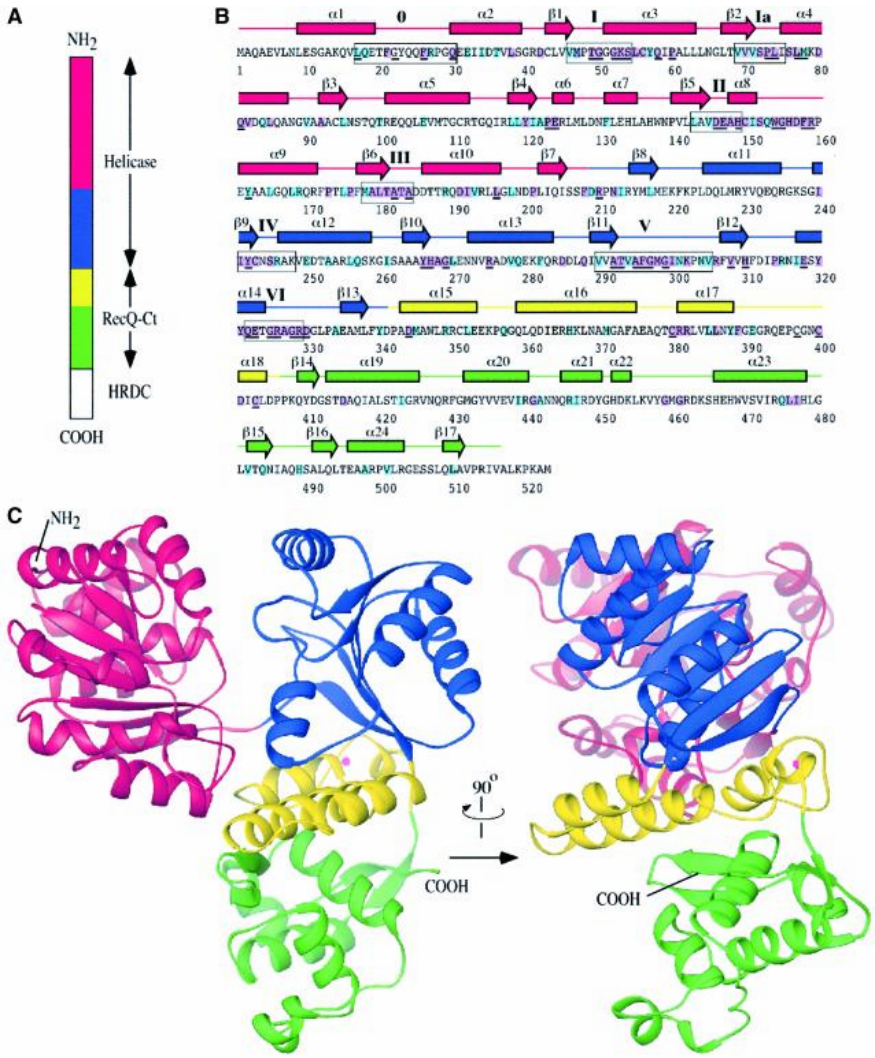


**Figure 1.11** Structure of the *E.coli* RecQ catalytic core. (**A**) Schematic diagram of *E.coli* RecQ. Three conserved regions, helicase, RecQ-Ct, and HRDC are labeled. The catalytic core of *E.coli* RecQ (RecQΔC) includes only the helicase and RecQ-Ct regions, and comprises four apparent subdomains in the structure: residues 1–208 in red, 209–340 in blue, 341–406 in yellow, and 407–516 in green. (**B**) Sequence and secondary structure of RecQΔC. Helices (boxes) and β-strands (arrows) are shown above the sequence and labeled sequentially. Color coding is the same as in (A). (**C**) Orthogonal views of a ribbon diagram of the crystal structure of RecQΔC, color-coded as in (A). A bound $Zn^{2+}$ ion is shown as a magenta sphere (Bernstein, Zittel et al. 2003).

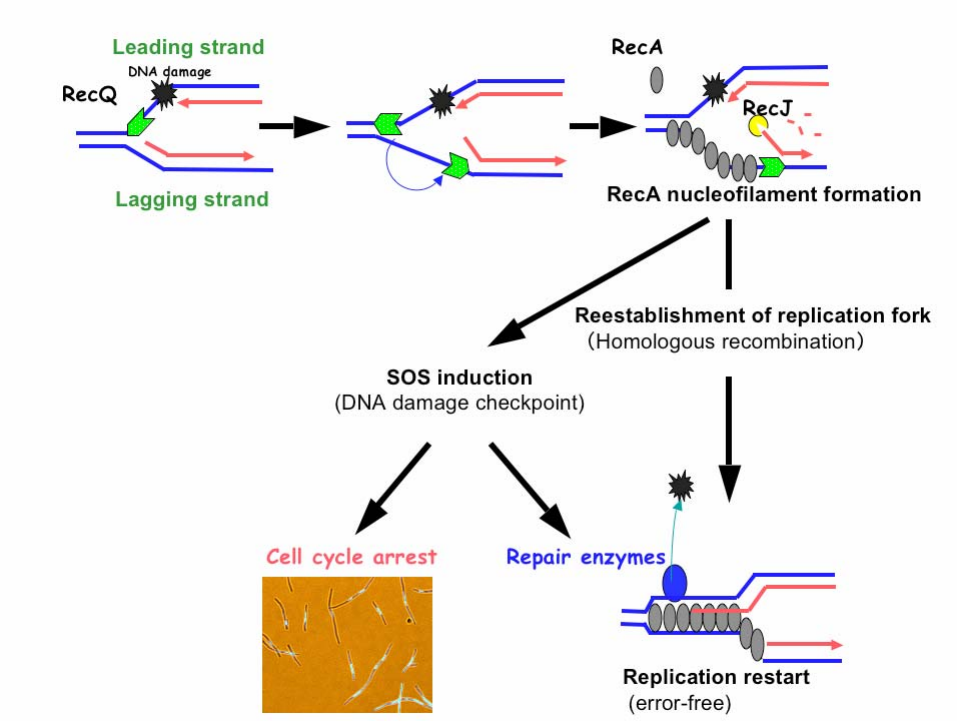


**Figure 1.12** The roles of RecQ in the rescue of a stalled replication fork. RecQ binds a ssDNA gap on the replication fork and creates an ssDNA region on the lagging strand by two-step reactions, which may be an initiating signal for RecA-dependent SOS induction and recombination repair (Hishida, Han et al. 2004).

*In vivo*, RecQ and other proteins in the RecF pathway of HR help repair stalled replication forks at sites of DNA damage (Courcelle, Carswell-Crumpton et al. 1997; Courcelle and Hanawalt 2001; Courcelle and Hanawalt 2003). *E.coli* RecQ suppresses illegitimate recombination between sequences with limited homology (Hanada, Ukita et al. 1997). RecQ is also involved in recruiting RecA for SOS induction and recombination at stalled replication forks, which then leads to cell cycle checkpoint and resumption of DNA replication (Heyer 2004; Hishida, Han et al. 2004). Recently, Magner *et al.* found that RecQ promotes the net accumulation of bimolecular recombination intermediates *in vivo*, indicating a second paradigm for the *in vivo* effect of RecQ-like proteins (Magner, Blankschien et al. 2007).

### 1.2.2 *Saccharomyces cerevisiae* Sgs1

The unicellular eukaryote *Sacchromyces cerevisiae* has only one RecQ helicase, named Sgs1. Sgs1 was identified as a genetic suppressor of the *top3* mutant phenotype (Gangloff, McDonald et al. 1994), and mutations in sgs1 are synthetically lethal with mutations in the Srs2 helicase (Lee, Johnson et al. 1999) or the SLX nuclease (Kaliraman, Mullen et al. 2001). Sgs1 forms complex with topoisomerase 3 (Top3) and Rmi1 that is implicated in resolving intermediates of HR (Mullen, Nallaseth et al. 2005; Mankouri and Hickson 2007). It is proposed that Sgs1 in conjunction with Top3 removes double-Holliday junction intermediates yielding non-crossover products, whereas Srs2 promotes the non-crossover synthesis-dependent strand-annealing pathway, apparently by regulating Rad51 binding during strand exchange (Ira, Malkova et al. 2003).

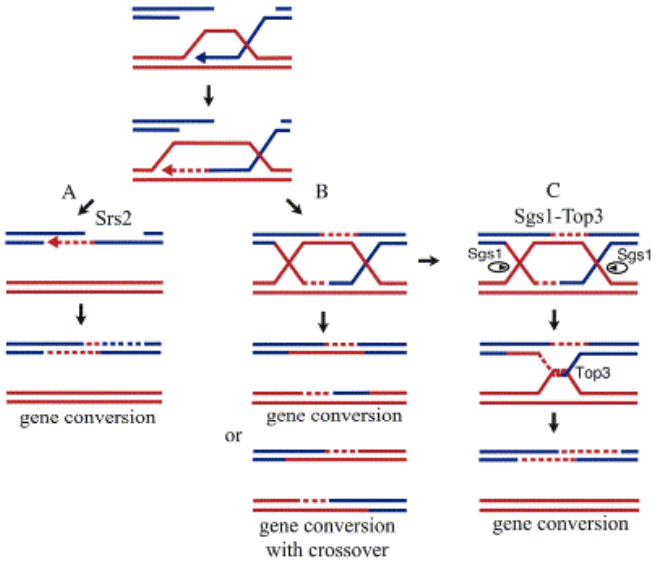


**Figure 1.13** Model of Sgs1- and Srs2-Dependent Crossover Suppression (A) Srs2 promotes the noncrossover pathway of HR. (B) A HJ resolvase cuts double Holliday junctions to give crossovers and noncrossovers. (C) Sgs1 acts together with Top3 to remove double Holliday junctions so that gene conversions will be recovered as noncrossovers. Adapted from (Ira, Malkova et al. 2003).

Sgs1 contains seven conserved helicase motifs and shows helicase activity (Lu, Mullen et al. 1996; Bennett, Sharp et al. 1998). The N-terminal region of the Sgs1 protein has been shown to be critical for interacting with Top2 and Top3 (Gangloff, McDonald et al. 1994; Bennett, Noirot-Gros et al. 2000; Fricke, Kaliraman et al. 2001). The function of the C-terminal region of Sgs1 remains unknown.

The Sgs1 protein exists in the nucleolus when the cells are young and migrates to the nucleoplasm as the cells senesce and the nucleolus gets fragmented (Sinclair, Mills et al. 1997). Sgs1 binds to Top2 and Top3 (Gangloff, McDonald et al. 1994) (Watt, Louis et al. 1995) and is tightly regulated throughout the cell cycle, accumulating in S phase and barely detectable in M and G1 phases (Frei and Gasser 2000). Sgs1 deficiency promotes aging processes such as nucleolar expansion and subsequent fragmentation, increases both illegitimate and homologous recombination and leads to hypersensitivity to DNA damaging agents such as methylmethanesulfonate and hydroxyurea (Miyajima, Seki et al. 2000). Recent data showed that Sgs1 prevents aberrant crossing-over by suppressing formation of multi-chromatid joint molecules and is required for efficient resolution of telomere recombination intermediates (Lee, Kozak et al. 2007; Oh, Lao et al. 2007).

### 1.2.3 Bloom syndrome helicase

Bloom syndrome (BS) is a rare genetic disorder arising from inherited mutations in both alleles of the BLM gene, one of the five human RecQ homologs. BS patients exhibit a high predisposition to development of all types of cancer affecting the general population. The most characteristic feature of BS cells is genomic instability manifested as an elevated frequency of chromosome breaks, interchanges between homologous chromosomes and sister chromatid exchanges (SCEs) (Enomoto 2001), which indicates an impairment of the ability to regulate crossovers during HR (Ababou, Dutertre et al. 2000)(Bussen, Raynard et al. 2007). Early studies on BS cells also showed a slow replication fork progression and the accumulation of abnormal replication intermediates (Enomoto 2001).

The BLM protein can act together with DNA topoisomerase IIIα (TOPOIIIα) to resolve HR intermediates into non-crossover products through a process called double-Holliday junction (DHJ) dissolution, as shown in Figure 1.14 (Hu, Beresten et al. 2001; Hickson 2003; Seki, Nakagawa et al. 2006; Bussen, Raynard et al. 2007). This activity of the BLM-Topo IIIα complex is thought to be critical for the suppression of DNA crossover formation in mitotic cells and cancer avoidance in humans (Bishop and Zickler 2004). Recently, BLAP75 protein (BLM-Associated Polypeptide, 75 kDa) was identified as a component of several BLM-containing complexes (Meetei, Sechi et al. 2003). In a subsequent study, it was shown that siRNA (small interfering RNA)-mediated depletion of cellular BLAP75 led to a decrease in BLM and TOPOIIIα protein levels in cells (Yin, Sobeck et al. 2005). Moreover, BLAP75 depletion resulted in increased frequency of sister chromatid exchanges, indicating a functional overlap between BLM and BLAP75. Recently, Bussen *et al.* proved that DHJ unwinding activity of the BLM/TopoIIIα complex is greatly enhanced as a result of its association with BLAP75 (Bussen, Raynard et al. 2007). Moreover, under physiological

conditions, DHJ dissolution is completely dependent on the presence of BLAP75 (Raynard, Bussen et al. 2006).

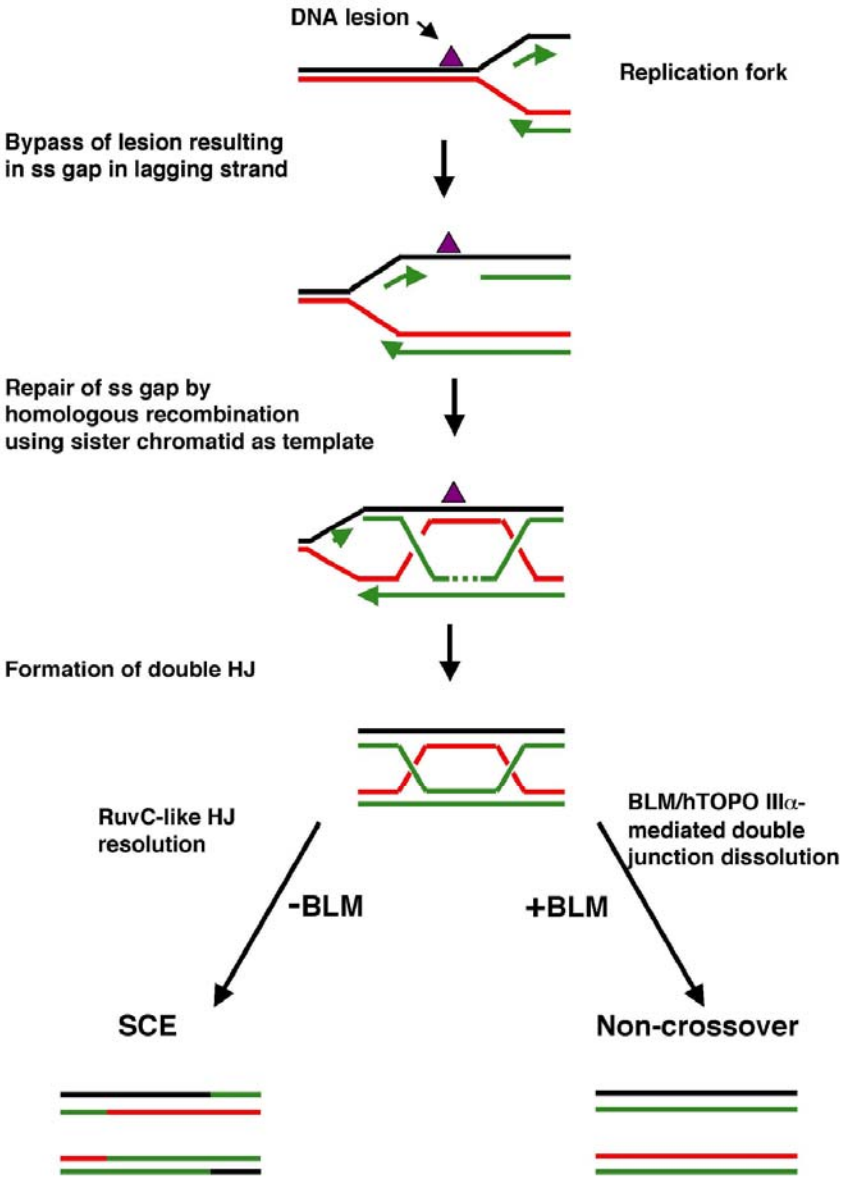


Figure 1.14 Model depicting pathways of DNA gap repair by homologous recombination. Double-Holliday junction (DHJ) intermediates are processed via classical HJ resolution, resulting in SCEs or via DHJ dissolution catalysed by the BLM/hTOPOIIIα complex, resulting in non-crossover products. Adapted from (Hickson 2003).

### 1.2.4 RECQ5 helicase

#### 1.2.4.1 *Drosophila melanogaster* RECQ5

In 1999, Sekelsky *et al.* discovered the *Drosophila melanogaster RECQ5* gene. They reported that *Drosophila* RecQ5 exists as three isoforms (Sekelsky, Brodsky et al. 1999). These include a large isoform RecQ5a (121kDa) and two small isoforms RecQ5b (54kDa) and RecQ5c that are almost identical (RecQ5c contains two additional amino acids at the C-terminus). Independently, Jeong *et al.* isolated the cDNA encoding for the large isoform of *Drosophila* RecQ5 and named the protein RECQ5/QE (Jeong SM 2000). The three isoforms of *Drosophila* RecQ5 are generated by alternative splicing (Figure1.15). The region encoding the helicase motifs is entirely present on the second exon, which can be joined to either of two alternative third exon start sites.

Two years later after the discovery of *Drosophila* RecQ5, the small isoform DmRecQ5 was expressed and purified from bacteria (Ozsoy, Sekelsky et al. 2001). The protein was shown to display single-stranded DNA-stimulated ATPase (dATPase) activity and 3′-5′ ATP (dATP)-dependent helicase activity (Ozsoy, Sekelsky et al. 2001). The purified DmRecQ5 was able to catalyze the unwinding of partial duplexes as long as 93 bp, but failed to unwind an 89bp blunt duplex substrate suggesting that a 3′ssDNA tail is essential for the unwinding activity of DmRecQ5 (Ozsoy, Sekelsky et al. 2001). Further experiments showed that DmRecQ5 is a structure specific helicase as other RecQ family members (Ozsoy, Ragonese et al. 2003). DmRecQ5 could efficiently unwind 3'-flap duplexes, three-way junctions and forked structures. Interestingly, DmRecQ5 showed a preference for binding at the fork junction in those substrates, suggesting a role in the repair of stalled replication forks (Ozsoy, Ragonese et al. 2003). DmRecQ5 was also shown to possess a DNA strand pairing and strand exchange activities (Machwe, Xiao et al. 2005).

Kawasaki *et al.* expressed and purified the large RECQ5/QE isoform using baculovirus system, since the initial attempts to express it in bacterial

were unsuccessful (Kawasaki, Maruyama et al. 2002). They found that RECQ5/QE formed oligomers (probably tetramers) and displayed a DNA helicase activity. Although RECQ5/QE hydrolysed GTP more efficiently than ATP in the presence of ssDNA, its DNA helicase activity was dependent only on ATP hydrolysis, Nevertheless, GTP had a stimulatory effect on this ATP-mediated helicase activity of RECQ5/QE (Kawasaki, Maruyama et al. 2002).

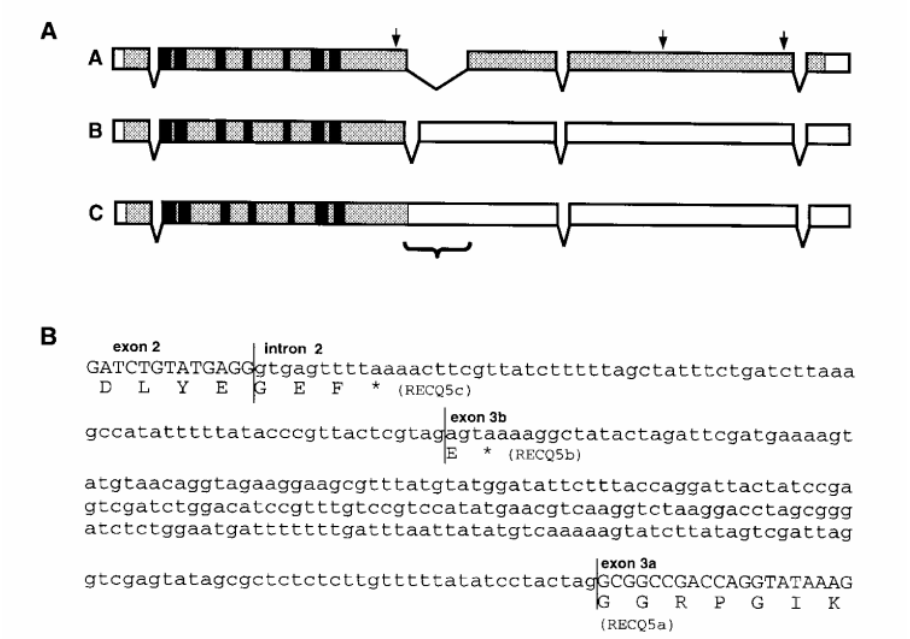


**Figure 1.15** Alternative splicing at *Drosophila RecQ5*. (**A**) Schematic of three alternative *RecQ5* transcripts. Each box represents one exon. Protein-coding regions are shaded; black boxes indicate the seven helicase motifs. Transcript A encodes a 121 kDa isoform (RecQ5a); transcripts B and C encode nearly identical 54 kDa isoforms RecQ5b and RecQ5c, respectively. (**B**) DNA sequence corresponding to the region of alternative splicing. Predicted amino acid sequences are shown, with asterisks indicating stop codones (Sekelsky, Brodsky et al. 1999).

*Drosophila* RecQ5 was found to localize to the nucleus when transiently expressed in *Drosophila* Schneider2 cells. Genetic studies indicated that *Drosophila RECQ5* is not an essential gene (Sekelsky, Brodsky et al. 1999).

Nevertheless, RECQ5/QE has been shown to accumulate specifically in early embryos, suggesting a role in development (Jeong SM 2000). Although the protein level of RECQ5/QE remains constant during cell-cycle in *Drosophila* S2 cells, both MMS and cisplatin treatment increased RECQ5/QE levels in these cells, suggesting a role for RECQ5/QE in the cellular response to DNA damage (Nakayama, Maruyama et al. 2006). Moreover, over-expression of RECQ5/QE in flies causes eye deformation and perturbs the normal cell-cycle progression in the presence of DNA damage. Those data suggest that RECQ5/QE might coordinate DNA repair with cell-cycle progression under genomic stress (Nakayama, Maruyama et al. 2006).

To understand the *in vivo* role of *Drosophila* RECQ5/QE, the *Drosophila* protein was expressed in yeast *sgs1* mutants. RECQ5/QE was able to complement the synthetic growth defect of *sgs1srs2* mutant; substitute Sgs1 function in the *top3* background when overexpressed; correct the hypersensitivity of *sgs1* mutants to hydroxyurea and MMS; and suppress the elevated rate of homologous recombination and sister chromatid exchanges (SCEs) in *sgs1* mutants. Further experiments showed that a QE/ΔC (8-463aa) mutant, which is nearly identical to the small isoforms DmRECQ5, is able to complement the Sgs1 function in *sgs1srs2,* but not in *sgs1top3* (Nakayama, Kawasaki et al. 2004).

#### 1.2.4.2 Human RECQ5 helicase

The human *RECQ5* gene was cloned by Kitao et al. in 1998 after a search for sequences similar to the RecQ helicase motifs in the expressed sequence tag database (Kitao, Ohsugi et al. 1998). In this study, a small isoform of RECQ5 was identified, which was later denoted RECQ5α (Shimamoto, Nishikawa et al. 2000). The cDNA for RECQ5 showed 48% homology to *Escherichia coli* RecQ in the helicase domain. The *RECQ5* gene was found to be expressed ubiquitously in all tissues examined with the highest levels in testis and ovary, and expression level of the *RECQ5* mRNA was almost constant throughout the cell cycle (Kitao, Ohsugi et al. 1998).

The same group who discovered the *Drosophila Melanogaster RECQ5* gene suggested that alternative splicing is also involved in generating different isoforms of human RECQ5 (Sekelsky, Brodsky et al. 1999). This proposal was confirmed by Shimamoto *et al.* (Shimamoto, Nishikawa et al. 2000). Three RECQ5 isoforms identified thus far include: RECQ5α (410aa), RECQ5β (991aa), and RECQ5γ (435aa). All three proteins contain the helicase domain with seven conserved motifs as shown in Figure 1.16 (Shimamoto, Nishikawa et al. 2000).

The small isoforms RECQ5α and RECQ5γ were found to localize in cytoplasm. In contrast, RECQ5β migrated exclusively to the nucleus (Shimamoto, Nishikawa et al. 2000). Interestingly, a deletion variant of RECQ5β containing the last 246 aa could also migrate to the nucleus, indicating that the C-terminal part of RECQ5β contains a nuclear localization signal (NLS) (Shimamoto, Nishikawa et al. 2000). The sequence KRPRSQQENPESQPQKRPR at the C-terminus (residues 854–872) of RECQ5β was suggested to be the potential NLS (Shimamoto, Nishikawa et al. 2000). The same authors also showed that RECQ5β formed complexes with TOPOIIIα and TOPOIIIβ and colocalized with these proteins in the nucleoplasm (Shimamoto, Nishikawa et al. 2000).

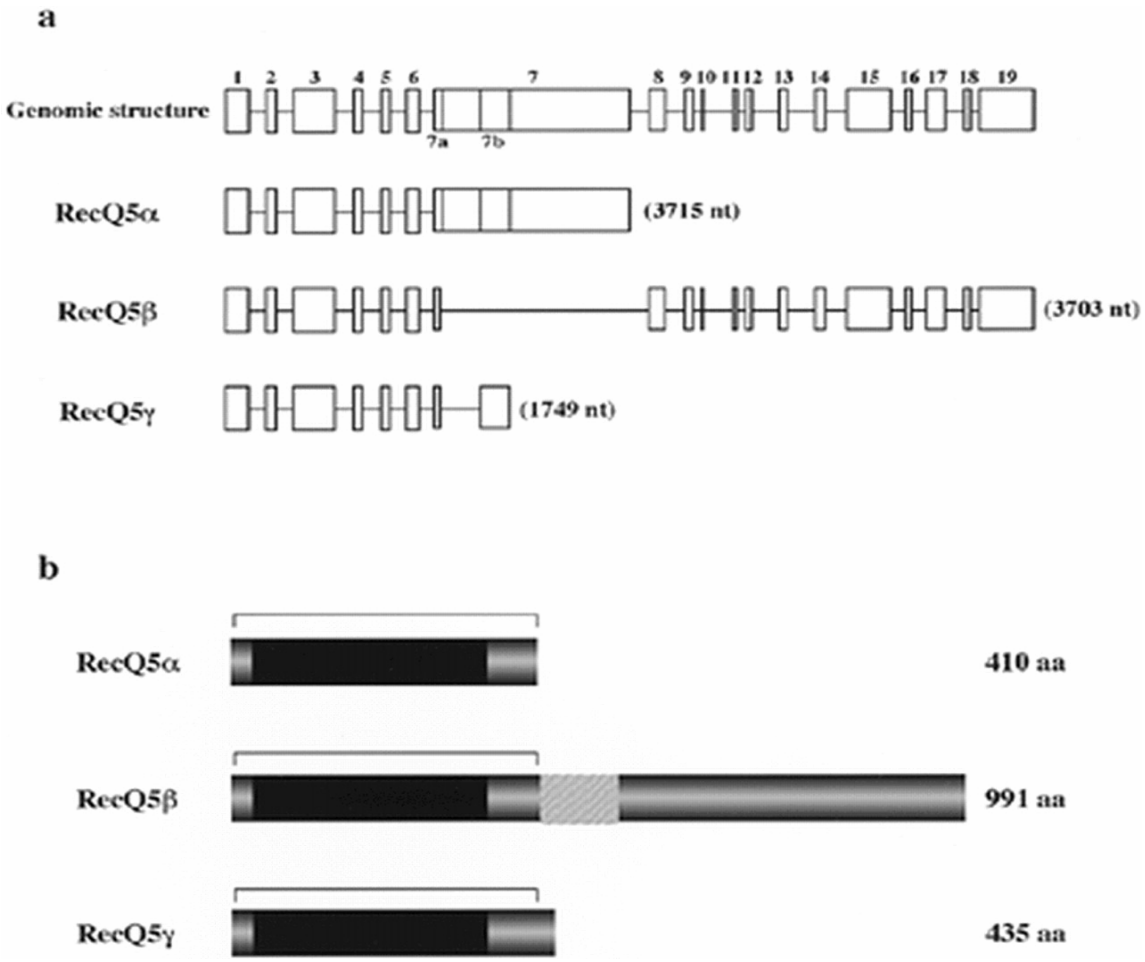


**Figure 1.16** Structure of the *RECQ5* gene and the encoded RecQ5 proteins. (**a**) Genomic structure of the RecQ5 gene and the exon uses of three RecQ5 mRNA isomers, RecQ5α, RecQ5β and RecQ5γ. (**b**) Schematic representation of three RecQ5 helicase isomers. The sizes of each protein are given on the right. The darkened areas indicate the locations of the helicase domains shared by the RecQ helicase family. The hatched area indicates the RECQ-C terminal domain. Adapted from (Shimamoto, Nishikawa et al. 2000).

Garcia *et al.* carried detailed biochemical characterization of human RECQ5β and found that RECQ5β is an ssDNA/dsDNA-dependent ATPase and an ATP-dependent 3'–5' DNA helicase with the ability to promote branch

migration of HJs (Garcia, Liu et al. 2004). More interestingly, RECQ5β was found to possess an intrinsic DNA strand-annealing activity that is inhibited by RPA (Garcia, Liu et al. 2004). Analysis of deletion variants of RECQ5β revealed that the DNA helicase activity resides in the conserved N-terminal portion of the protein, whereas the unique C-terminal domain mediates strand annealing. This is the first demonstration of a DNA helicase with an intrinsic DNA strand-annealing function residing in a separate domain. The unique biochemical properties of RECQ5β suggested that the protein might function in a DNA repair pathway that requires the coordinated action of DNA helicase and DNA strand-annealing activities (Garcia, Liu et al. 2004).

### *1.2.4.3* Mouse RecQ5

The mouse *Recq5* gene is located to chromosome 11E2, which has a syntenic relation to human 17q25.2-q25.3 where human *RECQ5* is present (Ohhata, Araki et al. 2001). To explore the role of RECQ5 in recombination, Hu *et al* inactivated *Recq5* gene in mouse ES cell by gene targeting (Hu, Lu et al. 2005). Although mouse *Recq5*$^{-/-}$ ES cells had similar growth rate and ionising radiation sensitivity to their parental mouse ES cells, the frequency of spontaneous SCE in *Recq5*$^{-/-}$ ES cells was significantly higher than that of the wild-type or heterozygous *Recq5*$^{+/-}$ cells. Hu *et al.* then reintroduced a single copy of functional Recq5 into *Recq5*$^{-/-}$ ES cells to see if the SCE phenotype could be rescued. Indeed their results directly demonstrated that the elevated SCE level of *Recql5*$^{-/-}$ ES cells is caused by the loss of *Recql5* function (Hu, Lu et al. 2005). They could also confirm this phenotype in mouse embryonic fibroblasts (MEFs) derived from *Recq5*$^{-/-}$ ES cells. Furthermore, they created the double knock-out *Recq5*$^{-/-}$*/Blm*$^{-/-}$ and observed an even higher frequency of SCE than in the case of mutating either one of these two genes alone. Their data implied that RECQ5 and BLM suppress SCEs *via* different mechanisms (Hu, Lu et al. 2005).

## 2 Aim and Scope

The aim of this thesis is to advance our understanding of the role of human RECQ5β helicase (hereafter RECQ5) in the maintenance of genomic stability. We started the project by searching for novel interaction partners of RECQ5 using two methods: (i) yeast-two-hyrid screening using RECQ5 as bait; and (ii) large-scale immunoprecipitation of RECQ5 from human cell extracts followed by mass spectrometry analysis. Both methods successfully led to the discovery of several interesting protein-interaction partners of RECQ5 (Results 3.1 and 3.2).

We then focused on studying the interaction of RECQ5 with PCNA, RAD51, and the MRE11/RAD50/NBS1 (MRN) complex that play important roles in DNA replication and maintenance of genomic integrity.

RECQ5 was found to interact with PCNA directly through a conserved PCNA interaction motif located at the C-terminus of RECQ5 polypeptide. RECQ5 also localized to DNA replication factories in S-phase nuclei and persisted at sites of stalled replication forks, suggesting a role in replication-associated repair processes (Results 3.3).

At biochemical level, RECQ5 helicase could displace RAD51 from single-stranded DNA through a direct protein-protein interaction, suggesting a mechanism by which RECQ5 controls inappropriate homologous recombination events in the cell (Results 3.4).

RECQ5 was also found to bind directly to the MRE11 subunit of the MRN complex and to inhibit the 3′-5′ exonuclease activity residing in this subunit. At cellular level RECQ5 colocalized with the MRN complex at sites of stalled replication fork and DNA double-strand breaks. Our data also suggested that the MRN complex recruits RECQ5 to the sites of DNA damage (Results 3.5). Taken together, our studies established RECQ5 as an important factor in DNA damage response and maintenance of genomic stability.

# 3 Results

## 3.1 Novel interaction partners of RECQ5 identified by yeast-two-hybrid screening

Among all the traditional genetic approaches to identify novel protein-protein interactions, yeast two-hybrid technology is probably the most powerful one to detect protein-protein interactions in eukaryotic system (Gietz, Triggs-Raine et al. 1997). The basis of the two-hybrid system relies on the fact that a functional transcriptional factor can be reconstituted when its activation domain (AD) and DNA binding domain (DBD) are in close proximity to each other (Fields and Song 1989; Young 1998).

To perform yeast two-hybrid assay, we constructed the bait plasmid pZL3. Briefly, the C-terminal part of the coding regions of RECQ5 spanning amino acids 411-991 (RECQ5$^{411-991}$) was amplified by PCR using the plasmid pPG10 (Garcia, Liu et al. 2004) as a template. The primer were designed with PstI site. After PstI digestion, the RECQ5$^{411-991}$ fragment was subcloned in the PstI site of the bait vector pBTM116 that contains a LexA DBD (Figure 3.1) (Pedrazzi, Perrera et al. 2001). As prey, we used a randomly primed human peripheral blood cDNA library cloned in the BglII site of the pACT2 vector that contains a GAL4 AD (Figure 3.2) (Clontech).

In case of positive interaction between RECQ5 and a DNA sequence from the library, the DBD and AD fused to these proteins are brought to close proximity, leading to expression of reporter genes. In our system, two reporters could be checked for validation of positive interactions: (i) expression of yeast nutrition His marker - positive clones could grow on selective medium lacking histine; (ii) *lacZ* gene, which could be tested in a color formation assay using X-Gal.

A

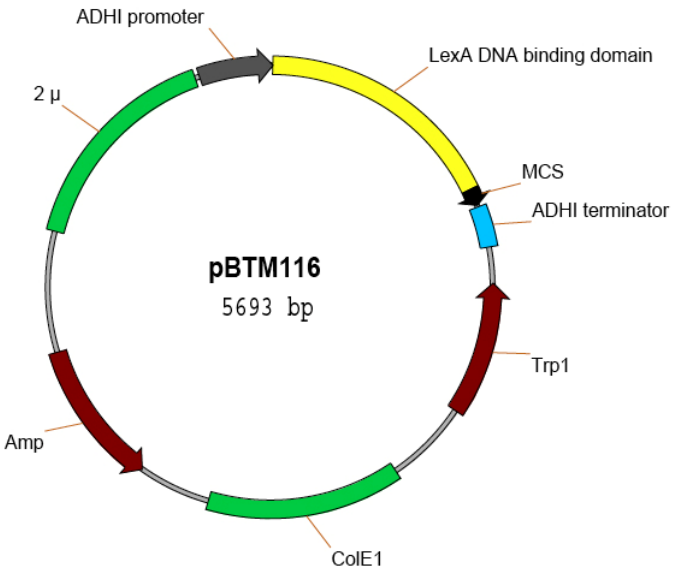


B

**LexA DNA binding domain (DNA-BD)**

```
ATT GAA GGG CTG GCG GTT GGG GTT ATT CGC AAC GGC GAC TGG CTG
I   E   G   L   A   V   G   V   I   R   N   G   D   W   L
```

**MCS**

***Eco*RI *Sma*I *Bam*HI *Sal*I *Pst*I stop**

```
GAA TTC CCG GGG ATC CGT CGA CCT GCA GCC AAG CTA ATT CCG GGC
E   F   P   G   I   R   R   P   A   A   K   L   I   P   G
```

**stop** **stop**

```
GAA TTT CTT ATG ATT TAT GAT TTT TAT TAT TAA
E   F   L   M   I   Y   D   F   Y   Y   *
```

**Figure 3.1** Bait vector pBTM116. (A) Schematic map of pBTM116. pBTM116 carries the yeast nutritional marker *TRP1* which is used for transformation selection. (B) Multiple cloning site (MCS) of pBTM116. Nucleotide triplets are shown in frame together with the corresponding amino acids (blue letters). Stop codons are in all three frames.

A

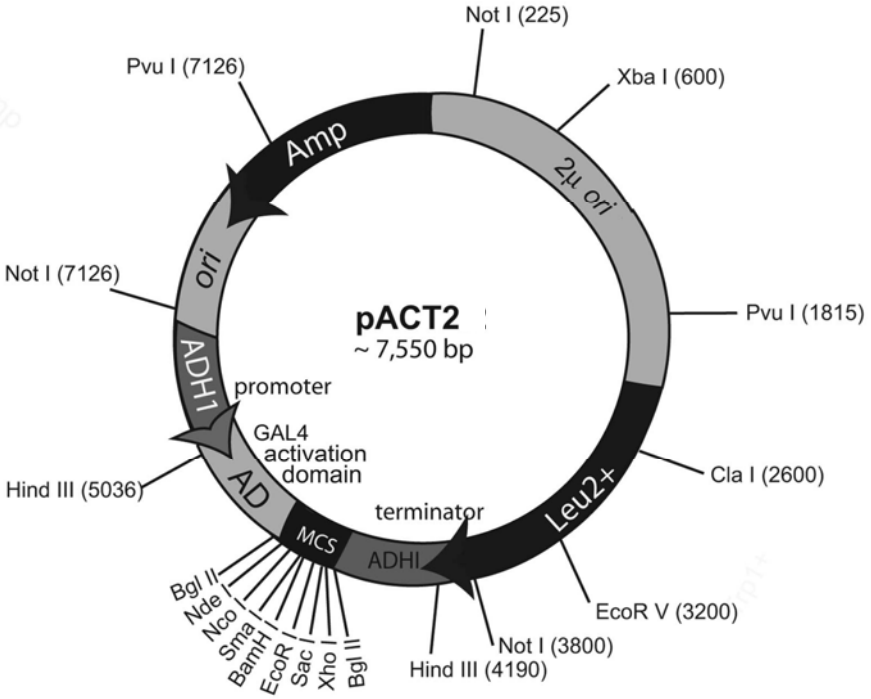


**B**

**MSC:**

| CAT ATG | GCC ATG GAG | GCC CCG GGG | ATC CGA ATT CGA | GCT CGA GAG ATC T |
|---|---|---|---|---|
| **Nde I** | **Nco I** | **Sma I** | **BamH I** **EcoR I** | **Sac I** **Xho I** **Bgl II*** |

*this site is not unique

**Figure 3.2** Prey vector pACT2. (A) Schematic map of pACT2. pACT2 carries the yeast nutritional marker *LEU2* which is used for transformation selection. (B) Multiple cloning site (MCS) of the pACT2 vector.

Transformation of yeast cells was performed essentially by modified lithium acetate (LiAc) method (Gietz, Triggs-Raine et al. 1997) (Gietz 2002). Briefly, yeast cultures were grown to $OD_{546}$ about 1.0. Cells were spun down at 2500rpm at 4°C. After washing with $ddH_2O$, cells were resuspended in $ddH_2O$ and split into 100µl aliquots on ice. To each cell suspension 240 µl of PEG3350 (50% w/v), 36 µl of 1.0 M LiAc, 25 µl of ssDNA and 1-10 µg of plasmid DNA to be transformed were added and vortexed vigorously. After incubation at room temperature for 10 minutes, cells were subjected to heat shock for 20 minutes at 42°C. Cell pellets were collected after centrifugation at 7000 rpm for 15 seconds, resuspended in 100 µl of $ddH_2O$ and spread onto an agar plate containing selective medium.

In our yeast two hybrid screening, the bait plasmid pZL3 and the cDNA library in the prey plasmid pACT2 were co-transformed into the L40 strain [MATa trp1 leu2 his3 LYS2::lexA-HIS3 URA3::lexA-lacZ] (Pedrazzi, Perrera et al. 2001) using the yeast transformation method described above, which was scaled up about 60 times. Approximately $1.4x10^7$ transformants were screened for grow on media lacking tryptophan (Trp), leucine (Leu), and histidine (His). To confirm the positive interactions, positive clones were analyzed by X-gal filter test assay for detection of *lacZ* reporter gene product through β-galactosidase activity. Out of $1.4x10^7$ yeast transformants, 198 colonies were scored as positive for reporter gene activity ($His^+$ and $LacZ^+$). All these clones were subjected to library plasmid DNA isolation and the cDNA inserts were sequenced. In total, 28 different cDNAs were identified. The list of all proteins identified in this yeast two-hybrid screen is shown in Table 3.1.

| No. | Number of clones | Name of the protein | Swiss-Prot Entry | Function |
|---|---|---|---|---|
| 1 | 21 | S-phase kinase-associated protein 1 (SKP1) | P63208 | SCF complex |
| 2 | 2 | SUMO-conjugating enzyme UBC9 | P63279 | Protein sumoylation |
| 3 | 1 | Ribosomal protein L19 (RPL19) | P84098 | Ribosomal protein |
| 4 | 2 | Ribosomal protein S3 (RPS3) | P23396 | Ribosomal protein |
| 5 | 26 | Nuclear autoantigen SP100 | P23497 | Gene expression PML bodies |
| 6 | 1 | F-box only protein 18 (FBXO18) | Q8NFZ0 | DNA helicase |
| 7 | 6 | DNA-directed RNA polymerase II subunit RPB2 (RPBII) | P30876 | RNA polymerase |
| 8 | 1 | BRCA1-associated protein (BRAP) | Q7Z569 | Binding to the NLS of BRCA1 |
| 9 | 1 | Guanine nucleotide binding protein (G protein), beta polypeptide | Q6FHM2 | Unknown |
| 10 | 2 | Beta-2-microglobulin (B2M), mRNA | Q6IAT8 | Beta-chain of major histocompatibility complex class I molecules |
| 11 | 1 | Maleylacetoacetate isomerase | O43708 | Glutathione S-transferase |

| | | | | |
|---|---|---|---|---|
| 12 | 1 | Endoplasmic reticulum aminopeptidase 1 (ARTS1) | Q9NZ08 | Peptide trimming |
| 13 | 1 | Activating transcription factor 4 | Q96AQ3 | Tax-responsive enhancer element |
| 14 | 1 | Ribosomal protein S6 (RPS6) | A2A3R5 | Ribosomal protein |
| 15 | 1 | Triosephosphate isomerase 1 (TPI1) | Q6FHP9 | Carbohydrate biosynthesis, gluconeogenesis |
| 16 | 2 | F-box/WD repeat-containing protein 7 | Q969H0 | F box protein, SCF complex |
| 17 | 1 | Cytochrome b-c1 complex subunit 1, mitochondria | P31930 | Component of the ubiquinol-cytochrome c reductase complex |
| 18 | 1 | Ribosomal protein L10a (RPL10A) | P62906 | Ribosomal protein |
| 19 | 1 | Splicing factor, arginine/serine-rich 18 | Q8TF01 | Splicing factor |
| 20 | 1 | S-adenosylmethionine synthetase isoform type-2 (MAT2A) | P31153 | Catalyzes the formation of S-adenosylmethionine |
| 21 | 1 | Glycine acyltransferase family-B | A5LGC7 | Unknown |
| 22 | 1 | CTD-binding SR-like protein rA9 (KIAA1542) | A6H8W1 | Unknown |
| 23 | 1 | DNA replication licensing factor MCM5 | P33992 | DNA replication |

| | | | | |
|---|---|---|---|---|
| 24 | 1 | ATP-binding domain 1 family member C | Q9UHW5 | Unknown |
| 25 | 1 | Fructose-bisphosphate aldolase A (ALDOA) | P04075 | Carbohydrate degradation, glycolysis |
| 26 | 1 | Polypyrimidine tract binding protein 1 (PTBP1) | Q9BUQ0 | Unknown |
| 27 | 1 | PRP18 pre-mRNA processing factor 18 homolog (PRPF18) | Q5T9P9 | Unknown |
| 28 | 1 | Kinesin family member 5B (KIF5B) | Q6P164 | Unknown |

**Table 3.1** List of protein interaction partners of RECQ5 identified by yeast-two-hybrid screening of human peripheral blood cell cDNA library. All proteins listed are human proteins. Functions of the proteins were derived from the Swiss-prot database or published data. Note that from clone #5 on, the DNAs were isolated and sequenced by Daniela Huehn.

Based on those 28 newly identified interaction partners, many new areas to study the function of RECQ5 could be suggested: DNA replication (MCM5), protein ubiquitination (Skp1, FBW7), protein sumoylation (UBC9), and transcription (RPB2).

### 3.2 Novel interaction partners of RECQ5 identified by mass spectrometric analysis of RECQ5 immunoprecipitates from human cells

Yeast-two-hybrid system is a very powerful tool to identify novel protein-protein interactions, but it has a major drawback since it produces a lot of false positives and thus might mislead us in designing our future experiments. To overcome this problem, we also employed a proteomic approach to identify new interaction partners of RECQ5. Specifically, we immunoprecipitated RECQ5 from a total extract of human 293T embryonic kidney fibroblasts and analysed the identity of co-precipitating proteins by mass spectrometry (MS).

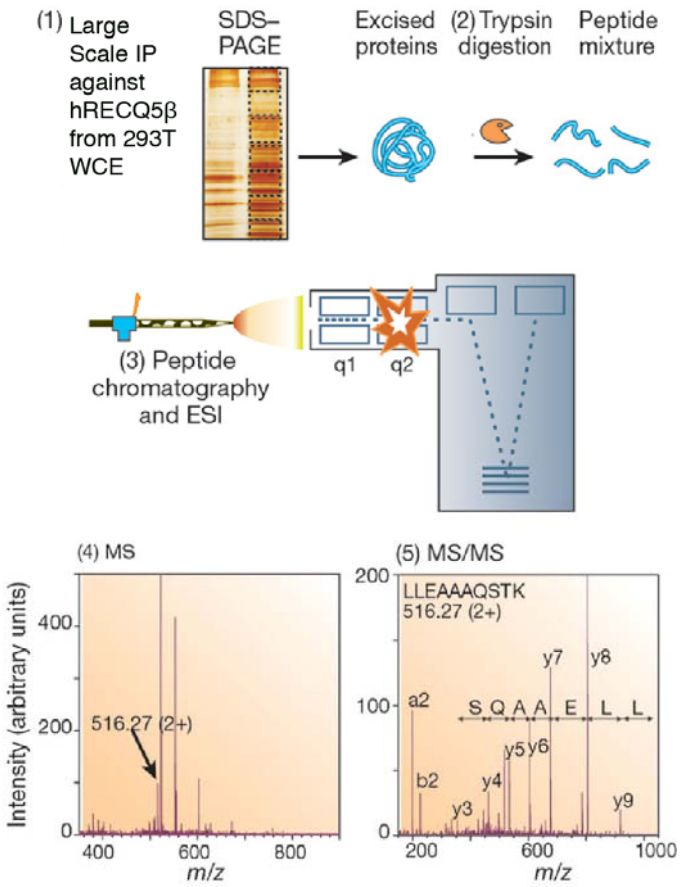


**Figure 3.3** The scheme of MS identification experiment, adapted from (Aebersold and Mann 2003).

As shown in Figure 3.3, the experiment consisted of five steps. First, a large-scale immunoprecipitation (IP) is performed. Briefly, whole cell extract (WCE) from human embryonic kidney cells (HEK 293T) was prepared in IP buffer (50 mM Tris–HCl, pH 8.0, 120 mM NaCl, 0.5% (v/v) NP-40, supplemented with a protease inhibitor cocktail (Complete, Mini; Roche). The extract (12 mg of total protein) was divided into four reaction tubes. Next, 3 μg of an affinity-purified rabbit polyclonal anti-RECQ5 antibody (Kanagaraj, Saydam et al. 2006) were added to each tube and the mixtures were incubated overnight at 4°C. As control, equal amount of IgGs purified from pre-immune serum was used in parallel experiment. Immune complexes were subsequently incubated with protein A/G–agarose beads (20 μl/tube, GE Healthcare) for 2 hours at 4°C. After extensive washing with IP buffer, beads were boiled at 95°C for 10 minutes in SDS loading buffer to release bound proteins. Supernatant was concentrated by speed vac and loaded on a 7.5 % (w/v) SDS poly-acrylamide gel. The gel was stained with Coomassie Brilliant Blue and excised protein bands were subjected to in gel trypsin digestion (Rosenfeld, Capdevielle et al. 1992; Hellman, Wernstedt et al. 1995; Cannavo 2006) to produce peptides with C-terminally protonated amino acids that could be analyzed in the subsequent MS peptide sequencing. Briefly, the gel was cut into nine pieces and each piece was further diced into smaller cubes (1mm) and subjected to two cycles of rehydration in 50 mM ammonium bicarbonate ($NH_4HCO_3$) and dehydration in 80% acetonitrile. Gel pieces were then incubated with 37 mM DTT solution at 50°C for 30 minutes. After two additional rounds of dehydration in 80% acetonitrile, proteins were incubated with 20 mM iodoacetamide for 15 minutes in dark for alkylation. After another three rounds of rehydration in 50 mM $NH_4HCO_3$ and shrinking in 80% acetonitrile, the gel pieces were incubated with freshly diluted **1**2.5ng /μl trypsin solution at 37°C for 4 hours and then at 25°C overnight. Digested peptides were finally extracted with 0.1% formic acid one time and 80% acetonitrile three times and

dried under vacuum.

In step three, the peptides are separated by chromatography and enter the mass spectrometer. In step four, the first mass spectrum (MS) of the eluting peptides is taken. A list of peptides was generated for further fragmentation and tandem mass spectrometric or 'MS/MS' experiments. Finally, the MS and MS/MS spectra were recorded and matched against the human portion (taxonomy ID: 9606) of the UniProt database (http://www.uniprot.org). The peptides identified were interrogated using the Mascot search algorithm (Perkins and Darryl J. C. Pappin 1999). RECQ5 protein itself was identified as one of the most significant hit [Mascot protein score where a value >65 was considered significant ($P<0.05$)], serving as the positive validation of the assay. In addition 63 proteins with significant peptide identification were considered as potential interaction partners of RECQ5 (Table 2.2).

| **No.** | **Name of the protein** | **Swiss-Prot Entry** | **Function** |
|---|---|---|---|
| 1 | DNA-dependent protein kinase catalytic subunit (DNA-PKcs) | P78527 | NHEJ |
| 2 | Microtubule-associated protein 1B (MAP 1B) | P46821 | Microtubules stabilization |
| 3 | Nijmegen breakage syndrome protein 1 (NBS1) | O60934 | DSB repair, DNA recombination |
| 4 | Heterogeneous nuclear ribonucleoprotein M (hnRNP M) | P52272 | Pre-mRNA binding |
| 5 | U1 small nuclear ribonucleoprotein 70 kDa (snRNP70) | P08621 | Pre-mRNA splicing |
| 6 | Myeloid/lymphoid or mixed-lineage leukemia protein 2 (MLL2) | O14686 | Transcriptional regulation |

| | | | |
|---|---|---|---|
| 7 | ATP-dependent RNA helicase DDX3X (DEAD box protein 3) | O00571 | RNA helicase |
| 8 | Polyadenylate-binding protein 1 (PABP 1) | P11940 | mRNA metabolism |
| 9 | Transcription intermediary factor 1-beta (TIF1B) | Q13263 | Transcription repression |
| 10 | Angiomotin | Q9HD27 | Junction maintenance |
| 11 | Vimentin | P08670 | Class-III intermediate filaments |
| 12 | Polyadenylate-binding protein 4 (PABP 4) | Q6P0N3 | mRNA metabolism |
| 13 | Nucleolin | P19338 | Transcriptional elongation |
| 14 | DNA-directed RNA polymerase II subunit RPB2 (RPBII) | P30876 | RNA polymerase |
| 15 | Coronin-1C | Q9ULV4 | Cytokinesis, signal transduction |
| 16 | Insulin-like growth factor 2 mRNA-binding protein 3 | O00425 | mRNA translation |
| 17 | Heterogeneous nuclear ribonucleoprotein K (hnRNP K) | P61978 | Nuclear metabolism of hnRNA |
| 18 | ATP-binding cassette sub-family D member 3 | P28288 | Transporter |
| 19 | Ras GTPase-activating protein-binding protein 1 | Q13283 | Stress granule assembly regulator |
| 20 | Heat shock protein 60 | P10809 | Mitochondrial protein import |

| | | | |
|---|---|---|---|
| 21 | Splicing factor, arginine/serine-rich 4 | Q08170 | Pre-mRNA splicing |
| 22 | ATP-dependent DNA helicase Q4 (RECQ4) | O94761 | DNA replication initiation, repair |
| 23 | Spectrin alpha chain, brain | Q13813 | Secretion |
| 24 | DNA replication licensing factor MCM7 | P33993 | DNA replication |
| 25 | Bcl-2-associated transcription factor 1 | Q9NYF8 | Transcriptional repressor |
| 26 | UDP-glucose 6-dehydrogenase | O60701 | Biosynthesis of glycosaminoglycans |
| 27 | Non-POU domain-containing octamer-binding protein (NONO) | Q15233 | DNA and RNA binding protein |
| 28 | E3 ubiquitin-protein ligase UBR5 | O95071 | E3 ubiquitin ligase |
| 29 | Splicing factor, proline- and glutamine-rich | P23246 | Essential pre-mRNA splicing factor |
| 30 | Pre-mRNA-processing-splicing factor 8<br>Synonyms (RPB 8) | O14547 | Central component of the spliceosome |
| 31 | Gephyrin | Q9NQX3 | Membrane protein-cytoskeleton interactions |
| 32 | DNA-directed RNA polymerase II subunit RPB1 | P24928 | RNA polymerase |
| 33 | Splicing factor, arginine/serine-rich 6 | Q13247 | Constitutive splicing |
| 34 | Desmoglein-2 | Q14126 | Cell-cell adhesion |
| 35 | Putative ATP-dependent RNA helicase DDX | P17844 | Pre-mRNA splicing |

| | | | |
|---|---|---|---|
| 36 | Spectrin beta chain, brain 1 | Q8IX99 | Secretion |
| 37 | Inverted formin-2 | Q6PK22 | Actin filaments |
| 38 | Zinc finger protein GLI3 | P10071 | Limb and brain development |
| 39 | SAPS domain family member 1 | Q9UPN7 | Regulatory subunit for PPP6 |
| 40 | Drebrin | Q9UFZ5 | Cell migration |
| 41 | 78 kDa glucose-regulated protein | P11021 | Multimeric protein complexes inside the ER |
| 42 | Insulin-like growth factor 2 mRNA-binding protein 1 | Q9NZI8 | mRNA nuclear export, translation |
| 43 | Suppressor of fused homolog (SUFU) | Q9NZ07 | Hedgehog signaling pathway |
| 44 | DNA repair protein RAD50 | Q92878 | DSB repair, DNA recombination |
| 45 | Nuclear receptor corepressor 2 | Q9Y618 | Transcriptional repression |
| 46 | Double-strand break repair protein MRE11A (MRE11) | P49959 | DSB repair, DNA recombination |
| 47 | Sodium/potassium-transporting ATPase subunit alpha-1 (AT1A1) | P05023 | ATP hydrolysis |
| 48 | Heat shock cognate 71 kDa protein | P11142 | Chaperone |
| 49 | Phenylalanyl-tRNA synthetase alpha chain (SYFA) | Q9Y285 | tRNA synthetase |
| 50 | Valyl-tRNA synthetase | P26640 | tRNA synthetase |
| 51 | Serine/arginine repetitive matrix protein 2 | Q9UQ35 | Pre-mRNA processing |

| | | | |
|---|---|---|---|
| 52 | Heterogeneous nuclear ribonucleoprotein U (HnRNP U) | Q9BQ09 | Double-and single-stranded DNA and RNA binding |
| 53 | Serine/arginine repetitive matrix protein 1 | Q8IYB3 | Pre-mRNA processing |
| 54 | Cytospin-A | Q69YQ0 | Cytokinesis and spindle organization |
| 55 | Zinc finger CCCH domain-containing protein 13 (ZC313) | Q5T200 | Unknown |
| 56 | Serine/threonine-protein kinase tousled-like 2 | Q86UE8 | Chromatin assembly, checkpoint |
| 57 | Protein phosphatase 1 regulatory subunit 12A | O14974 | Myosin phosphatase activity regulation |
| 58 | Insulin receptor substrate 4 (IRS4) | O14654 | Growth factor receptors possessing |
| 59 | Stress-70 protein, mitochondrial | P38646 | Cell proliferation, cellular aging |
| 60 | Heat shock 70 kDa protein 1 | P08107 | Chaperone |
| 61 | Tubulin alpha-1B chain | P68363 | Major constituent of microtubules |
| 62 | Heat shock protein HSP 90-beta | Q9NTK6 | Chaperone |
| 63 | Putative ATP-dependent RNA helicase DDX17 | Q92841 | RNA helicase |

**Table 3.2** List of proteins identified by MS analysis of RECQ5 immunoprecipitate from 293T cells. All proteins listed are human proteins. Functions of the proteins were derived from Swiss-prot database or published

data. Proteins with light grey color mark are involved in DNA metabolism including DNA repair, replication and recombination. Proteins with yellow mark are involved in RNA metabolism including RNA splicing, transcription, and tRNA synthesis.

In Figure 3.4, a short list of the novel interaction partners of RECQ5 discovered in this study (Results 3.1 and 3.2) was illustrated. Those interactions have linked RECQ5 to DNA replication, recombination and repair. In the following chapters, our work towards understanding the biological function of the interactions of RECQ5 with the PCNA (Results 3.3), RAD51 (Results 3.4) and MRN complex (Results 3.5) will be described.

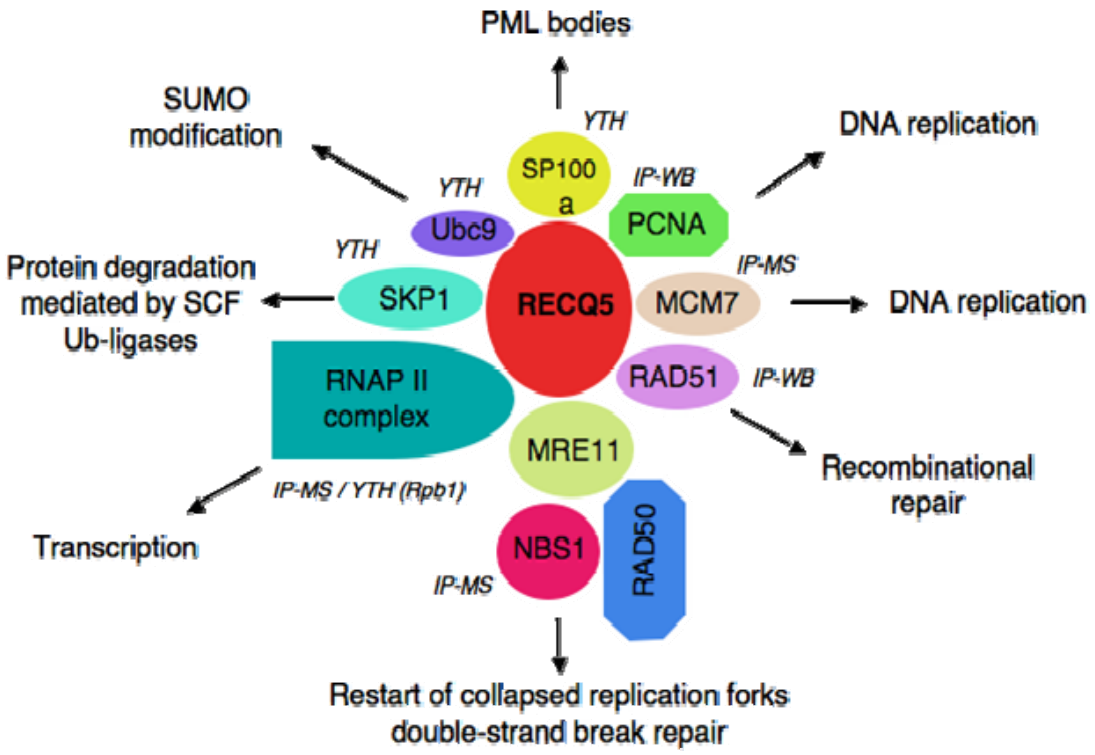


**Figure 3.4** Selected interaction partners of RECQ5 identified in this study.

## 3.3 Human RECQ5beta helicase promotes strand exchange on synthetic DNA structures resembling a stalled replication fork

Radhakrishnan Kanagaraj, Nurten Saydam, Patrick L. Garcia, **Lu Zheng**, and Pavel Janscak

Nucleic Acids Res. 2006; 34(18): 5217-31.

My contribution to this paper was to discover and confirm the interaction between RECQ5 and PCNA.

Published online 26 September 2006

Nucleic Acids Research, 2006, Vol. 34, No. 18 5217–5231
doi:10.1093/nar/gkl677

# Human RECQ5β helicase promotes strand exchange on synthetic DNA structures resembling a stalled replication fork

**Radhakrishnan Kanagaraj, Nurten Saydam, Patrick L. Garcia, Lu Zheng and Pavel Janscak***

Institute of Molecular Cancer Research, University of Zurich, Winterthurerstrasse 190, CH-8057 Zurich, Switzerland

Received July 25, 2006; Revised August 30, 2006; Accepted September 4, 2006

## ABSTRACT

**The role of the human RECQ5β helicase in the maintenance of genomic stability remains elusive. Here we show that RECQ5β promotes strand exchange between arms of synthetic forked DNA structures resembling a stalled replication fork in a reaction dependent on ATP hydrolysis. BLM and WRN can also promote strand exchange on these structures. However, in the presence of human replication protein A (hRPA), the action of these RecQ-type helicases is strongly biased towards unwinding of the parental duplex, an effect not seen with RECQ5β. A domain within the non-conserved portion of RECQ5β is identified as being important for its ability to unwind the lagging-strand arm and to promote strand exchange on hRPA-coated forked structures. We also show that RECQ5β associates with DNA replication factories in S phase nuclei and persists at the sites of stalled replication forks after exposure of cells to UV irradiation. Moreover, RECQ5β is found to physically interact with the polymerase processivity factor proliferating cell nuclear antigen *in vitro* and *in vivo*. Collectively, these findings suggest that RECQ5β may promote regression of stalled replication forks to facilitate the bypass of replication-blocking lesions by template-switching. Loss of such activity could explain the elevated level of mitotic crossovers observed in RECQ5β-deficient cells.**

## INTRODUCTION

The progression of DNA replication forks is frequently impaired by DNA damage, particularly if the blocking lesion is located on the leading-strand template (1). In this case, synthesis of the leading strand is halted at the lesion, while the lagging-strand synthesis continues beyond the lesion site, resulting in a fork structure with an extensive gap in the leading strand (2,3). Replication fork stalling poses a serious threat to genomic stability because it can trigger unscheduled DNA recombination events and hence lead to gross chromosomal re-arrangements that can induce tumorigenesis (4,5). To avoid these detrimental consequences of DNA replication arrest, cells can switch to different DNA damage bypass modes that permit replication across the lesion (1,3,6,7). One of these mechanisms is proposed to involve a transient template switch to the undamaged sister chromatid, allowing the replicative polymerase to synthesize the sequence complementary to the blocking lesion in an error-free manner (8). It is believed that such template-switching is achieved by a movement of the fork backward so as to re-anneal the original template strands and displace the newly synthesized strands which themselves anneal to generate a Holliday junction structure with a short arm (1). Indeed, such structures have been observed to accumulate upon replication arrest both in prokaryotic and in eukaryotic cells (8–11). However, it is not clear whether the formation of these structures is promoted enzymatically or occurs spontaneously.

Proteins belonging to the RecQ family of 3′–5′ DNA helicases are implicated in the processing of aberrant DNA structures arising during DNA replication and repair (12). Defects in three of the five known human RecQ homologues have been found to be associated with different autosomal recessive disorders characterized by genomic instability and cancer predisposition—mutations in BLM, WRN and RECQ4 give rise to Bloom syndrome, Werner syndrome and Rothmund–Thomson syndrome, respectively (12). BLM is known to suppress crossovers during homologous recombination (HR) presumably through its unique ability to act in conjunction with DNA topoisomerase IIIα to decatenate recombination intermediates containing double Holliday junctions (13). WRN promotes lagging-strand replication of G-rich telomeric regions and resolves telomeric D-loops in a manner regulated by the TRF1 and TRF2 proteins (14,15). RECQ4 is proposed to be important for the initiation of DNA replication by promoting the loading of replication protein A on unwound origins (16).

The role of the human RECQ5 protein in the maintenance of genomic stability remains to be elucidated. The inactivation

*To whom correspondence should be addressed. Tel: +41 44 635 3470; Fax: +41 44 635 3484; Email: pjanscak@imcr.unizh.ch

5218 Nucleic Acids Research, 2006, Vol. 34, No. 18

of the *Recq5* gene in mouse embryonic stem cells results in a significant increase in the frequency of sister chromatid exchanges (SCEs) comparable to that caused by *Blm* gene inactivation (17). Deletion of both *Recq5* and *Blm* genes leads to an even higher frequency of SCEs compared to the single mutants, suggesting that BLM and RECQ5 operate in different pathways that suppress mitotic recombination (17). In contrast to the other human RecQ homologues, RECQ5 exists in at least three different isoforms resulting from alternative mRNA splicing (18). The largest splice variant, RECQ5β functions not only as a 3′–5′ DNA helicase, but also possesses an intrinsic DNA strand-annealing activity residing in the unique C-terminal half of the protein (19). This strand-annealing activity is suppressed if the helicase is in its ATP-bound state, suggesting that RECQ5β may mediate DNA transactions that require a coordinated action of helicase and strand-annealing activities, such as replication fork regression.

Here we show that the RECQ5β helicase has the ability to promote strand exchange between arms of synthetic forked DNA structures that resemble a stalled replication fork in a reaction stimulated by the human replication protein A (hRPA). In contrast, hRPA is found to block strand exchange by BLM and WRN by driving these helicases to mediate unwinding of the parental duplex. On forked DNA structures with heterologous arms, RECQ5β preferentially unwinds the lagging-strand duplex, whereas BLM and WRN show a strong preference for unwinding of the parental duplex even in the absence of hRPA. The ability of RECQ5β to catalyze the lagging-strand unwinding and strand exchange on hRPA-coated forked structures is dependent on a short region located within the non-conserved portion of RECQ5β. In addition, we show by immunofluorescence microscopy that RECQ5β localizes to DNA replication factories in S phase nuclei and persists at the sites of stalled replication forks. Moreover, we have found that RECQ5β physically interacts with the polymerase processivity factor proliferating cell nuclear antigen (PCNA) *in vivo* and *in vitro*. Based on these findings, we propose that RECQ5β could mediate regression of stalled replication forks to facilitate DNA damage bypass by template-switching.

## MATERIALS AND METHODS

### Plasmid constructions and protein purifications

The bacterial expression vectors for the RECQ5β fragments encompassing the amino acid residues 1–774 (pPG13) and 542–991 (pPG14), fused to the C-terminus of glutathione-*S*-transferase (GST), were constructed by PCR amplification of the corresponding regions of the RECQ5β cDNA and their insertion in pGEX-2TK between the EcoRI and BamHI sites. The bacterial vectors expressing $RECQ5^{1–725}$ (pPG18), $RECQ5^{1–651}$ (pPG20), $RECQ5^{1–561}$ (pPG21) and $RECQ5^{1–475}$ (pPG19) as C-terminal fusions with a self-cleaving tag including chitin-binding domain (CBD) were constructed in the same way as the vector for the full-size RECQ5β (19). The BamHI–NcoI fragment of BLM cDNA in pcDNA3 (20), and the NcoI–XhoI fragment of pJK1 (21), including the remaining part of the BLM coding sequence fused C-terminally to a $His_6$ tag, were cloned in pFastBac1 via BamHI and XhoI sites to yield the plasmid pZL4, which was used to generate a bacmid for the expression of BLM in Sf9 cells by the means of baculovirus system.

The RECQ5β protein and its variants were produced in bacteria and purified as described previously (19). His-tagged BLM was produced in Sf9 by the means of baculovirus system and purified on a 5 ml HighTrap Chelating ($Ni^{2+}$) column under previously described conditions (21). To increase the purity, the BLM protein was further loaded on to a 1 ml MonoQ column equilibrated with buffer containing 50 mM Tris (pH 7.5), 10% (v/v) glycerol, 200 mM NaCl and 0.1 mM EDTA, and eluted with a linear concentration gradient of NaCl (200–650 mM). WRN, hRPA and PCNA were prepared essentially as described (22–24). *Escherichia coli* single-strand DNA-binding protein was purchased from Promega.

### Antibodies

An antibody against the C-terminal fragment of RECQ5β encompassing amino acids 675–991 was raised in rabbit (Clonestar Ltd, Czech Republic) and purified on a RECQ5β-Sepharose 4A column.

### DNA substrates

All oligonucleotides used for the preparation of DNA substrates were purchased PAGE-purified from Microsynth (Switzerland). The sequences of the oligonucleotides (RK1-7) and the schemes of DNA substrates are shown in Supplementary Table 1. Where required, oligonucleotides were labeled at the 5′ end with T4 polynucleotide kinase (NEB) and [$\gamma$-$^{32}$P]ATP using standard procedure. The oligonucleotides were annealed under conditions described previously (25).

### Strand exchange and helicase assays

Reactions were carried out at 37°C in buffer HA containing 20 mM Tris–acetate (pH 7.9), 50 mM KOAc, 10 mM $Mg(OAc)_2$, 1 mM DTT and 50 μg/ml BSA. Where required, $Mg(OAc)_2$ concentration was varied in the range from 0 to 10 mM. For the strand exchange assays, 1 nM RK1/RK2 partial duplex was incubated with 40 nM RECQ5β and either 1 nM RK3 oligonucleotide or 1 nM RK3/RK4 partial duplex in a volume of 100 μl of buffer HA to generate forked DNA structures depicted in Figures 1A and 2A, respectively. After 10 min, ATP was added to a final concentration of 2 mM. Aliquots (5 μl) were removed at different reaction time points (both before and after the addition of ATP) and analyzed. In the control experiment, ATP was substituted with ATPγS (2 mM). The 3′-flap duplex for strand-exchange assays with BLM (10 nM) and WRN (5 nM) was pre-formed by the spontaneous annealing of the constituent oligonucleotides RK1, RK2 and RK3, with the RK2 oligonucleotide being present in a 5-fold molar excess over the others. Helicase reactions were carried out as described previously (19). Where required, hRPA (20 nM) was added to DNA 1 min before the addition of RecQ proteins and ATP. All reactions were terminated by adding 0.5 reaction volumes of solution S (150 mM EDTA, 2% SDS, 30% glycerol and 0.1% bromophenol blue) and

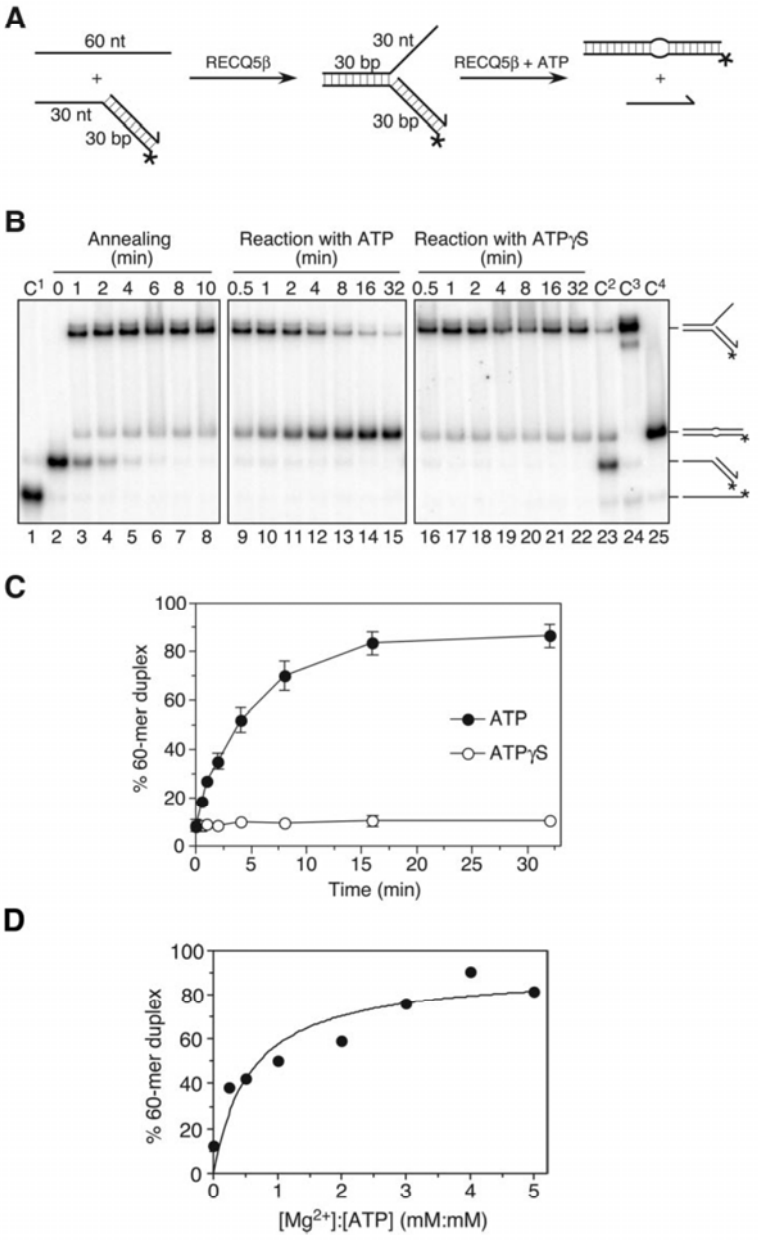


**Figure 1.** Strand-exchange by RECQ5β on synthetic forked DNA structure with homologous arms lacking the leading strand. (**A**) Scheme of the assay. The lengths of individual arms are indicated in nucleotides (nt) or base pairs (bp). The 3′ end of the lagging oligonucleotide is indicated by an arrow and the position of the 5′-$^{32}$P label is marked by an asterisk. The homologous leading and lagging arms have a 5 nt heterology at the fork junction to prevent spontaneous strand exchange. (**B**) 1 nM $^{32}$P-labeled 30mer/60mer duplex (RK1/RK2) was incubated with 1 nM 60mer complementary oligonucleotide (RK3) in the presence of 40 nM RECQ5β to form the forked DNA structure. After 10 min, either ATP or ATPγS were added to a final concentration of 2 mM. Aliquots from different reaction time points, before and after addition of the nucleotide, were analyzed by non-denaturing PAGE followed by phosphorimaging. $C^1$–$C^4$, markers for the DNA substrate and the reaction products. (**C**) Quantification of the ATP and ATPγS containing reactions. Relative concentration of the 60mer duplex product is plotted versus reaction time. The data points represent the average values from three independent experiments. (**D**) Dependence of the strand-exchange activity of RECQ5β on $Mg^{2+}$ ion concentration. Reaction mixtures contained 1 nM 3′-flap DNA substrate, 40 nM RECQ5β and 2 mM ATP with increasing concentrations of $Mg(OAc)_2$. Relative concentration of the 60mer duplex product after 32 min was measured as in (B) and (C). The lines drawn are only to guide the eye.

5220 Nucleic Acids Research, 2006, Vol. 34, No. 18

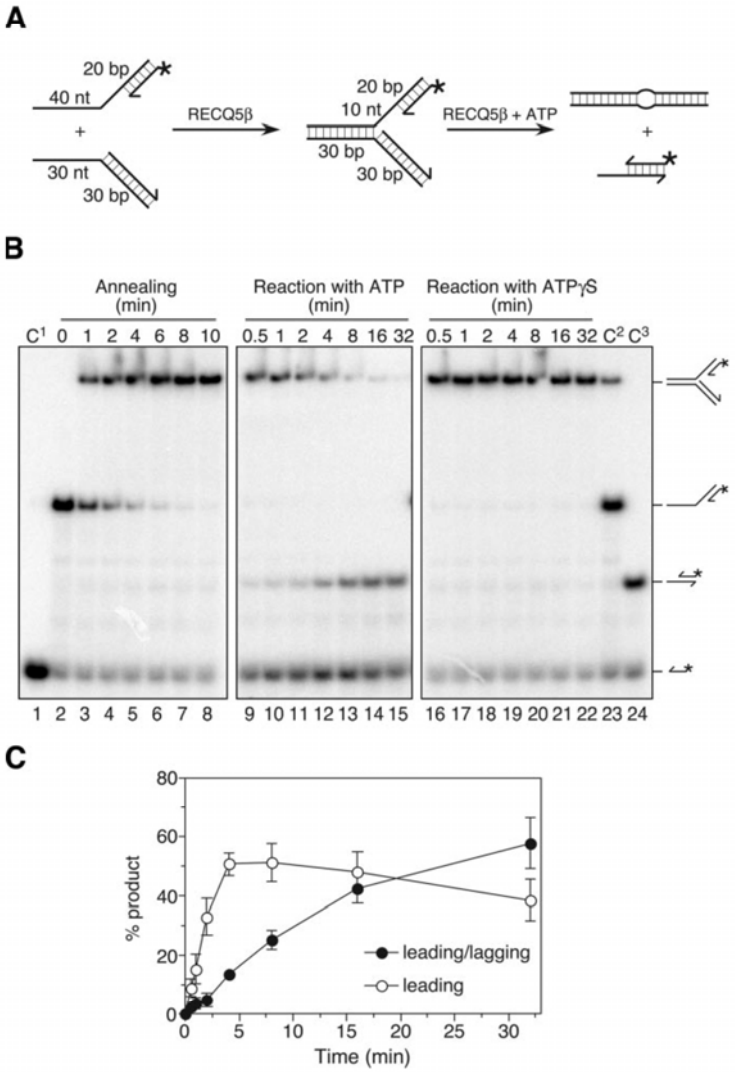


**Figure 2.** Strand-exchange by RECQ5β on synthetic forked DNA duplex with a leading-strand gap. (**A**) Scheme of the assay. The oligonucleotides used are the same as in Figure 1, except for an additional 20mer representing the leading strand. (**B**) 1 nM $^{32}$P-labeled 20mer/60mer duplex (RK1/RK2) was incubated with 1 nM 30mer/60mer duplex (RK3/RK4) in the presence of 40 nM RECQ5β to form the forked DNA structure. After 10 min, either ATP or ATPγS were added to a final concentration of 2 mM. Aliquots of the annealing and the nucleotide-driven reactions were analyzed by non-denaturing PAGE. $C^1$–$C^3$, markers for the DNA substrate and the reaction products. (**C**) Quantification of the ATP- driven reaction. The relative concentrations of the unwound 20mer oligonucleotide (leading strand; open circles) and subsequently formed 20mer/30mer partial duplex (leading/lagging duplex; closed circles) are plotted versus reaction time. The data points represent the average values from three independent experiments.

subsequently treated with proteinase K (0.1 mg/ml) at 37°C for 10 min. The reaction mixtures were resolved by electrophoresis in a 10% (w/v) non-denaturing polyacrylamide gel (PAGE; acrylamide/bis-acrylamide 19:1). Radiolabeled DNA species were visualized by autoradiography and quantified using a Molecular Dynamics Typhoon 9400 scanner with associated IMAGEQUANT software. The relative concentration of radiolabeled products was expressed as percentage of total DNA.

### Strand annealing assays

Strand annealing activity of RECQ5β and its deletion variants was measured using complementary 50mer oligonucleotides as described previously (19).

### Cell culture

All the cell lines used in this study were maintained in DMEM (OmniLab) supplemented with 10% fetal calf

serum (Life Technologies) and streptomycin/penicillin (100 U/ml). To prepare synchronized population of cells, cultures at ~60% confluency were treated with 2 mM hydroxyurea (HU) for 16 h. UV treatments (at a dose of 20 J/m$^2$) were carried out in a UV-Stratalinker 1800 equipped with a 254 nm UV lamp (Stratagene). Where required, *cis*-diamminedichloro-platinum (CDDP) was added to a final concentration of 20 μM. For cell cycle analyses, ethanol-fixed cells were stained with propidium iodide (20 μg/ml; Molecular Probes) and subjected to flow cytometry in a Becton Dickinson cell sorter.

### Immunofluorescence assays

Cells grown on cover slips were fixed in methanol for 30 min at −20°C, which was followed by incubation in acetone for 30 s. After blocking in PBS supplemented with 3% low-fat milk (blocking solution), cover slips were incubated overnight at 4°C with primary antibodies [rabbit polyclonal anti-RECQ5β (this study; 1:800) and mouse monoclonal anti-PCNA (PC-10, Santa Cruz; 1:200); all antibodies were diluted in blocking solution]. After washing with PBS, the cells were incubated with FITC-conjugated sheep anti-rabbit (Sigma; 1:700) and Texas Red-conjugated donkey anti-mouse (Abcam; 1:200) secondary antibodies for 1 h at 37°C. The nuclei were then counterstained with DAPI (0.1 μg/ml; Sigma) for 10 min, washed with water and mounted in SlowFade Antifade reagent (Molecular Probes). Images were captured by Olympus IX81 fluorescence microscope. At least 150 nuclei were analyzed in each experiment.

### Immunoprecipitation assays

Cells were subjected to trypsinization, harvested by centrifugation and resuspended in lysis buffer [50 mM Tris–HCl, pH 8.0, 120 mM NaCl and 0.5% (v/v) NP-40] supplemented with protease inhibitor cocktail (Complete, Mini; Roche). After a 30 min incubation on ice, the lysate was treated with 10 U of RNase-free DNase I (Roche) at 25°C for 30 min, and clarified by centrifugation. The protein extracts (1 mg) were incubated overnight at 4°C with purified rabbit anti-RECQ5β IgGs (1 μg) or with IgGs purified from pre-immune serum (1 μg). Immune complexes were subsequently incubated with protein A/G–agarose beads (20 μl, Amersham Biosciences) for 1 h at 4°C. Immunoprecipitates were analyzed by western blotting.

### GST/CBD pull-down assays

GST- and CBD-tagged fragments of RECQ5β were produced in *E.coli* BL21-CodonPlus(DE3)-RIL cells (Stratagene) and bound to Glutathione–Sepharose beads (20 μl; Amersham Biosciences) and chitin beads (20 μl; NEB), respectively, in NET-T150 buffer [10 mM Tris (pH 8.0), 1 mM EDTA, 150 mM NaCl and 0.1% (v/v) Triton X-100]. The beads were incubated with recombinant PCNA (0.5–2 μg) in 400 μl of NET-T150 buffer supplemented with ethidium bromide (50 μg/ml) for 2 h at 4°C. Bound proteins were analyzed by western blotting.

## RESULTS

### RECQ5β promotes strand exchange on synthetic DNA structures mimicking a stalled replication fork

To investigate whether the RECQ5β helicase is capable of promoting replication fork regression, we examined its activity on oligonucleotide-based forked structures with homologous arms, which had a 5 nt region of heterology adjacent to the three-way junction to prevent spontaneous branch migration. First, we prepared a partial forked duplex lacking the leading strand (3′-flap duplex) by RECQ5β-mediated annealing of a 60mer oligonucleotide representing the leading-strand template to a 3′-tailed duplex composed of a 30mer oligonucleotide and a $^{32}$P-labeled 60mer oligonucleotide representing the lagging strand and the corresponding template strand, respectively (Figure 1A). This resulted in a rapid formation of the forked structure as detected by electrophoresis in non-denaturing polyacrylamide gel followed by phosphorimaging (Figure 1B, lanes 2–8). A small amount of the 60mer duplex was also detected, which had presumably arisen from spontaneous branch migration. Remarkably, upon the addition of ATP to this mixture, a robust strand-exchange activity was observed, resulting in the formation of the $^{32}$P-labeled 60mer duplex (Figure 1B and C, lanes 9–15). Note that this duplex contains a small bubble due to the short region of heterology at the junction (Figure 1A). When ATP was substituted with its poorly hydrolysable analogue ATPγS, no strand exchange was observed over the period of 32 min, confirming that the RECQ5β-mediated strand exchange is dependent on the helicase activity of the enzyme (Figure 1B and C, lanes 16–22).

Certain RecQ DNA helicases such as human RECQ1 (26) have been shown to be sensitive to free magnesium cations. Hence, we sought to determine the optimal $Mg^{2+}$:ATP ratio for RECQ5β-mediated strand exchange reaction. To do so, we varied $Mg^{2+}$ concentration in the range from 0 to 10 mM keeping ATP at a fixed concentration of 2 mM. We found that the extent of RECQ5β-mediated strand exchange on the 3′-flap substrate increased with increasing $Mg^{2+}$ concentration in a hyperbolic fashion, reaching maximal values at $Mg^{2+}$:ATP ratios between 3 and 5 (Figure 1D). These data indicated that RECQ5β requires a molar excess of $Mg^{2+}$ over ATP for efficient strand exchange activity. Therefore, all further experiments were performed using 2 mM ATP and 10 mM $Mg(OAc)_2$.

Next we investigated whether RECQ5β can promote strand exchange if the forked structure contains both the lagging and the leading strands. To mimic the structure of a replication fork blocked by a lesion on the leading-strand template, the length of the leading strand was chosen to be 10 nt shorter than the length of the lagging strand. The DNA substrate was again assembled using the strand-annealing function of RECQ5β (Figure 2A). Upon the addition of ATP, a rapid accumulation of free $^{32}$P-labeled leading oligonucleotide was observed in the initial stages of the reaction which was followed by its annealing to the lagging oligonucleotide as evidenced by an accumulation of the 20mer/30mer duplex in the later stage of the reaction (Figure 2B and 2C, lanes 9–15). This indicates that RECQ5β has the ability to promote the displacement of both arms of the fork and subsequent annealing of the displaced leading and lagging strands

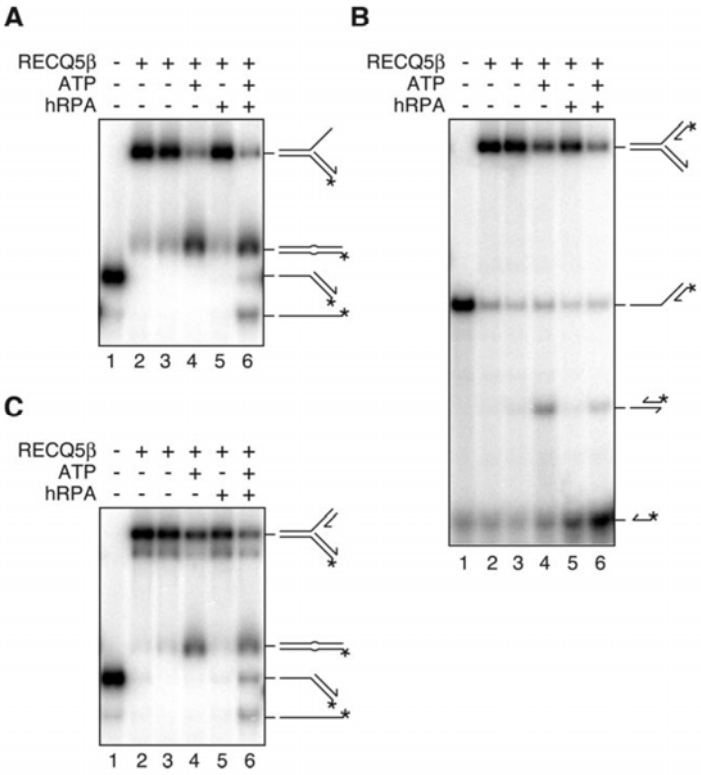


**Figure 3.** Effect of hRPA on RECQ5β-mediated strand exchange on forked DNA duplex lacking the leading strand (**A**) and forked DNA duplex with 10 nt leading-strand gap, radioactively labeled either on the leading-strand oligonucleotide (**B**) or on the lagging-strand template (**C**). The DNA substrates were prepared by RECQ5β mediated annealing as described in Materials and Methods and schematically indicated in Figures 1A and 2A. Reactions were carried out for 32 min as indicated. DNA, RECQ5β and hRPA were present at concentrations of 1, 40 and 20 nM, respectively. hRPA was added 2 min before the addition of ATP (2 mM).

(Figure 2B and C). No strand exchange was seen in the presence of ATPγS, indicating a requirement for the helicase activity of the enzyme (Figure 2B, lanes 16–22).

It is known that RPA covers single-stranded regions at stalled replication forks (27). Therefore, we investigated the effect of hRPA on the strand-exchange activity of RECQ5β using the synthetic forked structures described above. To monitor the annealing of the parental strands on the gapped fork structure, $^{32}$P-label was also placed on the lagging-strand template. These experiments indicated that hRPA did not impair the RECQ5β-mediated annealing of the parental strands (Figure 3A and C). However, it was found to partially inhibit the annealing of the displaced leading and lagging oligonucleotides (Figure 3B). This is consistent with our earlier studies, which indicated that hRPA inhibits RECQ5β-mediated strand annealing (19). A partial shift of the reaction towards unwinding of the parental duplex was also observed, particularly with the gapped substrate (Figure 3C, compare lanes 4 and 6). However, this is not likely to be the consequence of binding of hRPA to the leading arm, since the single-strand gap on the gapped fork structure is too short (10 nt) to accommodate hRPA, assuming that the size of the DNA-binding site for RPA is ~30 nt (28).

Collectively, the findings described above suggested that RECQ5β is capable of promoting fork regression *in vitro*.

### RPA blocks strand exchange by BLM and WRN

We also examined other human RecQ homologues, namely BLM and WRN, for the ability to promote strand exchange on the 3′-flap structure described above (Figure 1A). As WRN showed only negligible strand-annealing activity under the condition of our assay, the DNA substrate was prepared by spontaneous annealing of the constituent oligonucleotides, with the lagging oligonucleotide being present in a 5-fold molar excess over the parental strands. We found that both BLM and WRN could efficiently catalyze the conversion of the 3′-flap structure into the 60mer duplex (Figure 4A and B). However, if hRPA was present in the reaction, the action of both helicases was strongly biased toward unwinding of the parental duplex, as evidenced by the accumulation of the $^{32}$P-labeled 30mer/60mer duplex in the course of the reaction (Figure 4C and D). In contrast, these time course experiments revealed that hRPA significantly stimulated the rate and the extent of RECQ5β-mediated strand exchange on 3′-flap structure (Figure 4).

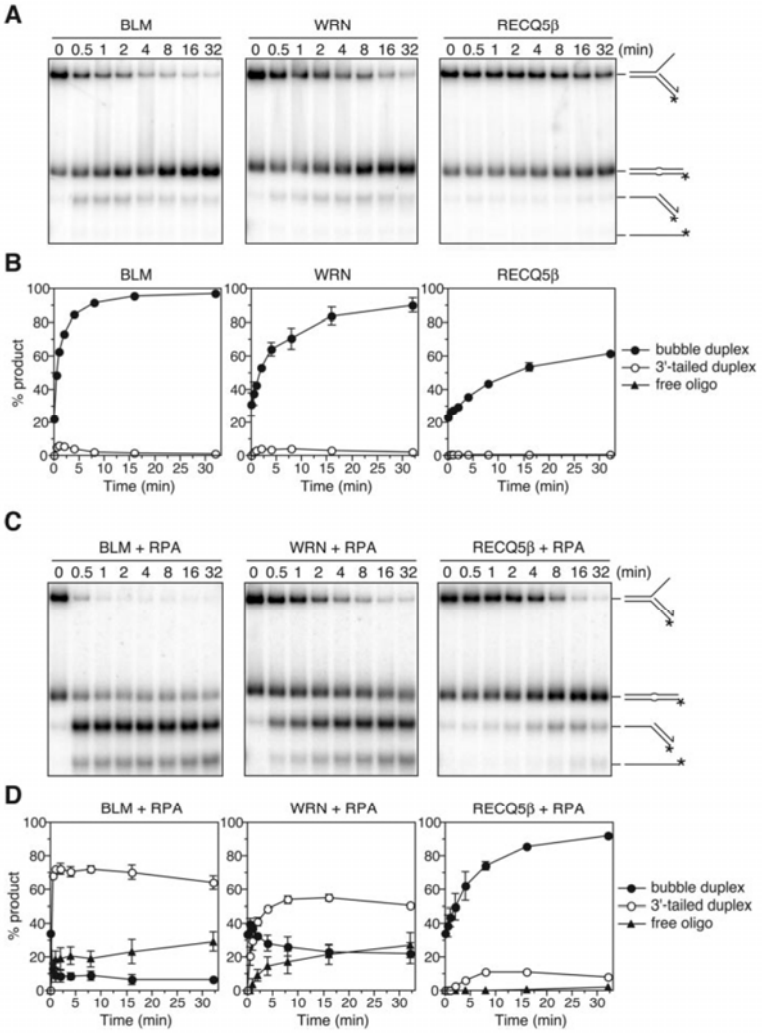


**Figure 4.** Strand exchange by BLM, WRN and RECQ5β in the absence and presence of hRPA. (**A**) Time course of reactions of 10 nM BLM, 5 nM WRN and 40 nM RECQ5β, respectively, with 1 nM forked DNA structure with homologous arms lacking the leading strand. (**B**) Quantification of reactions in (A). (**C**) Time course of reactions of 10 nM BLM, 5 nM WRN and 40 nM RECQ5β, respectively, with 1 nM DNA structure as in (A) in the presence of 20 nM hRPA. The DNA substrate was preincubated for 2 min with hRPA before addition of helicase. (**D**) Quantification of reactions in (C). The DNA substrate was the same as in Figure 1, except that it was prepared by spontaneous annealing of the component oligonucleotides as described in Materials and Methods. Reactions were analyzed as in Figure 1. In the graphs, relative concentrations of the products are plotted versus reaction time. The 60mer bubble duplex, filled circles; 3′-tailed 30mer/60mer duplex, open circles; free 60mer oligonucleotide, filled triangles. In all graphs, the data points represent the average values from three independent experiments.

These data indicate that there are mechanistic differences between RECQ5β and other human RecQ helicases in the mode of processing of forked DNA structures coated with hRPA.

### RECQ5β actively unwinds only the lagging-strand arm of the fork

To gain insights into the mechanism of RECQ5β-mediated strand exchange, we investigated the action of RECQ5β on synthetic forked structures with heterologous arms to monitor only DNA unwinding events. In agreement with data reported for the *Drosophila* RECQ5 homologue (29), we found that on partial forked duplex lacking the leading strand (3′-flap duplex), RECQ5β showed preference for unwinding of the lagging-strand arm (Figure 5A and B). Interestingly, this reaction was significantly enhanced if the DNA substrate was pre-incubated with hRPA (compare Figure 5A and B). This could be the consequence of binding of hRPA to the single-stranded leading arm that would prevent loading of

RECQ5β on this arm to initiate unwinding of the parental duplex. In agreement with this assumption, we found that hRPA inhibited RECQ5β-mediated unwinding of a 3′-tailed duplex if added to the DNA substrate prior to the helicase (data not shown). However, no significant stimulation of RECQ5β-mediated unwinding of the lagging-strand arm was observed with the *E.coli* single-stranded binding protein, indicating that this effect is specific for hRPA (Supplementary Figure S1).

To assess whether the RECQ5β helicase can actively unwind the leading arm of the fork, we examined its activity on partial forked duplex lacking the lagging strand (5′-flap duplex). We found that RECQ5β could catalyze only the unwinding of the parental arm on this structure, as evidenced by the accumulation of 5′-tailed duplex during the course of the reaction (Figure 5C and D). This was, however, seen only in the presence of hRPA, which is consistent with our previous finding that hRPA counteracts the intrinsic strand-annealing activity of RECQ5β (19). In the later stages of the hRPA-containing reaction, accumulation of the free leading oligonucleotide was also observed, which presumably resulted from a secondary unwinding event on the primary 5′-tail product. This observation is intriguing since the RECQ5β helicase was shown to exhibit a 3′–5′ polarity (19). It is possible that hRPA, if bound to the 5′-single stranded tail, can partially destabilize the duplex, which would allow loading of RECQ5β to mediate unwinding.

To further confirm that the RECQ5β helicase cannot actively remove the leading strand from the fork, we examined its action on a 5′-flap structure with homologous arms prepared from the same set of oligonucleotides as used in the previous strand exchange assays. If RECQ5β was capable of unwinding of the leading arm, it would promote strand exchange on this structure to form the 60mer duplex as it did on the homologous 3′-flap structure (Figure 1). However, RECQ5β did not show any strand-exchange activity on the 5′-flap structure, indicating that it cannot actively unwind the leading arm (Supplementary Figure S2).

We also examined the action of the BLM and WRN helicases on the forked DNA structures with heterologous arms described above. In contrast to RECQ5β, BLM and WRN displayed a strong preference for unwinding of the parental arm on all these structures, which was further enhanced by hRPA (Supplementary Figure S3). These findings are in agreement with previously published data (30) and further highlight mechanistic differences between RECQ5β and other human RecQ helicases in processing of forked DNA structures.

### A domain within the non-conserved portion of RECQ5β is important for RECQ5β-mediated processing of forked DNA structures

To identify the functional domains in RECQ5β that are required for its ability to unwind the lagging arm of the fork and to promote strand exchange on forked structures in the presence of hRPA, we purified a series of truncated variants of RECQ5β lacking different parts of the region distal to the conserved helicase domain (Figure 6A). The RECQ5β variants lacking the C-terminal 266 or 340 amino acids ($RECQ5^{1–725}$ and $RECQ5^{1–651}$) were found to be proficient in promoting strand exchange on hRPA-coated forked structure lacking the leading strand albeit with a reduced efficiency compared to the wild-type enzyme (Figure 6B). Moreover, these variants retained the capacity to preferentially unwind the lagging-strand duplex on the forked structure with heterologous arms, being even more efficient than the wild-type enzyme (Figure 6D). This correlates with the fact that these mutants were severely impaired in promoting strand annealing (Figure 6C). In contrast, the $RECQ5^{1–475}$ and $RECQ5^{1–561}$ mutants were defective in promoting strand exchange and unwinding of the lagging arm (Figure 6B and D). However, these mutants could catalyze unwinding of the parental arm on the partial forked duplex lacking the leading strand, indicating that they retained the capacity to initiate duplex unwinding from a single-stranded tail (Figure 6D).

Collectively, these data indicate that the region of RECQ5β spanning the amino acids 561–651 is important for the processing of forked structures by this helicase.

### RECQ5β is localized in DNA replication factories and persists at sites of stalled replication forks

To explore whether RECQ5β acts at DNA replications forks *in vivo*, we investigated its subcellular localization by immunofluorescence microscopy relative to PCNA that is widely used as a marker for DNA replication foci. It is known that PCNA foci undergo reproducible changes throughout S phase, with a fine punctuate pattern in early S, perinuclear and perinucleolar patterns in mid S and a characteristic late-S pattern with a few, but large foci (31). To monitor the RECQ5β localization pattern during S phase, we synchronized HeLa cells at the $G_1$/S transition by HU treatment and fixed them with methanol at different time points after release from the arrest. In addition to immunostaining, the cells were subjected to flow cytometry to determine the cell cycle distribution at individual time points. We observed that in HU-arrested cells, both PCNA and RECQ5β displayed exclusively nuclear staining, forming a large number of foci that partially co-localized (Figure 7). Three hours after the removal of HU (early S phase), >80% of PCNA foci in a single nucleus co-localized with RECQ5β foci in the majority of cells (Figure 7). Six hours after release (mid-S phase), the PCNA foci exhibited the characteristic peripheral pattern, while the RECQ5β foci were dispersed throughout the nucleus (Figure 7). Nine hours after release (late S phase), both PCNA and RECQ5β formed a few large foci that almost completely co-localized (Figure 7). We also examined the spatial distribution of RECQ5β and PCNA during S phase of U2OS osteosarcoma cells and obtained essentially the same results as in HeLa cells (Supplementary Figure S4). Moreover, in synchronized U2OS cells, the RECQ5β foci co-localized with sites of BrdU incorporation, a marker of ongoing DNA synthesis (Supplementary Figure S4). Using U2OS cells, we also found that the RECQ5β foci in late S phase co-localized with promyelocytic leukemia protein (PML), indicating that RECQ5β associates with PML nuclear bodies in this stage of the cell cycle (Supplementary Figure S5).

Next we investigated the effect of exogenously induced replication-blocking lesions on the cellular localization pattern of RECQ5β in non-synchronized HeLa cells. To induce

5226 Nucleic Acids Research, 2006, Vol. 34, No. 18

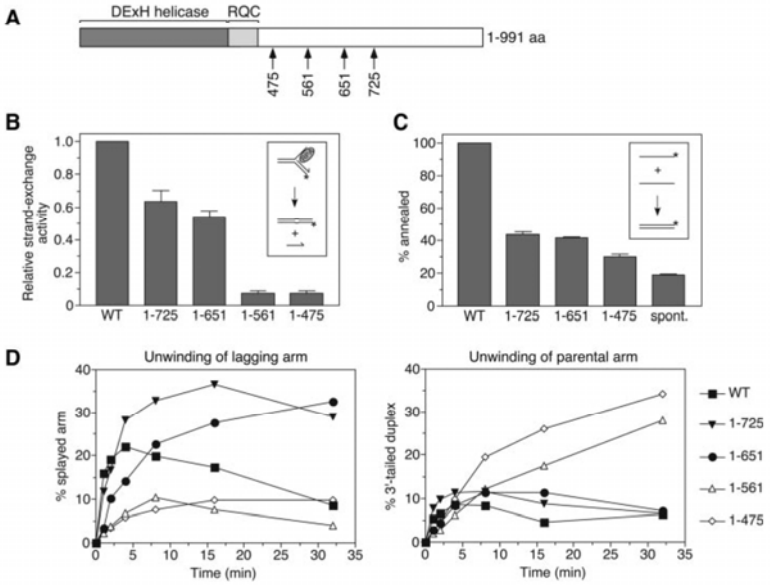


**Figure 6.** Characterization of RECQ5β mutants. (**A**) A schematic representation of the human RECQ5β protein demonstrating the location of the DExH helicase (dark gray) and RecQ C-terminal (RQC) (light gray) regions conserved among RecQ helicases. The arrowheads indicate the positions of the C-terminal ends of the truncated RECQ5β polypeptides used in this study. The numbers refer to the amino acid sequence of RECQ5β. (**B**) Comparison of strand-exchange activities of RECQ5β and its deletion variants (40 nM each) on forked DNA structure lacking the leading strand (1 nM) pre-coated with hRPA (20 nM). The reactions were incubated for 32 min and analyzed as described in Materials and Methods. Relative concentration of the 60mer duplex product was calculated for each reaction, and the values obtained were corrected by subtracting the background value (reaction without protein). Strand exchange activity of the mutants is expressed as a fraction of the wild-type activity. The inset shows the scheme of the reaction. (**C**) Annealing of 50mer complementary oligonucleotides, each at a concentration of 1 nM, in the presence of 20 nM wild-type and mutant RECQ5β proteins as indicated. Reactions were incubated for 32 min and the relative concentration of the strand-annealing product was determined as described in Materials and Methods. Values determined for spontaneous (spont.) reaction are also plotted. The inset shows the scheme of the reaction. (**D**) Kinetics of unwinding of 1 nM forked structure lacking the leading strand by 100 nM RECQ5β and its deletion variants as indicated. Reactions were carried out and analyzed as described in Materials and Methods. The graph on the left shows relative concentrations of splayed arm product resulting from unwinding of the lagging arm. The graph on the right shows relative concentration of the 3′-tailed duplex generated by unwinding of the parental arm. All data points represent the average values from three independent experiments.

the formation of bulky DNA adducts, cells were exposed to UVC irradiation or treated with CDDP. In asynchronous populations of cycling HeLa cells (~70% of cells in $G_1$ as judged from the FACS profile), PCNA showed mostly a diffuse nuclear staining, whereas RECQ5β displayed rather a punctuate distribution in the nucleus as well as a weak cytoplasmic staining (Figure 8). In a small percentage of cells (~15%), PCNA was concentrated in small nuclear foci, indicating that these cells were in S phase (data not shown). Most importantly, these PCNA foci largely co-localized with RECQ5β foci, which excludes the possibility that the pattern observed 3 h after HU removal was a consequence of DNA damage caused by HU treatment (data not shown; Figure 7).

After exposure of cells to UV irradiation at a dosage of 20 J/m$^2$, there was a dramatic increase in the percentage of cells in which PCNA foci co-localized with RECQ5β foci (Figure 8). Four hours after UV irradiation, ~80% of PCNA foci in a single nucleus co-localized with RECQ5β foci in 55% of cells. These foci appeared somewhat brighter than those observed in early S phase cells (compare Figure 7 and Figure 8) and persisted up to 6 h after irradiation (data not shown).

In HeLa cells treated with CDDP (20 μM), which predominantly causes intra-strand DNA cross-links mimicking pyrimidine–dimer adducts induced by UV light, RECQ5β and PCNA displayed essentially the same spatial distribution as in UV-irradiated cells, with the maximal co-localization being apparent 6 h after addition of the drug (Figure 8). Moreover, we examined spatial distribution of RECQ5β in SV40-immortalized human fibroblasts GM00637 and XP20SSV (XPA-deficient) before and after UV irradiation. We observed essentially the same patterns as in HeLa cells, excluding a cell-line specific effect (Supplementary Figure S6). In addition, the experiment with XPA-deficient cells ruled out the possibility that RECQ5β is present in the complexes that mediate repair synthesis following excision of DNA adducts by the nucleotide-excision repair pathway.

Taken together, these data suggest that RECQ5β is associated with the DNA replication machinery, particularly in early and late S phase and it is present in replication-repair factories at the sites of stalled replication forks.

### RECQ5β directly interacts with PCNA

In addition to serving as a sliding clamp required for processive DNA synthesis, PCNA provides attachment sites for various other proteins that function in DNA replication, DNA repair, cell cycle progression and chromatin assembly

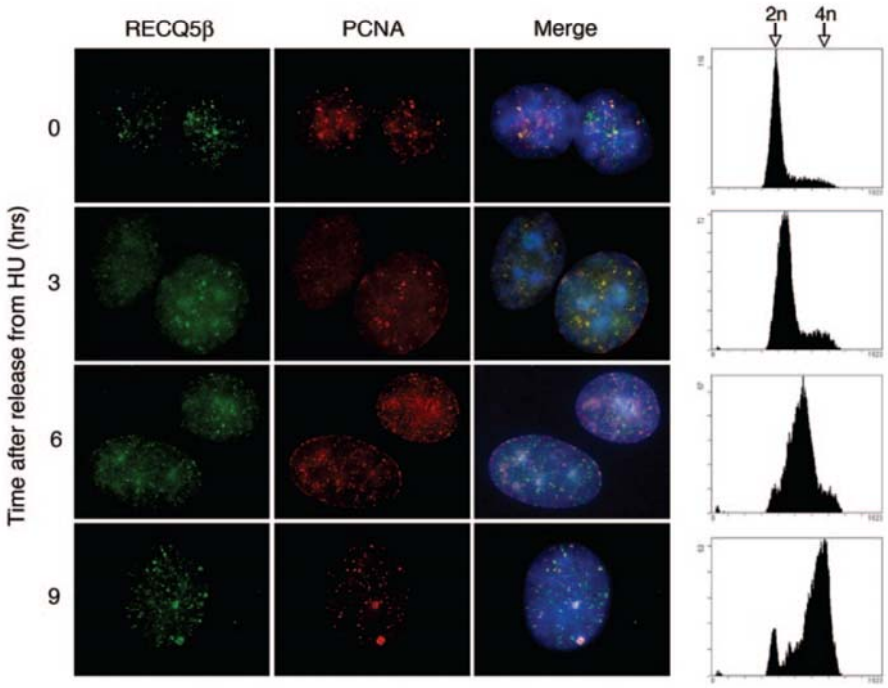


**Figure 7.** Co-localization of RECQ5β and PCNA in S phase nuclei of HeLa cells. Cells were synchronized at $G_1$/S transition by treatment with hydroxyurea (HU) for 16 h and then released to S phase by adding fresh medium without HU. At indicated time points, cells were fixed with methanol, triply stained for RECQ5β (green), PCNA (red) and DNA (blue) as described in Materials and Methods, and analyzed by fluorescence microscopy. Representative images are shown. Yellow colour in the superimposed images (Merge) indicates co-localization of RECQ5β and PCNA staining. In parallel, cells were subjected to FACS analysis. The resultant cell cycle profiles for each time point are shown on the right. Arrowheads indicate cell population in $G_1$ phase with a 2n DNA content and $G_2$/M with 4n DNA content; S phase cells have DNA content between 2n and 4n.

(32). To further explore the association of RECQ5β with the DNA replication machinery, we examined whether it interacts with PCNA, as suggested by the presence of a putative PCNA-binding motif at the C-terminus of RECQ5β (Figure 9A). First, we performed affinity pull-down assays with recombinant proteins produced in *E.coli*. We found that PCNA was bound to chitin beads coated with RECQ5β-CBD protein, but not to beads coated with McrA-CBD protein, indicating that the interaction was specific (Figure 9B). Moreover, using GST-tagged RECQ5β deletion variants, we found that the region spanning the last 200 amino acids of RECQ5β is essential for its interaction with PCNA, suggesting that this interaction is mediated through the putative PCNA-binding motif located in this region (Figure 9C).

We also examined the effect of PCNA on the strand exchange activity of RECQ5β using the synthetic forked DNA structure containing a 10 nt gap on the leading arm (Figure 2A). We found that PCNA did not affect the rate or the extent of RECQ5β-mediated strand exchange (Supplementary Figure S7).

To see whether RECQ5β interacts with PCNA *in vivo*, we conducted immunoprecipitation experiments with total extracts of human 293T embryonic kidney cells. Extracts were prepared not only from non-treated cells, but also from cells synchronized in early S phase and cells subjected to UV irradiation or CDDP treatment, since under these conditions, RECQ5β was found to localize to PCNA foci. We found that PCNA was precipitated with the anti-RECQ5β antibody, but not with control IgGs purified from pre-immune serum, indicating that RECQ5β and PCNA indeed form a complex *in vivo* (Figure 9D). Moreover, a significant larger amount of PCNA (~2 times) was detected in the immunoprecipitates of treated cells compared with non-treated cells, suggesting that the observed recruitment of RECQ5β to replication foci may occur via a direct interaction with PCNA (Figure 9D, compare lane 3 to lanes 4–6).

## DISCUSSION

There is growing evidence suggesting that RecQ DNA helicases operate in various DNA repair processes induced by DNA replication defects. However, the DNA transactions mediated by these proteins at damaged replication forks still remain elusive. Here we show that the human RECQ5β helicase possesses the ability to promote strand exchange on synthetic forked DNA structures that mimic a stalled replication fork. Moreover, we provide evidence suggesting that the RECQ5β protein is localized in the DNA replication factories

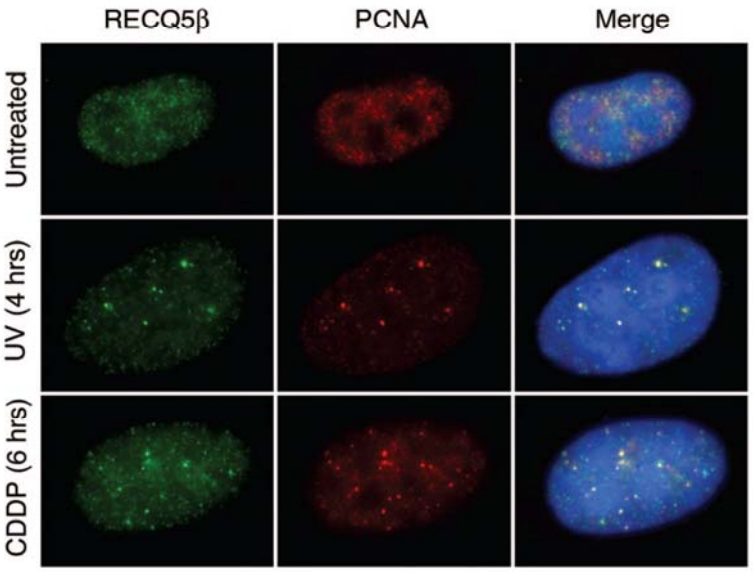


**Figure 8.** Co-localization of RECQ5β and PCNA in HeLa cells following UV irradiation and CDDP treatment. Non-synchronized cells were UV-irradiated at 20 J/m$^2$ and cultured for additional 4 h or treated with 20 μM CDDP for 6 h. After methanol fixation, cells were triply stained for RECQ5β (green), PCNA (red) and DNA (blue), and analyzed by fluorescence microscopy. Representative images are shown.

in S phase nuclei and persists at the sites of stalled replication forks. Based on these findings, we speculate that the RECQ5β helicase could mediate regression of stalled replication forks *in vivo* to facilitate DNA damage bypass by template-switching (Supplementary Figure S8). As mentioned above, such a DNA damage tolerance mechanism has been postulated to exist in both prokaryotic and eukaryotic organisms, but remains to be substantiated experimentally. In the budding yeast *Saccharomyces cerevisiae*, fork regression associated with template-switching is thought to be the underlying mechanism of the *RAD5*-subpathway of *RAD6*-dependent postreplicative repair, which is highly conserved from yeast to humans (33). As this DNA damage tolerance process, which involves non-destructive polyubiquitination of PCNA, is largely independent of the HR machinery, other means, such as helicase-promoted DNA unwinding, would be required to accomplish the strand-exchange events required for fork regression (33,34). At present, however, it is not clear whether Sgs1 helicase, the sole RecQ homologue in *S.cerevisiae*, is involved in the RAD6-dependent DNA damage tolerance, since the assessment of this possibility by epistatic analysis is complicated due to the involvement of Sgs1 in the HR pathway of postreplicative repair (6). Nevertheless, some evidence for such a function has been provided in the fission yeast *Saccharomyces pombe* by the observation that the formation of Rqh1 (Sgs1 homologue) foci upon UV irradiation is dependent on the presence of Rdh18/Rad18, a component of the Rad6 pathway (35).

Our hypothesis that RECQ5β operates in the repair of damaged replication forks is consistent with the finding that inactivation of the mouse RECQ5β homologue is associated with a significant increase in the frequency of SCEs (17), as these may represent cross-over outcomes of the HR-mediated repair of broken replication forks that arise as a consequence of the blockage of leading-strand extension by bulky lesions (Supplementary Figure S8). Similarly, elevated SCE levels have been observed in DT40 chicken cells lacking the trans-lesion polymerases Polζ and Polκ, or the Rad18 ubiquitin ligase (36). However, one cannot exclude the possibility that the increased level of mitotic recombination associated with RECQ5β deficiency results from a defect in another DNA repair mechanisms. For example, RECQ5β could operate in the synthesis-dependent strand-annealing pathway of DNA double-strand break repair by disrupting D-loops and promoting annealing of extended arms of the broken chromosome. Alternatively, RECQ5β could suppress unscheduled recombination during DNA replication by directly displacing inappropriately formed RAD51 filaments in the same manner as the Srs2 and UvrD helicases (37,38).

The biochemical and structural studies have revealed that the *E.coli* RecG helicase mediates fork regression by active unwinding of both the leading and lagging arms of the fork using a wedge domain that is simultaneously pushed into the lagging and the leading duplexes promoting strand displacement (39,40). In contrast to RecG, the RECQ5β helicase was found to unwind only the lagging-strand duplex, which raises the question of how it can promote fork regression beyond the leading-strand gap. We propose a mechanism in which RECQ5β binds to the fork junction and subsequently translocates along the lagging-strand template in the 3′–5′ direction to unwind the lagging-strand duplex. As a result, the parental strands will be free to re-anneal. Interestingly, we identified a region of 90 amino acids, located within the non-conserved portion of RECQ5β, as being required for its ability to unwind the lagging arm of the fork, but not for RECQ5β-mediated unwinding of 3′-tailed DNA duplexes.

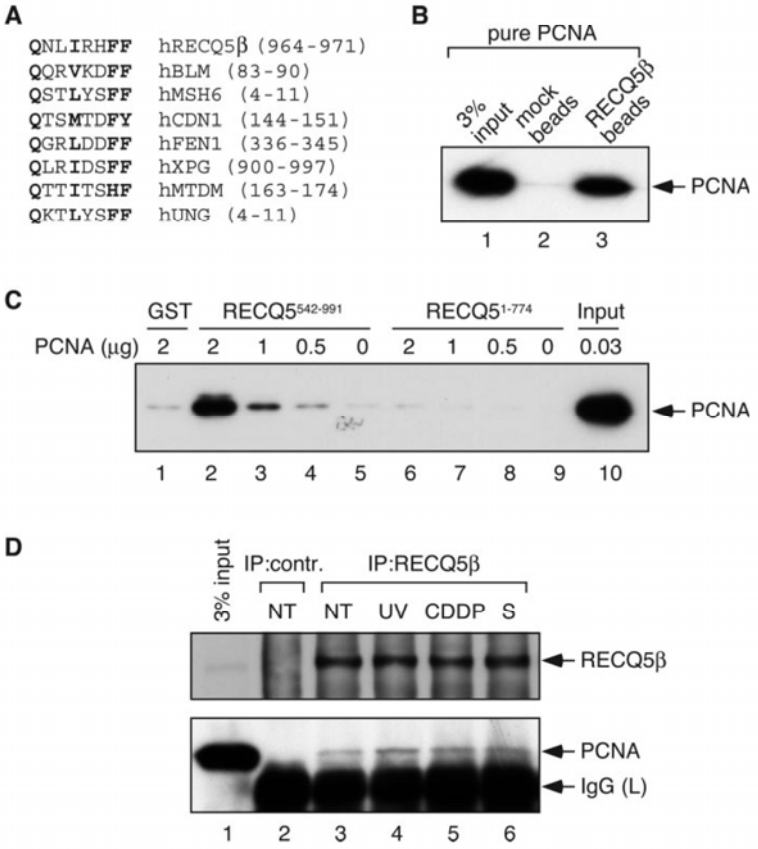


**Figure 9.** Interaction between RECQ5β and PCNA. (**A**) The putative PCNA-binding motif of human RECQ5β. The C-terminal amino acids 964–971 of RECQ5β are aligned with the PCNA-binding motifs identified in various PCNA-interacting proteins. The highly conserved residues are shown in boldface. (**B**) Direct interaction between RECQ5β and PCNA. Chitin beads coated with recombinant RECQ5β protein containing an intein-CBD tag were incubated with recombinant PCNA (1 μg) as described in Materials and Methods. In the control experiment, beads coated with the *E.coli* McrA endonuclease (mock beads) were used. Bound proteins were analyzed by SDS–PAGE and western blotting. Blots were probed with monoclonal anti-PCNA antibody (PC-10, Santa Cruz). (**C**) Mapping PCNA-interaction domain in RECQ5β. Glutathione beads coated with the GST-tagged RECQ5β deletion variants $RECQ5^{542-991}$ and $RECQ5^{1-774}$, respectively, were incubated with increasing amounts of purified PCNA as indicated. Bound proteins were analyzed as in (B). (**D**) Co-immunoprecipitation of PCNA with RECQ5β from extracts of 293T cells: non-treated (NT) cells (lane 3), UV-irradiated (40 J/m$^2$) cells incubated for 6 h (lane 4), cells treated with CDDP (20 μM) for 8 h (lane 5), cells arrested at $G_1$/S by HU (2 mM, 16 h) and subsequently released to S phase for 3 h (lane 6). Extracts were immunoprecipitated using affinity-purified rabbit polyclonal anti-RECQ5β antibody as described in Materials and Methods. IgGs purified from corresponding pre-immune serum served as a control (lane 2). The immunoprecipitates were analyzed as in (A). The blots were probed with anti-PCNA and anti-RECQ5β antibodies.

It is therefore plausible to propose that this domain may govern the loading of the RECQ5β helicase on the fork junction, placing the helicase motor on the parental duplex in such an orientation as to allow translocation towards the lagging arm. Furthermore, we propose that when the moving junction encounters the leading strand, spontaneous strand exchange will take place, resulting in the displacement of the leading strand and its annealing to the displaced lagging strand to form a four-way junction. This reaction will be favoured due to the concomitant unwinding of the lagging arm by RECQ5β. It is also possible that the annealing events occurring during the fork regression process are promoted by the C-terminal strand-annealing domain of RECQ5β, since we found that the deletion variants $RECQ5^{1-725}$ and $RECQ5^{1-651}$ were dramatically compromised for the strand-annealing activity and showed reduced strand-exchange activity relative to the wild-type protein.

A previous study demonstrated that BLM and WRN have the capacity to promote strand exchange on oligonucleotide-based substrates through combining their strand-pairing and helicase activities (41). More recently, the BLM helicase has been found to promote fork regression on plasmid-sized substrates, generating a four-way structure (42). Interestingly, we found that hRPA, which covers single-stranded regions at stalled forks (27), strongly modulated the action of the BLM and WRN helicases at the fork to favour unwinding of the parental duplex, which is consistent with the previous reports demonstrating that hRPA increases the processivity of the

BLM and WRN helicases through direct protein–protein interactions (43,44). However, these experiments using short DNA substrates cannot account for the possibility that fork regression is mediated by another helicase molecule loaded on the liberated lagging-strand template, an model proposed for the *E.coli* RecQ helicase (45). To assess which human RecQ helicase is more likely to promote fork regression *in vivo*, the effect of hRPA on fork regression by BLM, WRN and RECQ5β is currently being investigated using a plasmid-sized forked DNA structure containing an extensive leading-strand gap.

## SUPPLEMENTARY DATA

Supplementary Data are available at NAR Online.

## ACKNOWLEDGEMENTS

We thank Nina Mojas for help in fluorescence microscopy, Christiane Koenig for technical assistance and Josef Jiricny, Massimo Lopes and Ludovic Gillet for comments on the manuscript. This work was funded by the Swiss National Science Foundation and the Sassella Stiftung. Funding to pay the Open Access publication charges for this article was provided by the Swiss National Science Foundation.

*Conflict of interest statement.* None declared.

## REFERENCES

1. Cox,M.M. (2001) Recombinational DNA repair of damaged replication forks in *Escherichia coli*: questions. *Annu. Rev. Genet.*, **35**, 53–82.
2. Cordeiro-Stone,M., Makhov,A.M., Zaritskaya,L.S. and Griffith,J.D. (1999) Analysis of DNA replication forks encountering a pyrimidine dimer in the template to the leading strand. *J. Mol. Biol.*, **289**, 1207–1218.
3. Lopes,M., Foiani,M. and Sogo,J.M. (2006) Multiple mechanisms control chromosome integrity after replication fork uncoupling and restart at irreparable UV lesions. *Mol. Cell*, **21**, 15–27.
4. Hickson,I.D. (2003) RecQ helicases: caretakers of the genome. *Nat. Rev. Cancer*, **3**, 169–178.
5. Lambert,S., Watson,A., Sheedy,D.M., Martin,B. and Carr,A.M. (2005) Gross chromosomal rearrangements and elevated recombination at an inducible site-specific replication fork barrier. *Cell*, **121**, 689–702.
6. Barbour,L. and Xiao,W. (2003) Regulation of alternative replication bypass pathways at stalled replication forks and its effects on genome stability: a yeast model. *Mutat. Res.*, **532**, 137–155.
7. Heller,R.C. and Marians,K.J. (2006) Replication fork reactivation downstream of a blocked nascent leading strand. *Nature*, **439**, 557–562.
8. Higgins,N.P., Kato,K. and Strauss,B. (1976) A model for replication repair in mammalian cells. *J. Mol. Biol.*, **101**, 417–425.
9. Seigneur,M., Bidnenko,V., Ehrlich,S.D. and Michel,B. (1998) RuvAB acts at arrested replication forks. *Cell*, **95**, 419–430.
10. Zou,H. and Rothstein,R. (1997) Holliday junctions accumulate in replication mutants via a RecA homolog-independent mechanism. *Cell*, **90**, 87–96.
11. Sogo,J.M., Lopes,M. and Foiani,M. (2002) Fork reversal and ssDNA accumulation at stalled replication forks owing to checkpoint defects. *Science*, **297**, 599–602.
12. Bachrati,C.Z. and Hickson,I.D. (2003) RecQ helicases: suppressors of tumorigenesis and premature aging. *Biochem. J.*, **374**, 577–606.
13. Wu,L. and Hickson,I.D. (2003) The Bloom's syndrome helicase suppresses crossing over during homologous recombination. *Nature*, **426**, 870–874.
14. Crabbe,L., Verdun,R.E., Haggblom,C.I. and Karlseder,J. (2004) Defective telomere lagging strand synthesis in cells lacking WRN helicase activity. *Science*, **306**, 1951–1953.
15. Opresko,P.L., Otterlei,M., Graakjaer,J., Bruheim,P., Dawut,L., Kolvraa,S., May,A., Seidman,M.M. and Bohr,V.A. (2004) The Werner syndrome helicase and exonuclease cooperate to resolve telomeric D loops in a manner regulated by TRF1 and TRF2. *Mol. Cell*, **14**, 763–774.
16. Sangrithi,M.N., Bernal,J.A., Madine,M., Philpott,A., Lee,J., Dunphy,W.G. and Venkitaraman,A.R. (2005) Initiation of DNA replication requires the RECQL4 protein mutated in Rothmund-Thomson syndrome. *Cell*, **121**, 887–898.
17. Hu,Y., Lu,X., Barnes,E., Yan,M., Lou,H. and Luo,G. (2005) Recql5 and Blm RecQ DNA helicases have nonredundant roles in suppressing crossovers. *Mol. Cell. Biol.*, **25**, 3431–3442.
18. Shimamoto,A., Nishikawa,K., Kitao,S. and Furuichi,Y. (2000) Human RecQ5β, a large isomer of RecQ5 DNA helicase, localizes in the nucleoplasm and interacts with topoisomerases 3α and 3β. *Nucleic Acids Res.*, **28**, 1647–1655.
19. Garcia,P.L., Liu,Y., Jiricny,J., West,S.C. and Janscak,P. (2004) Human RECQ5β, a protein with DNA helicase and strand-annealing activities in a single polypeptide. *EMBO J.*, **23**, 2882–2891.
20. Gaymes,T.J., North,P.S., Brady,N., Hickson,I.D., Mufti,G.J. and Rassool,F.V. (2002) Increased error-prone non homologous DNA end-joining—a proposed mechanism of chromosomal instability in Bloom's syndrome. *Oncogene*, **21**, 2525–2533.
21. Karow,J.K., Chakraverty,R.K. and Hickson,I.D. (1997) The Bloom's syndrome gene product is a 3′–5′ DNA helicase. *J. Biol. Chem.*, **272**, 30611–30614.
22. Orren,D.K., Brosh,R.M., Jr., Nehlin,J.O., Machwe,A., Gray,M.D. and Bohr,V.A. (1999) Enzymatic and DNA binding properties of purified WRN protein: high affinity binding to single-stranded DNA but not to DNA damage induced by 4NQO. *Nucleic Acids Res.*, **27**, 3557–3566.
23. Henricksen,L.A., Umbricht,C.B. and Wold,M.S. (1994) Recombinant replication protein A: expression, complex formation, and functional characterization. *J. Biol. Chem.*, **269**, 11121–11132.
24. Podust,L.M., Podust,V.N., Sogo,J.M. and Hubscher,U. (1995) Mammalian DNA polymerase auxiliary proteins: analysis of replication factor C-catalyzed proliferating cell nuclear antigen loading onto circular double-stranded DNA. *Mol. Cell. Biol.*, **15**, 3072–3081.
25. Janscak,P., Garcia,P.L., Hamburger,F., Makuta,Y., Shiraishi,K., Imai,Y., Ikeda,H. and Bickle,T.A. (2003) Characterization and mutational analysis of the RecQ core of the Bloom syndrome protein. *J. Mol. Biol.*, **330**, 29–42.
26. Sharma,S., Sommers,J.A., Choudhary,S., Faulkner,J.K., Cui,S., Andreoli,L., Muzzolini,L., Vindigni,A. and Brosh,R.M., Jr. (2005) Biochemical analysis of the DNA unwinding and strand annealing activities catalyzed by human RECQ1. *J. Biol. Chem.*, **280**, 28072–28084.
27. Zou,L. and Elledge,S.J. (2003) Sensing DNA damage through ATRIP recognition of RPA-ssDNA complexes. *Science*, **300**, 1542–1548.
28. Kim,C., Snyder,R.O. and Wold,M.S. (1992) Binding properties of replication protein A from human and yeast cells. *Mol. Cell. Biol.*, **12**, 3050–3059.
29. Ozsoy,A.Z., Ragonese,H.M. and Matson,S.W. (2003) Analysis of helicase activity and substrate specificity of Drosophila RECQ5. *Nucleic Acids Res.*, **31**, 1554–1564.
30. Brosh,R.M., Jr., Waheed,J. and Sommers,J.A. (2002) Biochemical characterization of the DNA substrate specificity of Werner syndrome helicase. *J. Biol. Chem.*, **275**, 23500–23508.
31. Leonhardt,H., Rahn,H.P., Weinzierl,P., Sporbert,A., Cremer,T., Zink,D. and Cardoso,M.C. (2000) Dynamics of DNA replication factories in living cells. *J. Cell. Biol.*, **149**, 271–280.
32. Warbrick,E. (2000) The puzzle of PCNA's many partners. *Bioessays*, **22**, 997–1006.
33. Torres-Ramos,C.A., Prakash,S. and Prakash,L. (2002) Requirement of *RAD5* and *MMS2* for postreplication repair of UV-damaged DNA in *Saccharomyces cerevisiae*. *Mol. Cell. Biol.*, **22**, 2419–2426.
34. Hoege,C., Pfander,B., Moldovan,G.L., Pyrowolakis,G. and Jentsch,S. (2002) RAD6-dependent DNA repair is linked to modification of PCNA by ubiquitin and SUMO. *Nature*, **419**, 135–141.
35. Laursen,L.V., Ampatzidou,E., Andersen,A.H. and Murray,J.M. (2003) Role for the fission yeast RecQ helicase in DNA repair in G2. *Mol. Cell. Biol.*, **23**, 3692–3705.

36. Hochegger,H., Sonoda,E. and Takeda,S. (2004) Post-replication repair in DT40 cells: translesion polymerases versus recombinases. *Bioessays*, **26**, 151–158.
37. Krejci,L., Van Komen,S., Li,Y., Villemain,J., Reddy,M.S., Klein,H., Ellenberger,T. and Sung,P. (2003) DNA helicase Srs2 disrupts the Rad51 presynaptic filament. *Nature*, **423**, 305–309.
38. Veaute,X., Delmas,S., Selva,M., Jeusset,J., Le Cam,E., Matic,I., Fabre,F. and Petit,M.A. (2005) UvrD helicase, unlike Rep helicase, dismantles RecA nucleoprotein filaments in *Escherichia coli*. *EMBO J.*, **24**, 180–189.
39. McGlynn,P. and Lloyd,R.G. (2001) Rescue of stalled replication forks by RecG: simultaneous translocation on the leading and lagging strand templates supports an active DNA unwinding model of fork reversal and Holliday junction formation. *Proc. Natl Acad. Sci. USA*, **98**, 8227–8234.
40. Singleton,M.R., Scaife,S. and Wigley,D.B. (2001) Structural analysis of DNA replication fork reversal by RecG. *Cell*, **107**, 79–89.
41. Machwe,A., Xiao,L., Groden,J., Matson,S.W. and Orren,D.K. (2005) RecQ family members combine strand pairing and unwinding activities to catalyze strand exchange. *J. Biol. Chem.*, **280**, 23397–23407.
42. Ralf,C., Hickson,I.D. and Wu,L. (2006) The Bloom's syndrome helicase can promote the regression of a model replication fork. *J. Biol. Chem.*, **281**, 22839–22846.
43. Brosh,R.M., Jr., Li,J.L., Kenny,M.K., Karow,J.K., Cooper,M.P., Kureekattil,R.P., Hickson,I.D. and Bohr,V.A. (2000) Replication protein A physically interacts with the Bloom's syndrome protein and stimulates its helicase activity. *J. Biol. Chem.*, **275**, 23500–23508.
44. Brosh,R.M., Jr., Orren,D.K., Nehlin,J.O., Ravn,P.H., Kenny,M.K., Machwe,A. and Bohr,V.A. (1999) Functional and physical interaction between WRN helicase and human replication protein A. *J. Biol. Chem.*, **274**, 18341–18350.
45. Hishida,T., Han,Y.W., Shibata,T., Kubota,Y., Ishino,Y., Iwasaki,H. and Shinagawa,H. (2004) Role of the *Escherichia coli* RecQ DNA helicase in SOS signaling and genome stabilization at stalled replication forks. *Genes Dev.*, **18**, 1886–1897.

## 3.3 RECQL5/Recql5 helicase regulates homologous recombination and suppresses tumor formation via disruption of Rad51 presynaptic filaments

Yiduo Hu, Steven Raynard, Michael G. Sehorn, Xincheng Lu, Wendy Bussen, **Lu Zheng**, Jeremy M. Stark, Ellen L. Barnes, Peter Chi, Pavel Janscak, Maria Jasin, Hannes Vogel, Patrick Sung and Guangbin Luo

Genes Dev. 2007 Dec 1;21(23):3073-84.

My contribution to this paper was to discover and confirm the interaction between RECQ5 and RAD51 protein.


# RECQL5/Recql5 helicase regulates homologous recombination and suppresses tumor formation via disruption of Rad51 presynaptic filaments

Yiduo Hu, Steven Raynard, Michael G. Sehorn, Xincheng Lu, Wendy Bussen, Lu Zheng, Jeremy M. Stark, Ellen L. Barnes, Peter Chi, Pavel Janscak, Maria Jasin, Hannes Vogel, Patrick Sung and Guangbin Luo

*Genes & Dev.* 2007 21: 3073-3084; originally published online Nov 14, 2007;
Access the most recent version at doi:10.1101/gad.1609107



# RECQL5/Recql5 helicase regulates homologous recombination and suppresses tumor formation via disruption of Rad51 presynaptic filaments

**Yiduo Hu,[1,7,8] Steven Raynard,[2,7] Michael G. Sehorn,[2,9] Xincheng Lu,[1] Wendy Bussen,[2] Lu Zheng,[3] Jeremy M. Stark,[4] Ellen L. Barnes,[1] Peter Chi,[2] Pavel Janscak,[3] Maria Jasin,[5] Hannes Vogel,[6] Patrick Sung,[2,10] and Guangbin Luo[1,11]**

[1]Department of Genetics, Case Comprehensive Cancer Centre, University Hospitals of Cleveland and Case Western Reserve University, Cleveland, Ohio 44106, USA; [2]Department of Molecular Biophysics and Biochemistry, Yale University School of Medicine, New Haven, Connecticut 06520, USA; [3]Institute of Molecular Cancer Research, University of Zurich, Winterthurerstrasse 190, CH-8057 Zurich, Switzerland; [4]Department of Radiation Biology, Beckman Research Institute of the City of Hope National Medical Center, Duarte, California 91010, USA; [5]Developmental Biology Program, Memorial Sloan-Kettering Cancer Center, New York, New York 10021, USA; [6]Department of Pathology, Stanford University Medical Center, Stanford, California 94305, USA

**Members of the RecQ helicase family play critical roles in genome maintenance. There are five RecQ homologs in mammals, and defects in three of these (BLM, WRN, and RECQL4) give rise to cancer predisposition syndromes in humans. RECQL and RECQL5 have not been associated with a human disease. Here we show that deletion of Recql5 in mice results in cancer susceptibility. Recql5-deficient cells exhibit elevated frequencies of spontaneous DNA double-strand breaks and homologous recombination (HR) as scored using a reporter that harbors a direct repeat, and are prone to gross chromosomal rearrangements in response to replication stress. To understand how RECQL5 regulates HR, we use purified proteins to demonstrate that human RECQL5 binds the Rad51 recombinase and inhibits Rad51-mediated D-loop formation. By biochemical means and electron microscopy, we show that RECQL5 displaces Rad51 from single-stranded DNA (ssDNA) in a reaction that requires ATP hydrolysis and RPA. Together, our results identify RECQL5 as an important tumor suppressor that may act by preventing inappropriate HR events via Rad51 presynaptic filament disruption.**

[*Keywords*: Recql5 helicase; DNA repair; homologous recombination; tumor suppressor; Rad51 recombinase]

Supplemental material is available at http://www.genesdev.org.

Received August 27, 2007; revised version accepted September 27, 2007.

Homologous recombination (HR) is a fundamental molecular process in all organisms. In meiosis, HR is necessary for the proper segregation of homologous chromosomes and generates genetic diversity through the shuffling of parental alleles (Paques and Haber 1999; Symington 2002). In mitotic cells, HR is an important pathway for repairing chromosomal breaks and gaps, and for restarting damaged or stalled DNA replication forks (Symington 2002; Wu and Hickson 2006). However, inappropriate or untimely HR events can have mutagenic and oncogenic consequences. For example, reciprocal exchanges (crossovers) between homologous chromosomes can lead to somatic loss of heterozygosity (LOH), while crossovers between nonhomologous chromosomes can result in translocation. Also, crossovers between repeated sequences on the same chromosome can result in deletions or inversions. For these reasons, specific mechanisms have evolved for regulating HR to minimize these potentially deleterious rearrangements (Sung and Klein 2006; Wu and Hickson 2006).

[7]**These authors contributed equally to this work.**
**Present addresses: [8]Dana-Farber Cancer Institute and Department of Genetics, Harvard Medical School, Boston, MA 02115, USA; [9]Department of Genetics and Biochemistry, Clemson University, Clemson, SC 29634, USA.**
**Corresponding authors.**
**[10]E-MAIL Patrick.Sung@yale.edu; FAX (203) 785-6404.**
**[11]E-MAIL guangbin.luo@case.edu; FAX (216) 368-3432.**
Article published online ahead of print. Article and publication date are online at http://www.genesdev.org/cgi/doi/10.1101/gad.1609107.

Genetic analyses in *Saccharomyces cerevisiae* indicate that two DNA helicases, Srs2 and Sgs1, function in different pathways to suppress crossover events in mitotic cells (Ira et al. 2003). Mutations in either Srs2 or Sgs1 result in a hyperrecombination phenotype (Aguilera and Klein 1988; Onoda et al. 2000; Liberi et al. 2005). In humans, mutations in *BLM*, which encodes the human ortholog of Sgs1, give rise to the rare hereditary disorder Bloom's syndrome (Ellis et al. 1995). This disorder is marked by an elevated rate of sister chromatid exchange (SCE), increased chromosomal instability, and a high incidence of cancer (German 1993; Hickson 2003). BLM suppresses SCEs by acting in conjunction with the Type 1A topoisomerase, Topo IIIα, and a recently identified protein, BLAP75, to mediate the dissolution of double Holliday junctions (DHJ; a late HR intermediate), a process that yields solely noncrossover recombinants (Wu and Hickson 2003; Raynard et al. 2006; Sung and Klein 2006; Wu et al. 2006). Like its human counterpart, Sgs1 forms a complex with the Top3 topoisomerase (Gangloff et al. 1994; Bennett et al. 2000) and Rmi1 (the BLAP75 ortholog) (Chang et al. 2005; Mullen et al. 2005), suggesting that it might function to suppress SCEs by a similar mechanism.

Srs2 is a superfamily 1 helicase with similarities to the bacterial UvrD/Rep helicases. The mechanistic basis of the Srs2 function was elucidated by biochemical studies that revealed its ability to bind Rad51 and to dismantle the Rad51-ssDNA (single-stranded DNA) nucleoprotein filament, the key catalytic intermediate in recombination reactions (Krejci et al. 2003; Veaute et al. 2003; Sung and Klein 2006). To date, no apparent Srs2 ortholog has been identified in other eukaryotes, although the recently identified Fbh1 helicase shows some structural similarity to the Srs2 helicase family and studies in *Schizosaccharomyces pombe* suggest that Fbh1 plays a role in processing HR intermediates (Osman et al. 2005; Morishita et al. 2005). However, Fbh1-deficient DT40 cells show no prominent sensitivity to DNA damaging agents, and exhibit only a mild SCE phenotype (Kohzaki et al. 2007). This raises the question as to whether attenuation of HR by disruption of the Rad51 presynaptic filament represents a significant mechanism for HR regulation in higher eukaryotes.

Sgs1 and BLM are members of the RecQ family of DNA helicases. Sgs1 is the sole RecQ helicase in budding yeast. Interestingly, humans have a total of five RecQ helicase encoding genes (*RECQL*, *BLM*, *WRN*, *RECQL4*, and *RECQL5*). They share a conserved seven-motif helicase domain but are otherwise distinct from one another by their unique amino acid composition outside the helicase domain, suggesting that they have related but different roles (Hickson 2003). In addition to BLM, defects in both WRN and RECQL4 are also associated with heritable genome instability and cancer disorders (Hickson 2003). Therefore, while BLM likely represents the Sgs1 ortholog, the other RECQ-like helicases represent potential candidates as the functional equivalent of Srs2 in humans. We recently reported that mouse cells deficient in the RECQL5 homolog Recql5 exhibit an elevated level of SCEs, thus implicating this helicase in the regulation of HR (Hu et al. 2005). Importantly, deletion of both Recql5 and Blm further increases the SCE frequency, consistent with Recql5 acting to regulate SCEs in mitotic cells via a mechanism that is distinct from Blm, perhaps by functioning similarly to Srs2 to suppress the channeling of DNA lesions into HR.

In this paper, we show that deletion of Recql5 in mice results in increased susceptibility to cancer. Recql5-deficient cells exhibit elevated frequencies of spontaneous double-strand breaks (DSBs) and HR between direct repeats, and are prone to the accumulation of gross chromosomal rearrangements (GCRs) in response to replication stress. Moreover, by biochemical means, we provide a mechanistic basis by which RECQL5 functions in suppressing GCRs and tumorigenesis. Specifically, we show that human RECQL5 binds the Rad51 recombinase, and a catalytic quantity of this helicase inhibits Rad51-mediated D-loop formation markedly. Furthermore, we show that RECQL5 displaces Rad51 from ssDNA in a reaction that requires ATP hydrolysis by RECQL5 and is stimulated by the ssDNA-binding protein RPA. Taken together, our data provide compelling evidence that this unique member of the RecQ helicase family functions to minimize the propensity of oncogenic rearrangements by suppressing the accumulation of DSBs and attenuating HR by disrupting the Rad51 presynaptic filament.

## Results

### *Recql5-deficient mice are highly cancer prone*

To examine whether Recql5 suppresses tumorigenesis, we generated large cohorts of *Recql5* knockout mice and their wild-type littermates and monitored their phenotypes. No significant differences between the two groups were observed after 1 yr. However, as these animals aged further, a significantly higher percentage of *Recql5* knockout mice developed cancer. Specifically, by 22 mo of age, 23 out of 50 (46%) of the knockout mice and only two out of 32 (6%) wild-type animals developed cancer (Fig. 1A–F). The only two cancer cases in the wild-type were both lymphomas. In mutant mice, approximately half of the cancer incidences were lymphomas, with late-onset follicular lymphoma, which is a common type of malignant lymphoma in humans, accounting for 36% (five out of 14) of the total lymphoma incidences. The rest of the cancers were solid tumors of different tissue origins. Intriguingly, lung adenocarcinomas predominated among them (six out 12, or 50%) (Fig. 1B,D). Three *Recql5* knockout mice had two different types of primary cancers each (Fig. 1B). Interestingly, aside from the striking cancer susceptibility phenotype, *Recql5* knockout mice were indistinguishable from their wild-type siblings. In particular, except for those animals that succumbed to cancer, *Recql5* knockout mice had a lifespan that was not different from wild-type animals. Collectively, these data show that Recql5 is not required for normal embryonic development or for postnatal life in mice, but it has a potent tumor suppression function.

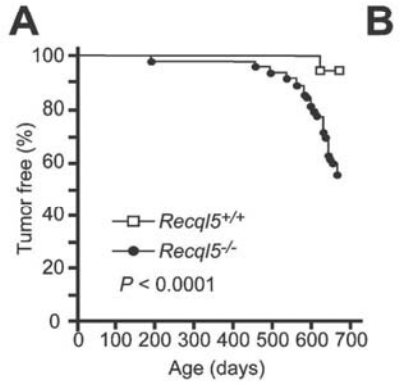


**B** **Tumors found in Recql5 deficient mice[1]**

| Tumor type | Number | Percentage (%) | Age (days) |
|---|---|---|---|
| Lymphomas | 14 | 28% | |
| Thymic lymphoma | 1 | 2% | 193 |
| Follicular lymphoma | 5 | 10% | 647[3] |
| Plasmacytoid lymphoma | 8 | 16% | 606[3] |
| Solid tumors | 12 | 24% | |
| Squamous cell carcinoma | 1 | 2% | 480 |
| Lung adenocarcinoma | 6 | 12% | 613[3] |
| Heptocellular carcinoma | 1 | 2% | 660 |
| Breast carcinoma | 1 | 2% | 647 |
| Liver hemangioma | 3 | 6% | 588[3] |
| Total | 26[2] | 52% | |

[1] 50 *Recql5*$^{-/-}$ and 32 *Recql5*$^{+/+}$ mice were aged up to 22 months (660 days) and monitored daily for tumor development. 2 wild type mice (6%) developed mild lymphomas at the end of the study.
[2] 26 tumors found in 23 *Recql5*$^{-/-}$ mice (46%). 3 mice (6%) had multiple tumors.
[3] Average ages of all cases.

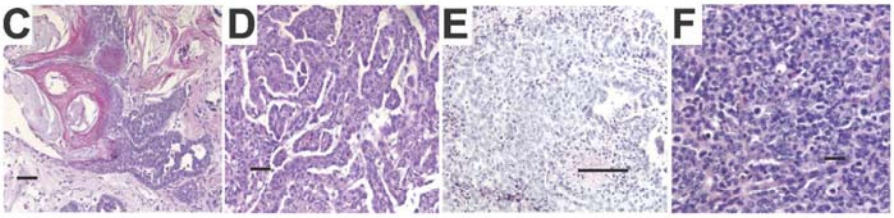


**Figure 1.** Cancer susceptibility phenotype of *Recql5*$^{-/-}$ mice. (*A*) Cancer-free survival of wild-type ($n = 32$) and *Recql5* knockout ($n = 50$) mice. The animals were monitored for up to 22 mo or until they succumbed to cancer. The two wild-type mice with cancer were identified when they were sacrificed at 22 mo of age. All tumor cases were determined based on the results of pathological analysis. (*B*) A table summarizing the cancers observed in *Recql5*$^{-/-}$ mice, including the types of cancers, the frequency for individual type of cancers, and their ages (or average ages) of on-set. (*C–F*) Images of hematoxylin and eosin (H&E) histology of four representative cancers found in *Recql5*$^{-/-}$ mice. (*C*) A well-differentiated squamous cell carcinoma with keratin formation and focal invasion. (*D*) A well-differentiated lung adenocarcinoma of the predominantly papillary type. (*E*) A breast carcinoma characteristic of malignant epithelial cells with poor gland formation by axillary mass histopathology. (*F*) A follicular lymphoma exhibiting characteristic mixture of small and medium-sized abnormal lymphocytes with features of centroblasts and centrocytes. Bars: *C–E*, 50 μm; *F*, 10 μm.

### *Recql5 deficiency is not associated with an elevated frequency of LOH*

As Blm and Recql5 have nonredundant roles in suppressing SCEs in mitotic cells (Hu et al. 2005), our finding that *Recql5* knockout mice are highly cancer prone suggests that misregulation of HR may be the underlying basis for the cancer phenotype in these animals. Mutations in both human *BLM* and mouse *Blm* result in elevated rates of LOH and engender cancer susceptibility (German 1993; Luo et al. 2000; Goss et al. 2002; Hickson 2003). Thus, we first examined whether the elevated SCEs in Recql5-deficient cells is also associated with an increased frequency of LOH. Consistent with a previous report (Luo et al. 2000), we found that *Blm* knockout embryonic stem (ES) cells exhibited a significant increase in LOH at the *Rad50* locus compared with their wild-type counterparts (Supplementary Fig. S1A,B). In contrast, *Recql5* knockout ES cells had similar frequencies of LOH as wild-type ES cells at both the *Rad50* locus (Supplementary Fig. S1A,C) and the *Recql5* locus (Supplementary Fig. S1D,E). This finding suggests that alteration in LOH is not the primary underlying mechanism of cancer susceptibility in *Recql5* knockout mice. It also suggests that the main function of Recql5 with respect to suppressing SCEs does not lie at the dissolution of DHJ, a deduction that is consistent with our previous finding that Blm and Recql5 have nonredundant roles in suppressing SCEs in mitotic cells (Hu et al. 2005).

### *Recql5-deficient cells exhibit an increased frequency of Rad51 and γ-H2AX foci*

HR can also be regulated at an early step—for instance, during the assembly of presynaptic filaments of the Rad51 recombinase (Sung and Klein 2006). To determine whether Recql5 functions at this stage, we examined the effect of *Recql5* ablation on the kinetics of HR induced by DSBs. We reasoned that if Recql5 suppresses SCEs by affecting the channeling of DSBs into HR, deletion of *Recql5* should result in an elevated frequency of HR. First, γ-H2AX and Rad51 foci were used as indicators of DSB induction and HR activation, respectively, whereas the colocalization of γ-H2AX and Rad51 foci was used to monitor HR-mediated DSB repair (Paull et al. 2000; Rothkamm et al. 2003). We found that in mouse embry-

onic fibroblasts (MEFs) derived from *Recql5* knockout mice, the percentage of cells with >10 Rad51 foci was significantly higher than wild-type MEFs (Fig. 2A; Supplementary Fig. S2A). Unexpectedly, Recql5-deficient MEFs also had elevated frequencies of cells with >10 spontaneous γ-H2AX foci (Fig. 2B). No significant

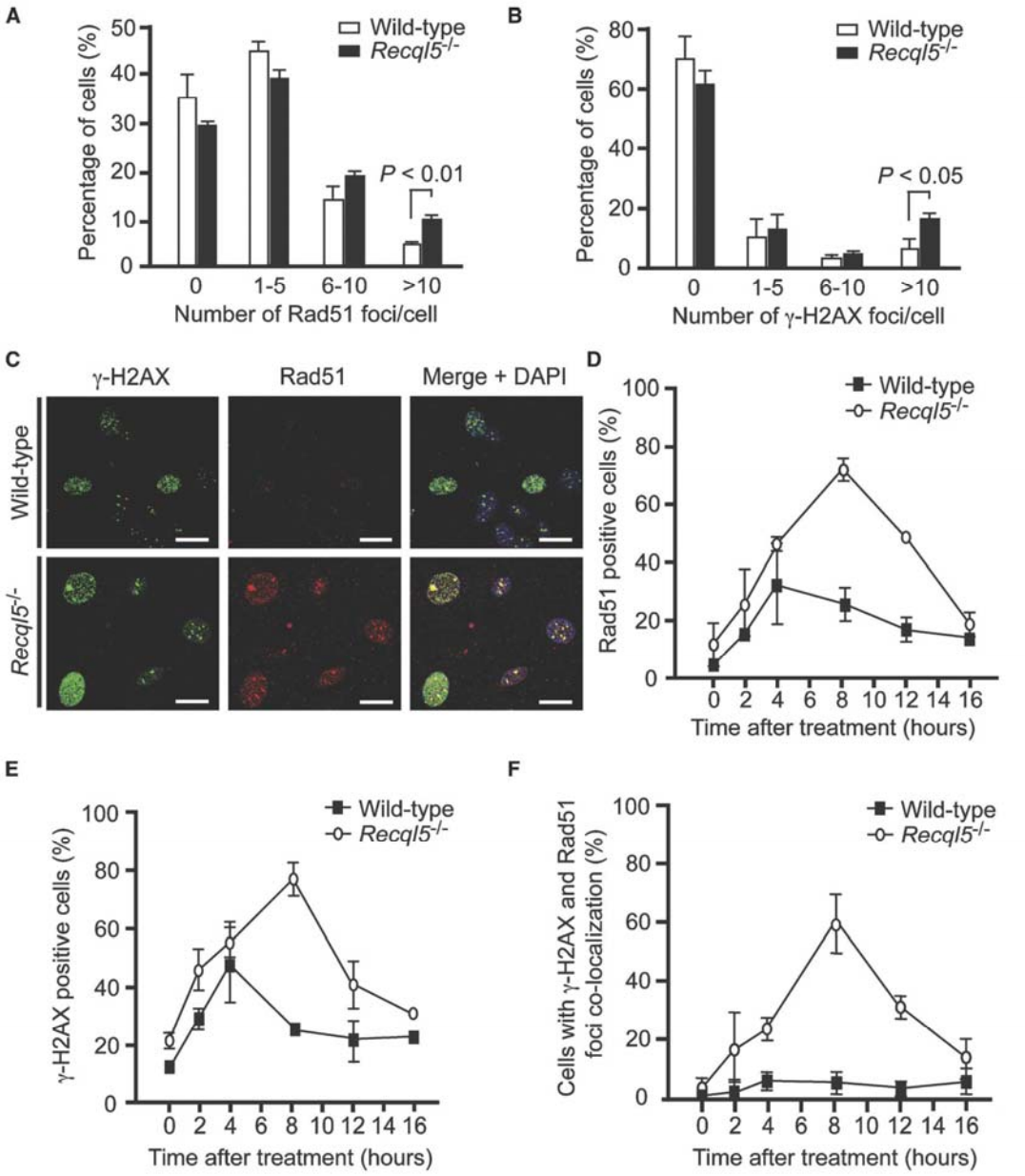


**Figure 2.** Detection of γ-H2AX and Rad51 focus formation in MEFs by immunostaining. Detection of spontaneous Rad51 (*A*) and γ-H2AX (*B*) foci in MEFs. (*C*) Representative images of cells with γ-H2AX, and/or Rad51 foci. (*D–F*) The accumulation of MEF cells with Rad51 foci (*D*), γ-H2AX foci (*E*), and cells with γ-H2AX and Rad51 foci colocalization (*F*) at various time points after exposure to 50 nM CPT. In each data set, only cells with >10 foci were scored as positive. Each data point represents the mean ± SEM from at least 500 nuclei examined in two independent experiments. Bars, 10 μm.

difference in the frequency of S-phase cells or tetraploid cells between the wild-type and Recql5-deficient MEFs was seen by flow cytometry analysis (data not shown), ruling out the possibility that the increased percentages of cells with >10 γ-H2AX or Rad51 foci were due to differences in the cell cycle distributions. The majority of the spontaneous γ-H2AX foci were detected in PCNA positive cells (data not shown), suggesting that they arise during DNA replication. Consistent with this hypothesis, we found that after exposure to a sublethal dose of camptothecin (CPT), a potent S-phase-specific DSB inducer (Pommier et al. 2003), the proportion of cells with Rad51 foci increased dramatically in both mutant and wild-type MEFs, with the fraction of such cells being much higher in the mutant than wild-type (Fig. 2C,D). Importantly, the CPT-induced Rad51 foci persisted much longer in the mutant cells as compared with wild-type cells (Fig. 2D). The *Recql5* mutant cells also exhibited more γ-H2AX foci and for a much longer length of time than wild-type cells (Fig. 2C,E). Moreover, γ-H2AX and Rad51 foci colocalization was rarely observed in wild-type MEFs, even after CPT treatment. In comparison, there were a significantly higher percentage of mutant cells with >10 γ-H2AX foci, of which at least 80% of the foci colocalized with Rad51. Parallel experiments using ES cells showed a similar trend (Supplementary Fig. S2B). In addition, Western blotting showed that chromatin-bound Rad51 was enriched in mutant ES cells compared with the wild-type control following CPT treatment (Supplementary Fig. S3).

### *Recql5 suppresses DSB-induced HR*

The finding that deletion of *Recql5* leads to a dramatic increase in γ-H2AX foci-positive cells strongly suggests that Recql5 has a role in suppressing the accumulation of DSBs. Therefore, it seemed possible that the elevated Rad51 foci and Rad51/γ-H2AX colocalization in Recql5-deficient cells could be an indirect consequence of the increased accumulation of DSBs, rather than an inability to suppress HR. To distinguish between these two possibilities, we examined whether Recql5 deficiency affects the efficiency of HR-mediated repair of I-SceI-induced DSBs. An *SCneo* cassette for monitoring HR-mediated repair (Johnson et al. 1999) was introduced into the *Rb* locus in both wild-type and *Recql5* knockout ES cells by gene targeting. Within this reporter system, a single DSB could be induced in the mutated version of a G418 resistance selection marker gene by the I-SceI endonuclease. The DSB triggers HR-mediated repair with a nonmutated fragment of the neomycin gene to generate G418-resistant clones (Fig. 3A; Johnson et al. 1999). Since Recql5 deletion does not seem to affect either HJ resolution (Supplementary Fig. S1) or nonhomologous end joining (Hu et al. 2005), differences in the proficiency of reconstructing a functional G418 resistance gene between wild-type and Recql5-deficient ES cells likely reflect differences in the channeling of DSBs into HR. The result showed that the frequency of G418-resistant colonies arising from Recql5-deficient ES cells was almost

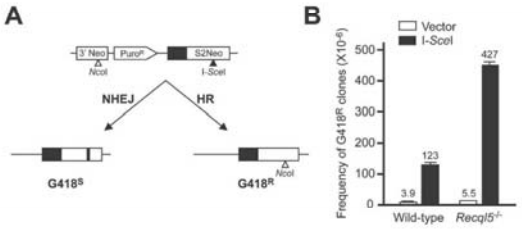


**Figure 3.** HR-mediated repair of I-SceI-induced DSBs in mouse ES cells. (*A*) Schematic illustration of the *SCneo* system for monitoring HR-mediated repair of I-SceI-induced DSBs. A single copy of the *SCneo* substrate was introduced into the *Rb* locus in both wild-type and *Recql5* knockout ES cells by gene targeting. Repair of the DSB by HR results in the reconstitution of a functional *Neo* cassette and G418 resistance. (*B*) Recovery of G418-resistant colonies from cells containing the *SCneo* cassette. ES cells containing the *SCneo* cassette were cultured in medium containing G418 after transfection with either the expression vector for I-SceI or the corresponding empty vector by electroporation. G418-resistant colonies were scored at 10 d after transfection. The average values from three independent experiments are presented *above* the histograms.

3.5-fold higher than that from wild-type ES cells (Fig. 3B). Taken together, these data indicate that Recql5 deficiency is associated with increased DSB repair by HR.

### *Recql5 is required for genome stability in response to replicative stress*

Both the accumulation of DSBs and unchecked inappropriate HR events that accompany *Recql5* deletion can result in genome instability. To address this important issue, we examined metaphase chromosome spreads from both wild-type and Recql5-deficient ES cells. As reported previously, spontaneous GCRs are very rare in both wild-type and Recql5-deficient cells (Hu et al. 2005) and therefore difficult to quantify. Thus, to better assess the impact of Recql5 deficiency on GCRs, we compared the frequency of chromosomal aberrations between wild-type, *Blm*, and *Recql5* mutant ES cells following exposure to a sublethal dose (50 nM) of CPT, a potent inducer of GCRs (Pommier et al. 2003). This treatment had only a modest impact on genome stability in the wild-type and *Blm* knockout ES cells, but it resulted in a dramatic increase in the incidence of chromosomal aberrations in the *Recql5*$^{-/-}$ mutant cells. The aberrations included chromatid and chromosome gaps, as well as multiradial structures (Fig. 4A–D). These data provide evidence that Recql5 deficiency elevates the susceptibility for GCRs.

### *Human RECQL5 physically interacts with Rad51 and suppresses Rad51-mediated D-loop formation*

To delineate how Recql5 regulates HR at the mechanistic level, we expressed human RECQL5 in *Escherichia coli* as a C-terminal fusion with a self-cleaving affinity

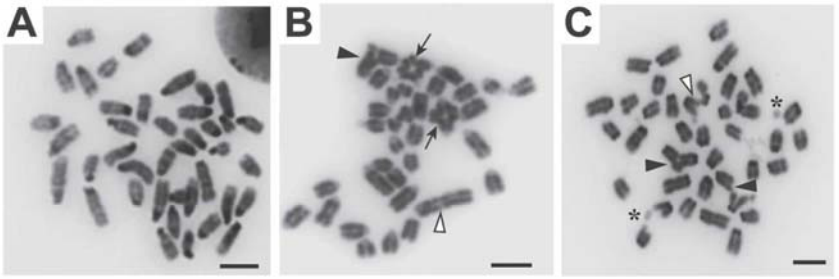


D

**Chromosomal abnormalities and rearrangements after CPT treatment[1]**

| | Total metaphases | Broken chromatid | Broken chromosome | Triradial | Quadriradial | Complex rearrangements | Fusion | Other[2] | Total aberrant chromosomes | % of aberrant metaphase |
|---|---|---|---|---|---|---|---|---|---|---|
| Wild-type | 400 | 3 | 2 | 3 | 2 | 0 | 6 | 0 | 16 | 3.3 |
| *Recql5*$^{-/-}$ | 400 | 43 | 19 | 22 | 26 | 14 | 25 | 10 | 159 | 20.0 |
| *Blm*$^{-/-}$ | 400 | 1 | 0 | 1 | 8 | 0 | 7 | 1 | 18 | 4.5 |

[1] ES cells were treated with CPT (50 nM) for a period of 16 hours and released into fresh medium for 28 hours. Colcemid (30 ng/ml) was added in the last hour of incubation before cells were collected for making metaphase spreads.
[2] Other abnormalities include fragmented chromosomes, premature sister chromatid separation and double minutes.

**Figure 4.** Effect of CPT treatment on chromosome stability in ES cells. (*A*) A metaphase spread from a wild-type cell. (*B*,*C*) Representative images of two metaphase spreads from CPT-treated *Recql5* knockout ES cells. A number of abnormal features, including triradial (solid arrowheads), quadriradial (solid arrows), DNA fragments (asterisks), and end-to-end fusion (open arrowheads) are indicated. Bars, 5 µm. (*D*) Summary of the data from the metaphase spread analysis.

tag composed of an Mxe-intein fragment and a chitin-binding domain (CBD) (Supplementary Fig. S4A; Garcia et al. 2004). RECQL5 was purified to near homogeneity using two chromatographic fractionation steps coupled with affinity chromatography on chitin beads (Supplementary Fig. S4B). Three independently purified RECQL5 preparations gave the same results in all the biochemical analyses.

Since human RECQL5 physically interacts with both Topo IIIα and its isoform, Topo IIIβ (Shimamoto et al. 2000), we first considered the possibility that RECQL5 helps mediate DHJ dissolution as has been shown for BLM (Wu and Hickson 2003). However, using a previously described DHJ dissolution assay (Wu and Hickson 2003), we could find no evidence of RECQL5 and Topo IIIα or Topo IIIβ being capable of dissolving the DHJ. The same negative result was obtained with the inclusion of BLAP75 in the reaction (data not shown).

We then entertained the possibility that RECQL5 regulates the activity of the human Rad51 recombinase. To test this premise, we first examined whether RECQL5 is capable of associating with Rad51. Interestingly, we found that Rad51 can be coimmunoprecipitated with RECQL5 from U2OS cell extracts (Supplementary Fig. S5A). Likewise, Rad51 in HEK293 cell extracts bound to chitin beads coated with purified RECQL5-CBD protein, but not to control beads containing *E. coli* McrA-CBD protein (Supplementary Fig. S5B). This interaction is direct, as purified RECQL5 and Rad51 can be efficiently coimmunoprecipitated (Fig. 5A).

A D-loop assay (Fig. 5B; Petukhova et al. 1998; Mazin et al. 2000) was used to test whether RECQL5 has an effect on the recombinase activity of Rad51. We initially used the Rad51 K133R protein, which binds ATP but is greatly attenuated for ATP hydrolysis, in the D-loop reaction. Since ATP hydrolysis prompts the dissociation of Rad51 from DNA, Rad51 K133R forms a highly stable presynaptic filament (Chi et al. 2006), and its use facilitated our analyses. Coimmunoprecipitation verified that RECQL5 has the same affinity for Rad51 K133R as Rad51 (data not shown). To enhance the efficiency of the D-loop reaction, the accessory factor Hop2-Mnd1 (Petukhova et al. 2005) was included. As expected, Rad51 K133R, and Hop2-Mnd1 catalyzed efficient D-loop formation both in the presence and absence of the ssDNA-binding factor, RPA (Fig. 5C, lanes 2,3). The addition of a catalytic quantity of RECQL5 with Rad51 K133R strongly inhibited D-loop formation when RPA was present (Fig. 5C,E). As little as 15 nM of RECQL5 suppressed the D-loop reaction by four- to fivefold. Interestingly, no significant inhibition by RECQL5 was observed upon the omission of RPA (Fig. 5C, lane 7). Exactly the same results—i.e., RPA-dependent inhibition of the D-loop reaction by RECQL5—were obtained when wild-type Rad51 was used (Supplementary Fig. S6A). To address the specificity of the reaction, we substituted RECQL5 with another human RecQ helicase, WRN, which was previously reported to directly interact with Rad51 (Otterlei et al. 2006). WRN, even at 45 nM, did not affect the D-loop reaction catalyzed by either Rad51 K133R (Fig. 5D,E) or Rad51 (Supplementary Fig. S6A, lanes 5,6). However, this specific WRN preparation was

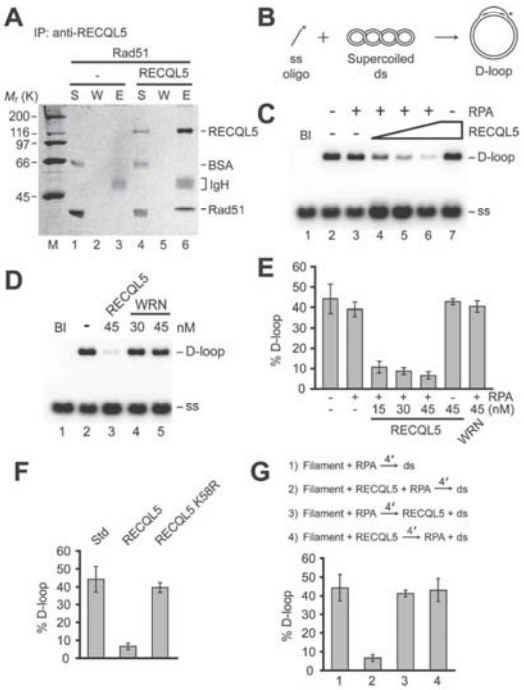


**Figure 5.** Human RECQL5 binds Rad51 and inhibits the D-loop reaction. (*A*) Purified RECQL5 and Rad51 were mixed and subjected to immunoprecipitation with anti-RECQL5 antibodies. The reaction supernatant (S), wash (W), and eluate (E) were analyzed by SDS-PAGE. (IgH) Immunoglobulin heavy chains. (*B*) D-loop reaction scheme. (*C*,*D*) Rad51 K133R presynaptic filaments were incubated with RECQL5 or WRN and RPA (where indicated) before Hop2-Mnd1 and pBluescript form I DNA were incorporated. (Bl) Blank containing DNA substrates only. (*E*) The average values ± SEM from three or more independent experiments are plotted. (*F*) D-loop reactions with RPA and RECQL5 or RECQL5 K58R. (Std) Standard reaction with RPA but no RECQL5 or RECQL5 K58R. (*G*) Effects of order of addition of reaction components. Presynaptic filaments of Rad51 K133R were incubated with the rest of the components in the indicated orders. Hop2-Mnd1 was added together with the dsDNA to all the reactions. The concentration of RECQL5 and RECQL5 K58R was 45 nM. The average values ± SEM from three or more independent experiments are plotted in *F* and *G*.

quite adept at dissociating a HJ substrate—in fact, much more so than RECQL5 (Supplementary Fig. S7A,B).

### *D-loop inhibitory action is dependent on ATP hydrolysis by RECQL5 and order of addition of proteins*

We used the ATPase-defective RECQL5 K58R mutant (Garcia et al. 2004) to ask whether suppression of D-loop formation requires ATP hydrolysis by RECQL5. RECQL5 K58R retains the ability to interact with Rad51 and Rad51 K133R (data not shown), but has no effect on the D-loop reaction, indicating that the RECQL5 ATPase activity is required for inhibition (Fig. 5F). Rad51 forms a functional presynaptic filament in the presence of the nonhydrolyzable ATP analog AMP-PNP (Chi et al. 2006). The D-loop reaction catalyzed by Rad51 with AMP-PNP as the nucleotide cofactor is impervious to RECQL5 (data not shown), a result that further supports the conclusion that ATP hydrolysis by RECQL5 is needed for Rad51 inhibition.

A series of order-of-addition experiments were conducted to test the possibility that RECQL5 might use its helicase activity to dissociate the D-loop product. Interestingly, for RECQL5 to inhibit the D-loop reaction, it must be added with RPA during the assembly of the presynaptic filament (Fig. 5G; Supplementary Fig. S6B). This finding argues that RECQL5 acts not by unwinding the D-loop product, but by interfering with the presynaptic filament assembly process.

### *RECQL5 disrupts the Rad51 presynaptic filament*

We employed a topoisomerase-linked assay previously used to characterize the presynaptic filament disruption function of Srs2 (Krejci et al. 2003) to enquire whether RECQL5 can catalyze the transfer of Rad51 K133R from ssDNA to a double-stranded DNA (dsDNA) trap. A preassembled presynaptic filament of Rad51 K133R was treated with RECQL5 with or without RPA and, after a brief incubation, an excess of topologically relaxed dsDNA was added to trap Rad51 K133R molecules displaced from the ssDNA. The binding of Rad51 K133R to topologically relaxed dsDNA induces lengthening of the DNA (Ogawa et al. 1993; Sung and Robberson 1995) that can be monitored as a change in the DNA linking number upon incubation with calf thymus topoisomerase I (Fig. 6A; Krejci et al. 2003). The product, Form U DNA, is well separated from the topologically relaxed substrate in an agarose gel (Fig. 6B; Krejci et al. 2003). Control experiments show that RPA and RECQL5 do not make Form U DNA (Fig. 6B, lane 8). The addition of a catalytic amount of RECQL5 resulted in the generation of Form U, indicating that it promotes the transfer of Rad51 K133R from the presynaptic filament to the dsDNA trap (Fig. 6C). The RECQL5-mediated release of Rad51 K133R from the ssDNA is enhanced by RPA (Fig. 6C, cf. lanes 7,8 and 4,5). In contrast, WRN is incapable of mediating the release of Rad51 K133R from the presynaptic filament, regardless of whether RPA is included (Fig. 6C, lane 11) or not (data not shown). The disruptive action of RECQL5 on the presynaptic filament is dependent on its ATPase activity, as the RECQL5 K58R mutant protein is completely inactive in this regard (Fig. 6C, lanes 9,10).

Electron microscopy was used to visualize disruption of the presynaptic filament by RECQL5. Incubation of Rad51 K133R with a 150-mer oligonucleotide and ATP produced abundant presynaptic filaments with distinctive striations (Fig. 7A). Nucleoprotein complexes of RPA with ssDNA were nondescript (Fig. 7B). The dissociation of the Rad51 K133R presynaptic filaments was

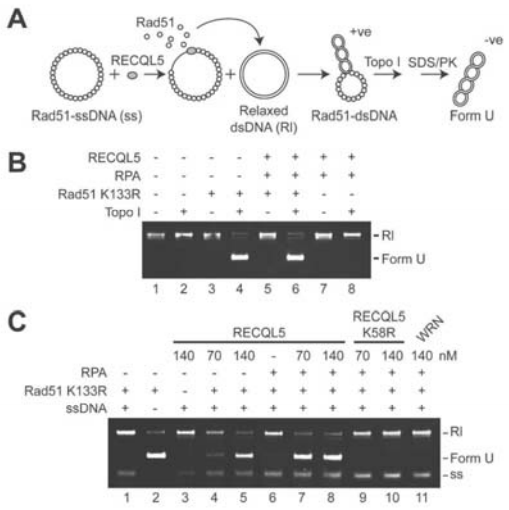


**Figure 6.** Turnover of the presynaptic filament as revealed by Topoisomerase-linked DNA topology modification. (*A*) The reaction scheme. (PK) Proteinase K. (*B*) Topologically relaxed duplex DNA was incubated with the indicated proteins, with or without calf thymus topoisomerase I. Only Rad51 K133R makes form U DNA. (*C*) Rad51 K133R presynaptic filaments were assembled and then incubated with RECQL5, RECQL5 K58R, or WRN, with or without RPA. Topologically relaxed duplex DNA and topoisomerase were subsequently added to complete the reaction. Form U DNA marker was run in lane 2. (RI) Topologically relaxed duplex DNA; (ss) ssDNA.

quantified by determining the relative frequencies of filaments and RPA–ssDNA complexes. At least 2500 nucleoprotein complexes were counted for each reaction. In congruence with the biochemical data, incubation of the Rad51 K133R presynaptic filaments with RECQL5 in the presence of ATP led to its replacement by RPA–ssDNA complexes (Fig. 7C). As anticipated, the Rad51 K133R filaments were impervious to RECQL5 K58R and WRN (Fig. 7C). RECQL5, but not RECQL5 K58R or WRN, also catalyzed the dismantling of presynaptic filaments that comprise Rad51 protein (Supplementary Fig. S8A–C). Thus, the electron microscopic analyses provide clear validation that RECQL5 catalyzes disassembly of the Rad51 presynaptic filament in an ATPase-dependent fashion.

## Discussion

Inappropriate or untimely HR events can have deleterious consequences. For example, the formation of crossovers can result in chromosome translocation, deletion, inversion, and LOH, which are potentially oncogenic in mammals; whereas inappropriate HR repair can lead to GCRs (Sung and Klein 2006; Wu and Hickson 2006). It is therefore not surprising that mammals have evolved multiple pathways for regulating HR-mediated repair in order to suppress potential oncogenic rearrangement in mitotic cells. The importance of this regulation is attested by several human cancer-prone disorders that are associated with aberrant or deregulated HR events (Thompson and Schild 2002). Recent studies have established that in yeast, HR is regulated by the Srs2 and Sgs1 helicases at the initiation and resolution stages, respectively (Sung and Klein 2006). In mammals, BLM appears to be the functional equivalent of yeast Sgs1. The relevance of BLM-dependent DHJ resolution in cancer avoidance has already been clearly established (German 1993; Luo et al. 2000; Goss et al. 2002).

Recently, we demonstrated that Blm and Recql5 act in nonredundant pathways to suppress mitotic SCEs in mice (Hu et al. 2005). In this study, we provide new data showing that deletion of *Recql5* in mice results in an increased susceptibility to cancer. Further, we show that Recql5-deficient cells exhibit elevated frequencies of spontaneous DSBs and HR between direct repeats, and are prone to GCRs in response to replication stress. We suggest that elevated spontaneous GCRs represent the primary underlying basis for the cancer susceptibility in Recql5 knockout mice. We also provide evidence that the GCR phenotype is due to a failure to regulate HR. Importantly, using biochemical approaches, we elucidate the mechanism by which RECQL5 regulates HR. Specifically, we demonstrate that human RECQL5 binds the Rad51 recombinase, and a catalytic quantity of this helicase inhibits Rad51-mediated D-loop formation markedly. Furthermore, we show that RECQL5 displaces Rad51 from ssDNA in a reaction that requires ATP hydrolysis by RECQL5. This reaction is stimulated by the ssDNA-binding protein RPA, probably due to the sequestering of ssDNA by RPA after Rad51 removal to prevent Rad51 renucleation on the DNA (Fig. 8). In contrast, the related WRN helicase is incapable of such a

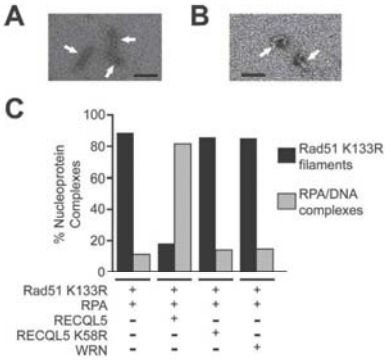


**Figure 7.** Analysis of presynaptic filament dissociation by electron microscopy. (*A*) Presynaptic filaments of Rad51 K133R on the 150-mer ssDNA. (*B*) Nucleoprotein complexes of RPA and the 150-mer ssDNA. The black scale bar in *A* and *B* denotes a length of 50 nm. (*C*) The relative abundance of Rad51 K133R presynaptic filaments and RPA–ssDNA complexes in reactions that contained the indicated protein components. Over 2500 nucleoprotein complexes were counted in each case.

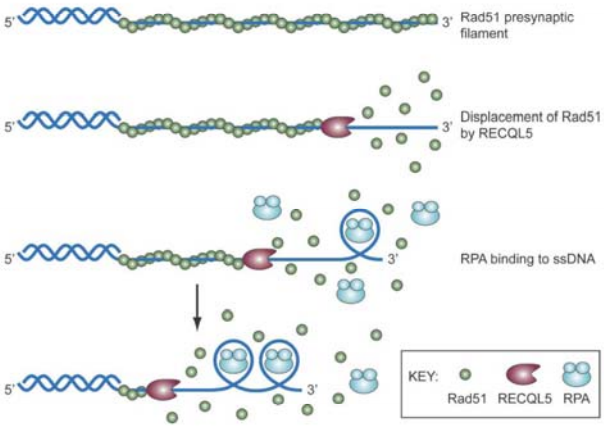


**Figure 8.** Model depicting the action mechanism of RECQL5 on Rad51 presynaptic filaments. RECQL5 utilizes the free energy from ATP hydrolysis to catalyze the dismantling of the Rad51 presynaptic filament. The ssDNA generated as a result of Rad51 removal is immediately occupied by RPA to prevent the reloading of Rad51.

feat, even though it is considerably more active than RECQL5 in HJ unwinding. Similarly, the RECQL helicase unwinds the HJ much more efficiently than RECQL5 but is incapable of Rad51 removal from ssDNA (our unpublished data).

Our combined genetic, cell biological, and biochemical data provide compelling evidence that RECQL5/Recql5 functions as the mammalian equivalent of yeast Srs2 in suppressing inappropriate HR events. Interestingly, our data also indicate that in the absence of Recql5, cells accumulate excessive DSBs despite having an elevated HR capacity. This observation suggests that this helicase plays an important role in mitigating the lesions associated with damaged or collapsed replication forks. If a replication fork does collapse, RECQL5/Recql5 then functions to suppress the HR-mediated repair of the one-ended DNA break associated with the collapsed fork.

Recent studies show that RECQL5 forms nuclear foci that colocalize with the DNA replication machinery in S-phase nuclei (Kanagaraj et al. 2006). Moreover, the RECQL5 foci persist at sites of stalled replication forks upon exposure of cells to UV irradiation. RECQL5 physically interacts with the DNA polymerase processivity factor PCNA (Kanagaraj et al. 2006). This interaction could serve to target RECQL5 to stalled replication forks where it may act to suppress spurious HR events, by channeling the stalled or damaged replication forks into a nonrecombinational repair pathway. We note that such a postulated means of targeting RECQL5 would be analogous to the PCNA-mediated recruitment of the Srs2 helicase to DNA replication forks (Papouli et al. 2005; Pfander et al. 2005).

In an accompanying paper, Bugreev et al. (2007) provide evidence that the BLM helicase can also disrupt presynaptic filaments of Rad51. In aggregate, the published information and the new findings indicate that in both the mouse and humans, BLM/Blm and RECQL5/Recql5 function via two distinct pathways to regulate the HR process at both early and late stages to prevent excessive crossovers and other inappropriate HR events. Specifically, RECQL5/Recql5 suppresses HR via Rad51 presynaptic filament disruption that serves to channel DNA lesions into the appropriate alternative mechanism(s), whereas BLM/Blm, in addition to providing a presynaptic filament disruptive function (Bugreev et al. 2007), acts to resolve a late HR intermediate in favor of gene conversions (Wu and Hickson 2003). Importantly, both mechanisms are required for tumor suppression.

## Materials and methods

See the Supplemental Material for details of protein purification, cell culture, and DNA substrates.

### *Establishment and culture of mouse ES cells and MEFs*

Culture and genetic manipulation of mouse ES cells was performed as described (Hu et al. 2005). The detailed information for individual genetically modified ES cell lines used in this study is described in the Supplemental Material. Primary MEF cultures were derived from 13.5-d-post-coitus (13.5-dpc) embryos of various genotypes, as described (Hu et al. 2005; Mann et al. 2005), except that a low oxygen condition (3% $O_2$, 5% $CO_2$, and 92% $N_2$) was used to reduce oxidative damage-induced stress (Parrinello et al. 2003). All MEF cells used in experiments were under passage number 4.

### *Mouse and pathological analysis of tumors*

*Recql5*$^{+/+}$ and *Recql5*$^{-/-}$ mice were generated by crossing between *Recql5*$^{+/-}$ mice in a mixed genetic background of 129Sv/Ev and C57BL/6. Mice were maintained in a standard transgenic mouse facility and monitored daily. Individual mice were autopsied, and potential lesions were recorded and fixed in 10% phosphate-buffered formalin. After the fixation, an experienced pathologist examined each animal again. All lesions identified were processed and subjected to standard histological and pathological analyses.

### *Immunofluorescence*

Anti-γ-H2AX (1:200, Upstate Biotechnology; 1:100, Trevigen), anti-Rad51 (1:100, Santa Cruz Biotechnology), and anti-PCNA (1:200, Santa Cruz Biotechnology) antibodies were used in im-

munofluorescence experiments. Passage 3 MEFs were seeded on glass coverslips for 24 h before drug treatment. After treatment, coverslips were washed briefly in PBS and processed by treating in 0.5% Triton X-100 in PBS (pH 7.1) for 5 min, followed by fixation with 3.7% paraformaldehyde (pH 7.1) for 10 min. Coverslips were incubated with primary antibodies overnight at 4°C and then with Alexa Fluor-conjugated secondary antibodies (Molecular Probes) for 1 h at room temperature, and then were counterstained with DAPI (Vector Laboratories). Images were captured using a confocal microscope (TCS SP2, UV/spectral confocal laser scanner, Leica) and analyzed using Adobe Photoshop (Adobe Systems).

*Repair of I-SceI-induced DSBs in mouse ES cells*

The *SCneo* substrate was introduced into the *Rb* locus in both wild-type and *Recql5* knockout ES cells by gene targeting essentially as described (Stark and Jasin 2003), except that the *Hyg* selection marker was replaced by a *Puro* marker and puromycin was used to select for transfected cells. After the correctly targeted ES cell lines were obtained, individual cell lines containing the *SCneo* cassette were transfected with either the expression vector for I-SceI or the corresponding empty vector by electroporation. The transfected cells were divided equally into several plates and then cultured in medium with or without 180 μg/mL G418. The number of colonies from each plate was scored at 10 d after transfection. For each data point, the average frequency of recovering G418-resistant colonies was calculated by dividing the number of G418-resistant colonies by the estimated total number of cells plated after adjusting to the corresponding plating efficiencies. Each experiment was repeated three times.

*Chromosome and mitotic abnormalities*

Conventional cytogenetic protocols were used for analyzing chromosomal abnormalities as described (Hu et al. 2005; Mann et al. 2005).

*RECQL5–Rad51 coimmunoprecipitation*

All the incubation steps were performed at 4°C. Purified RECQL5 or RECQL5 K58R and Rad51 or Rad51 K133R, 4 μg each, were incubated in 30 μL of K buffer (20 mM $KH_2PO_4$ at pH 7.4, 10% glycerol, 1 mM DTT, 0.5 mM EDTA, 0.01% Igepal) containing 150 mM KCl and 100 μg $mL^{-1}$ BSA for 10 min, and then rabbit polyclonal anti-RECQL5 antibody (0.1 μg) (Kanagaraj et al. 2006) was added, followed by a 30-min incubation. To capture RECQL5 and associated Rad51, the reactions were incubated for 30 min with 10 μL of Protein-G-coupled magnetic beads (Dynal Biotech) with frequent agitation. The magnetic beads and bound proteins were isolated using a magnet and, after washing the beads twice with 15 μL of K buffer containing 150 mM KCl, the bound proteins were eluted with 30 μL of SDS-PAGE sample loading buffer. The supernatant (S) that contained unbound proteins, the wash (W), and the SDS eluate (E), 10 μL each, were subject to 10% SDS-PAGE and staining with Coomassie blue to visualize proteins.

*D-loop reaction*

Buffer R (25 mM Tris-HCl at pH 7.5, 2 mM ATP, 1 mM $MgCl_2$, 50 mM KCl, 1 mM DTT, 100 μg $mL^{-1}$ BSA, containing an ATP-regenerating system consisting of 20 mM creatine phosphate and 20 μg $mL^{-1}$ creatine kinase) was used for the D-loop reactions, and all the incubation steps were performed at 37°C. Rad51 K133R (1 μM) was incubated with the 5′-end-labeled 90-mer oligonucleotide D1 (3 μM nucleotides) in 11 μL of buffer R for 5 min, followed by the incorporation of Hop2-Mnd1 (300 nM) in 0.75 μL of K buffer and a 1-min incubation. The reaction was initiated by adding pBluescript replicative form I DNA (50 μM base pairs) in 0.75 μL of water. The reactions were terminated after 6 min by the addition of 0.8 μL each of 10% SDS and proteinase K (10 mg $mL^{-1}$). Following a 3-min incubation, the reaction mixtures were resolved in 0.9% agarose gels in TAE buffer (40 mM Tris acetate at pH 7.4, 0.5 mM EDTA). The gels were dried and subjected to phosphorimaging analysis. When present, RPA (135 nM) and RECQL5 (15–45 nM), WRN (30 and 45 nM), or RECQL5 K58R (45 nM) were added to the preassembled Rad51 filament, followed by a 4-min incubation before the incorporation of Hop2-Mnd1 and replicative form I DNA.

*Topoisomerase I-linked DNA topology modification*

Buffer R was used for the reactions and all the incubation steps were performed at 37°C. Rad51 K133R (1.5 μM) was incubated for 5 min with pBluescript (–) strand (6 μM nucleotides) in 10.5 μL of buffer R. RECQL5, RECQL5 K58R, or WRN (70 and 140 nM each) and RPA (150 nM) were each added in 0.5 μL of K buffer, followed by a 4-min incubation. Topologically relaxed ϕX174 (7 μM base pairs) in 0.5 μL of water and 2.5 U calf thymus topoisomerase I (Invitrogen) were then incorporated to complete the reaction. The reaction mixtures were incubated for 6 min, terminated, and analyzed as above.

*Electron microscopy*

Buffer R was used for the reactions and all the incubation steps were performed at 37°C. Rad51 K133R (4 μM) was incubated with 150-mer ssDNA (12 μM nucleotides) for 5 min in 11.5 μL of buffer R, followed by addition of RPA (0.55 μM) in 0.5 μL of K buffer and either buffer, RECQL5, RECQL5 K58R, or WRN (90 nM each) in 0.5 μL of K buffer. After a 4-min incubation, the reactions were diluted eightfold with buffer, and a 4-μL aliquot was applied to 400-mesh grids coated with carbon film that was glow-discharged in air. After staining for 30 sec with 2% uranyl acetate, the samples were examined in a Tecnai 12 Biotwin electron microscope (FEI Company) equipped with a tungsten filament at 100 keV. Digital images were captured with a Morada (Olympus Soft Imaging Solutions) charge-coupled device camera at a nominal magnification of ×87,000.

## Acknowledgments

We are grateful to Daniel Camerini-Otero for the Hop2-Mnd1 expression plasmid and to Alessandro Vindigni for the recombinant RECQL baculovirus. This study was supported by grants RO1 CA110415, RO1 CA88939, P20 CA103736, RO1 ES015632, and RO1 ES015252 from the US National Institutes of Health, the Searle Scholar Program (01-E-109), and the Swiss National Science Foundation.

## References

Aguilera, A. and Klein, H.L. 1988. Genetic control of intrachromosomal recombination in *Saccharomyces cerevisiae*. I. Isolation and genetic characterization of hyper-recombination mutations. *Genetics* **119:** 779–790.

Bennett, R.J., Noirot-Gros, M.F., and Wang, J.C. 2000. Interaction between yeast Sgs1 helicase and DNA Topoisomerase III. *J. Biol. Chem.* **275:** 26898–26905.

Bugreev, D.V., Yu, X., Egelman, E.H., and Mazin, A.V. 2007. Novel pro- and anti-recombination activities of the Bloom's syndrome helicase. *Genes & Dev.* (this issue), doi: 10.1101/gad.1609007.

Chang, M., Bellaoui, M., Zhang, C., Desai, R., Morozov, P., Delgado-Cruzata, L., Rothstein, R., Freyer, G.A., Boone, C., and Brown, G.W. 2005. *RMI1/NCE4*, a suppressor of genome instability, encodes a member of the RecQ helicase/Topo III complex. *EMBO J.* **24:** 2024–2033.

Chi, P., Van Komen, S., Sehorn, M.G., Sigurdsson, S., and Sung, P. 2006. Roles of ATP binding and ATP hydrolysis in human Rad51 recombinase function. *DNA Repair (Amst.)* **5:** 381–391.

Ellis, N.A., Groden, J., Ye, T.Z., Straughen, J., Lennon, D.J., Ciocci, S., Proytcheva, M., and German, J. 1995. The Bloom's syndrome gene product is homologous to RecQ helicases. *Cell* **83:** 655–666.

Gangloff, S., McDonald, J.P., Bendixen, C., Arthur, L., and Rothstein, R. 1994. The yeast type I topoisomerase Top3 interacts with Sgs1, a DNA helicase homolog: A potential eukaryotic reverse gyrase. *Mol. Cell. Biol.* **14:** 8391–8398.

Garcia, P.L., Liu, Y., Jiricny, J., West, S.C., and Janscak, P. 2004. Human RECQ5β, a protein with DNA helicase and strand-annealing activities in a single polypeptide. *EMBO J.* **23:** 2882–2891.

German, J. 1993. Bloom syndrome: A Mendelian prototype of somatic mutational disease. *Medicine (Baltimore)* **72:** 393–406.

Goss, K.H., Risinger, M.A., Kordich, J.J., Sanz, M.M., Straughen, J.E., Slovek, L.E., Capobianco, A.J., German, J., Boivin, G.P., and Groden, J. 2002. Enhanced tumor formation in mice heterozygous for *Blm* mutation. *Science* **297:** 2051–2053.

Hickson, I.D. 2003. RecQ helicases: Caretakers of the genome. *Nat. Rev. Cancer* **3:** 169–178.

Hu, Y., Lu, X., Barnes, E., Yan, M., Lou, H., and Luo, G. 2005. Recql5 and Blm RecQ DNA helicases have nonredundant roles in suppressing crossovers. *Mol. Cell. Biol.* **25:** 3431–3442.

Ira, G., Malkova, A., Liberi, G., Foiani, M., and Haber, J.E. 2003. Srs2 and Sgs1-Top3 suppress crossovers during double-strand break repair in yeast. *Cell* **115:** 401–411.

Johnson, R.D., Liu, N., and Jasin, M. 1999. Mammalian XRCC2 promotes the repair of DNA double-strand breaks by homologous recombination. *Nature* **401:** 397–399.

Kanagaraj, R., Saydam, N., Garcia, P.L., Zheng, L., and Janscak, P. 2006. Human RECQ5β helicase promotes strand exchange on synthetic DNA structures resembling a stalled replication fork. *Nucleic Acids Res.* **34:** 5217–5231.

Kohzaki, M., Hatanaka, A., Sonoda, E., Yamazoe, M., Kikuchi, K., Vu Trung, N., Szuts, D., Sale, J.E., Shinagawa, H., Watanabe, M., et al. 2007. Cooperative roles of vertebrate Fbh1 and Blm DNA helicases in avoidance of crossovers during recombination initiated by replication fork collapse. *Mol. Cell. Biol.* **27:** 2812–2820.

Krejci, L., Van Komen, S., Li, Y., Villemain, J., Reddy, M.S., Klein, H., Ellenberger, T., and Sung, P. 2003. DNA helicase Srs2 disrupts the Rad51 presynaptic filament. *Nature* **423:** 305–309.

Liberi, G., Maffioletti, G., Lucca, C., Chiolo, I., Baryshnikova, A., Cotta-Ramusino, C., Lopes, M., Pellicioli, A., Haber, J.E., and Foiani, M. 2005. Rad51-dependent DNA structures accumulate at damaged replication forks in *sgs1* mutants defective in the yeast ortholog of BLM RecQ helicase. *Genes & Dev.* **19:** 339–350.

Luo, G., Santoro, I.M., McDaniel, L.D., Nishijima, I., Mills, M., Youssoufian, H., Vogel, H., Schultz, R.A., and Bradley, A. 2000. Cancer predisposition caused by elevated mitotic recombination in Bloom mice. *Nat. Genet.* **26:** 424–429.

Mann, M.B., Hodges, C.A., Barnes, E., Vogel, H., Hassold, T.J., and Luo, G. 2005. Defective sister-chromatid cohesion, aneuploidy and cancer predisposition in a mouse model of type II Rothmund-Thomson syndrome. *Hum. Mol. Genet.* **14:** 813–825.

Mazin, A.V., Zaitseva, E., Sung, P., and Kowalczykowski, S.C. 2000. Tailed duplex DNA is the preferred substrate for Rad51 protein-mediated homologous pairing. *EMBO J.* **19:** 1148–1156.

Morishita, T., Furukawa, F., Sakaguchi, C., Toda, T., Carr, A.M., Iwasaki, H., and Shinagawa, H. 2005. Role of the *Schizosaccharomyces pombe* F-Box DNA helicase in processing recombination intermediates. *Mol. Cell. Biol.* **25:** 8074–8083.

Mullen, J.R., Nallaseth, F.S., Lan, Y.Q., Slagle, C.E., and Brill, S.J. 2005. Yeast Rmi1/Nce4 controls genome stability as a subunit of the Sgs1–Top3 complex. *Mol. Cell. Biol.* **25:** 4476–4487.

Ogawa, T., Yu, X., Shinohara, A., and Egelman, E.H. 1993. Similarity of the yeast RAD51 filament to the bacterial RecA filament. *Science* **259:** 1896–1899.

Onoda, F., Seki, M., Miyajima, A., and Enomoto, T. 2000. Elevation of sister chromatid exchange in *Saccharomyces cerevisiae sgs1* disruptants and the relevance of the disruptants as a system to evaluate mutations in Bloom's syndrome gene. *Mutat. Res.* **459:** 203–209.

Osman, F., Dixon, J., Barr, A.R., and Whitby, M.C. 2005. The F-Box DNA helicase Fbh1 prevents Rhp51-dependent recombination without mediator proteins. *Mol. Cell. Biol.* **25:** 8084–8096.

Otterlei, M., Bruheim, P., Ahn, B., Bussen, W., Karmakar, P., Baynton, K., and Bohr, V.A. 2006. Werner syndrome protein participates in a complex with RAD51, RAD54, RAD54B and ATR in response to ICL-induced replication arrest. *J. Cell Sci.* **119:** 5137–5146.

Papouli, E., Chen, S., Davies, A.A., Huttner, D., Krejci, L., Sung, P., and Ulrich, H.D. 2005. Crosstalk between SUMO and ubiquitin on PCNA is mediated by recruitment of the helicase Srs2p. *Mol. Cell* **19:** 123–133.

Paques, F. and Haber, J.E. 1999. Multiple pathways of recombination induced by double-strand breaks in *Saccharomyces cerevisiae*. *Microbiol. Mol. Biol. Rev.* **63:** 349–404.

Parrinello, S., Samper, E., Krtolica, A., Goldstein, J., Melov, S., and Campisi, J. 2003. Oxygen sensitivity severely limits the replicative lifespan of murine fibroblasts. *Nat. Cell Biol.* **5:** 741–747.

Paull, T.T., Rogakou, E.P., Yamazaki, V., Kirchgessner, C.U., Gellert, M., and Bonner, W.M. 2000. A critical role for histone H2AX in recruitment of repair factors to nuclear foci after DNA damage. *Curr. Biol.* **10:** 886–895.

Petukhova, G., Stratton, S., and Sung, P. 1998. Catalysis of homologous DNA pairing by yeast Rad51 and Rad54 proteins. *Nature* **393:** 91–94.

Petukhova, G.V., Pezza, R.J., Vanevski, F., Ploquin, M., Masson, J.Y., and Camerini-Otero, R.D. 2005. The Hop2 and Mnd1 proteins act in concert with Rad51 and Dmc1 in meiotic recombination. *Nat. Struct. Mol. Biol.* **12:** 449–453.

Pfander, B., Moldovan, G.L., Sacher, M., Hoege, C., and Jentsch, S. 2005. SUMO-modified PCNA recruits Srs2 to prevent recombination during S phase. *Nature* **436:** 428–433.

Pommier, Y., Redon, C., Rao, V.A., Seiler, J.A., Sordet, O., Takemura, H., Antony, S., Meng, L., Liao, Z., Kohlhagen, G., et al. 2003. Repair of and checkpoint response to topoisomerase I-mediated DNA damage. *Mutat. Res.* **532:** 173–203.

Raynard, S., Bussen, W., and Sung, P. 2006. A double Holliday junction dissolvasome comprising BLM, topoisomerase IIIα, and BLAP75. *J. Biol. Chem.* **281:** 13861–13864.

Rothkamm, K., Kruger, I., Thompson, L.H., and Lobrich, M. 2003. Pathways of DNA double-strand break repair during the mammalian cell cycle. *Mol. Cell. Biol.* **23:** 5706–5715.

Shimamoto, A., Nishikawa, K., Kitao, S., and Furuichi, Y. 2000. Human RecQ5β, a large isomer of RecQ5 DNA helicase, localizes in the nucleoplasm and interacts with topoisomerases 3α and 3β. *Nucleic Acids Res.* **28:** 1647–1655.

Stark, J.M. and Jasin, M. 2003. Extensive loss of heterozygosity is suppressed during homologous repair of chromosomal breaks. *Mol. Cell. Biol.* **23:** 733–743.

Sung, P. and Klein, H. 2006. Mechanism of homologous recombination: Mediators and helicases take on regulatory functions. *Nat. Rev. Mol. Cell Biol.* **7:** 739–750.

Sung, P. and Robberson, D.L. 1995. DNA strand exchange mediated by a RAD51-ssDNA nucleoprotein filament with polarity opposite to that of RecA. *Cell* **82:** 453–461.

Symington, L.S. 2002. Role of RAD52 epistasis group genes in homologous recombination and double-strand break repair. *Microbiol. Mol. Biol. Rev.* **66:** 630–670.

Thompson, L.H. and Schild, D. 2002. Recombinational DNA repair and human disease. *Mutat. Res.* **509:** 49–78.

Veaute, X., Jeusset, J., Soustelle, C., Kowalczykowski, S.C., Le Cam, E., and Fabre, F. 2003. The Srs2 helicase prevents recombination by disrupting Rad51 nucleoprotein filaments. *Nature* **423:** 309–312.

Wu, L. and Hickson, I.D. 2003. The Bloom's syndrome helicase suppresses crossing over during homologous recombination. *Nature* **426:** 870–874.

Wu, L. and Hickson, I.D. 2006. DNA helicases required for homologous recombination and repair of damaged replication forks. *Annu. Rev. Genet.* **40:** 279–306.

Wu, L., Bachrati, C.Z., Ou, J., Xu, C., Yin, J., Chang, M., Wang, W., Li, L., Brown, G.W., and Hickson, I.D. 2006. BLAP75/RMI1 promotes the BLM-dependent dissolution of homologous recombination intermediates. *Proc. Natl. Acad. Sci.* **103:** 4068–4073.

### 3.5 MRE11 complex links RECQ5 helicase to sites of DNA damage

**Lu Zheng**, Radhakrishnan Kanagaraj, Boris Mihaljevic, Sybille Schwendener, Alessandro A. Sartori, Bertran Gerrits, Igor Shevelev and Pavel Janscak

Nucleic Acids Research Advance Access published online on March 6, 2009
Nucleic Acids Research, doi:10.1093/nar/gkp147

I identified the interaction between RECQ5 and MRN complex, and performed most of the experiements in the manuscript.

**Nucleic Acids Research Advance Access published March 6, 2009**

*Nucleic Acids Research, 2009, 1–13*
*doi:10.1093/nar/gkp147*

# MRE11 complex links RECQ5 helicase to sites of DNA damage

**Lu Zheng[1], Radhakrishnan Kanagaraj[1], Boris Mihaljevic[1], Sybille Schwendener[1], Alessandro A. Sartori[1], Bertran Gerrits[2], Igor Shevelev[3] and Pavel Janscak[1,3,*]**

[1]Institute of Molecular Cancer Research, University of Zurich, [2]Functional Genomics Center Zurich, UZH/ETH Zurich, Winterthurerstrasse 190, CH-8057 Zurich, Switzerland and [3]Institute of Molecular Genetics, Academy of Sciences of the Czech Republic, Videnska 1083, 14300 Prague, Czech Republic

Received December 22, 2008; Revised and Accepted February 19, 2009

## ABSTRACT

**RECQ5 DNA helicase suppresses homologous recombination (HR) possibly through disruption of RAD51 filaments. Here, we show that RECQ5 is constitutively associated with the MRE11–RAD50–NBS1 (MRN) complex, a primary sensor of DNA double-strand breaks (DSBs) that promotes DSB repair and regulates DNA damage signaling via activation of the ATM kinase. Experiments with purified proteins indicated that RECQ5 interacts with the MRN complex through both MRE11 and NBS1. Functional assays revealed that RECQ5 specifically inhibited the 3′→5′ exonuclease activity of MRE11, while MRN had no effect on the helicase activity of RECQ5. At the cellular level, we observed that the MRN complex was required for the recruitment of RECQ5 to sites of DNA damage. Accumulation of RECQ5 at DSBs was neither dependent on MDC1 that mediates binding of MRN to DSB-flanking chromatin nor on CtIP that acts in conjunction with MRN to promote resection of DSBs for repair by HR. Collectively, these data suggest that the MRN complex recruits RECQ5 to sites of DNA damage to regulate DNA repair.**

## INTRODUCTION

Proteins belonging to the RecQ DNA helicase family are highly conserved from bacteria to mammals. In human cells, five RecQ homologs have been identified and named RECQ1, BLM, WRN, RECQ4 and RECQ5. Inherited defects in the genes encoding for BLM, WRN and RECQ4 have been found to cause distinct autosomal recessive disorders associated with various forms of genomic instability, premature aging and predisposition to cancer (1). Numerous biochemical and cellular studies have shown that the RecQ homologs in human cells have nonredundant roles in the maintenance of genomic stability (2). Several lines of evidence suggest that BLM suppresses crossovers during homologous recombination (HR) by acting in concert with DNA topoisomerase IIIα to catalyze dissolution of double Holliday junctions (3,4). WRN acts specifically at telomeres to promote lagging-strand replication of G-rich telomeric regions, preventing telomere erosion and subsequent recombination (5,6). RECQ4 accumulates on chromatin during initiation of DNA replication to promote loading of replication factors at unwound origins (7,8).

The role of human RECQ5 protein in the maintenance of genomic stability is not well understood. RECQ5 exists in at least three different isoforms resulting from alternative RNA splicing, but only the largest splice variant, RECQ5β, localizes to the nucleus and possesses DNA helicase activity (9 11). Like other RecQ helicases, RECQ5β promotes branch migration of Holliday junctions and exhibits strand-annealing and strand-exchange activities *in vitro* (11,12). It can also disrupt RAD51 presynaptic filaments in a reaction dependent on its ATPase activity and the presence of replication protein A (RPA) (13). In proliferating cells, RECQ5β associates with the replication machinery and accumulates at sites of stalled replication forks (12). Hereafter RECQ5β will be referred to as RECQ5.

Mice lacking the Recql5 gene are viable, but are highly prone to various types of cancer (13). Recql5-deficient

*To whom correspondence should be addressed. Tel: +41 44 635 3470; Fax: +41 44 635 3484; Email: pjanscak@imcr.uzh.ch
Present address:
Lu Zheng, Department of Chemistry, University of Basel, Spitalstrasse 51, CH-4056 Basel, Switzerland

The authors wish it to be known that, in their opinion, the second and third authors should be regarded as joint Second Authors.

cells accumulate Rad51 and γ-H2AX foci and are prone to gross chromosomal rearrangements in response to replication stress (13). Moreover, Recql5 deficiency is associated with a significant increase in the frequency of both spontaneous and DNA-damage-induced HR (13,14). These findings establish Recql5/RECQ5 as a tumor suppressor that plays a role in the control of HR, possibly through disruption of inappropriately formed Rad51 filaments (13).

The MRE11 NBS1 RAD50 (MRN) complex exhibits 3′→5′ exonuclease activity on double-stranded (ds) DNA and endonuclease activity on single-stranded (ss) DNA and hairpin DNA structures in a reaction stimulated by ATP (15). The nuclease active site resides in MRE11, while RAD50 contains a bipartite ATP binding domain split by a long repeat region that fold into an anti-parallel coiled-coil domain (16). The coiled-coil domain of RAD50 can dimerize via a hook structure located on the tip of this domain, which gives the MRN complex the capacity to tether DNA ends (16,17). NBS1 does not possess any enzymatic function, but it enhances the endonuclease activity of the MRE11 RAD50 complex (18).

The MRN complex is required for the maintenance of the integrity of DNA replication forks, double-strand break (DSB) repair, G2/M checkpoint activation, telomere length maintenance and meiotic recombination (15,19). Accumulating evidence suggests that it functions as a DSB sensor activating the ATM-dependent signaling pathway, which coordinates cell cycle arrest with DNA repair (20,21). In higher eukaryotes, null mutations in all components of the MRN complex are lethal (19), while hypomorphic mutations in the human MRE11 and NBS1 genes can give rise to Ataxia telangiectasia-like disorder (ATLD) and Nijmegen breakage syndrome (NBS), respectively, which are characterized by neurological abnormalities, radiosensitivity, genomic instability and cancer predisposition (19).

Here we show that RECQ5 and the MRN complex constitutively associate *in vivo* and colocalize at nuclear foci in response to replication arrest and chromosomal breakage. The interaction between RECQ5 and MRN is direct and can be mediated through both MRE11 and NBS1. We further show that the recruitment of RECQ5 to sites of DNA damage is dependent on MRN. Moreover, biochemical experiments reveal that RECQ5 inhibits the 3′→5′ exonuclease activity associated with the MRE11 protein. Together, these data suggest a functional relationship between RECQ5 and the MRN complex in the cellular response to DNA damage.

## MATERIALS AND METHODS

### Protein purification

The RECQ5 protein was produced in bacteria as fusion with self-cleaving chitin-binding domain (CBD) and purified as described previously (11). *Escherichia coli* RecQ was purified as described (22). Baculoviruses expressing $(His)_6$-MRE11, $(His)_6$-NBS1 and RAD50, respectively, were a kind gift from Dr Vilhelm Bohr. The MRN and MR complexes as well as the individual MRN subunits were produced in Sf9 cells infected with appropriate baculoviruses. Cells harvested at 72 h after infection were suspended in buffer A [50 mM sodium phosphate (pH 7.0), 0.3 M NaCl, 0.5% (v/v) Tween 20, 10% (v/v) glycerol, 2 mM β-mercaptoethanol] supplemented with 20 mM imidazole and 2 mM phenylmethylsulfonylfluoride (PMSF) and disrupted by sonication. Cell extract was clarified by centrifugation at 100 000*g* for 1 h and loaded on a 5-ml HiTrap $Ni^{2+}$-Sepharose column (GE Healthcare) equilibrated with buffer A containing 20 mM imidazole. Bound proteins were eluted with a linear concentration gradient of imidazole (50 ml; 50 350 mM) in buffer A. Fractions containing MRN proteins were pooled, dialyzed against buffer B [20 mM Tris HCl (pH 8.0), 100 mM NaCl, 10% (v/v) glycerol and 1 mM DL-Dithiothreitol (DTT)] and loaded onto a 1-ml HiTrap Q Sepharose FF column (GE Healthcare). Bound proteins were eluted with a linear concentration gradient of NaCl (12 ml; 50 500 mM) in buffer B. The RAD50 protein was purified only via HiTrap Q Sepharose FF column as it was expressed without a histidine tag. Purified proteins were stored at −80°C. The concentration of purified proteins was determined by Bradford assay. The values obtained in Bradford assay were divided by predicted molecular mass of appropriate protein to calculate molar concentration. The MRN complex was assumed to have an 2:2:1 (M:R:N) stoichiometry (23).

### Antibodies

Rabbit polyclonal antibody against the C-terminal portion of RECQ5 (amino acids 675 991) was affinity purified as described previously (12). Additionally, the following commercially available antibodies were used in this study: mouse monoclonal anti-MRE11 antibody, clone 12D7 (Novus Biologicals), mouse monoclonal anti-RAD50 antibody, clone 13B3 (GeneTex), rabbit polyclonal anti-NBS1 antibody, ab-398 (Abcam), mouse monoclonal anti-NBS1 antibody, clone 1D7 (GeneTex), mouse monoclonal anti-γ-H2AX antibody, clone JBW301 (Upstate Biotechnology), rabbit polyclonal anti-TFIIH p89 antibody (S-19), sc-293 (Santa Cruz Biotechnology), mouse monoclonal anti-RAD51 antibody, ab1837 (Abcam), rabbit polyclonal anti-ATM antibody (Abcam), mouse monoclonal anti-RPA antibody (Ab-3), clone RPA34-20 (Calbiochem), mouse monoclonal anti-Cyclin B1 antibody, clone GNS3 (Upstate) and mouse monoclonal anti-CtIP antibody (24).

### Cell culture and generation of DNA damage

U2OS, HeLa and HEK 293T cells were maintained in Dulbecco modified Eagle's medium (DMEM; OmniLab) supplemented with 10% fetal calf serum (FCS; Life Technologies) and streptomycin/penicillin (100 U/ml). Immortalized ATLD1 cells transduced with retrovirus expressing the wild-type MRE11 cDNA (ATLD1-MRE11) or retrovirus harboring the empty vector were a kind gift from Dr Matthew Weitzman (25) and grown in DMEM supplemented with 20% FCS, streptomycin/penicillin (100 U/ml) and 1 μg/ml puromycin (Sigma-Aldrich).

NBS cells stably transfected with vector containing the wild-type NBS1 cDNA (NBS-NBS1) as well as the parental NBS cells (GM7166 VA7) were obtained from Dr Yosef Shiloh and described in (26). Growth medium of complemented NBS cells was supplemented with hygromycin B (100 μg/ml). MDC1$^{+/+}$ and MDC1$^{-/-}$ mouse embryonic fibroblasts (MEFs) were cultured under the same conditions as U2OS cells (27). Where indicated, cells were treated with 2 mM hydroxyurea (HU) for 16 h or with 20 μM cis-diamminedichloroplatinum (CDDP) for 8 h. Laser microirradiation to generate DNA DSBs in defined nuclear volumes was performed using a MMI CELLCUT system containing a UVA laser of 355 nm (Molecular Machines & Industries). Prior to irradiation, cells were grown for 24 h in the presence of 10 μM bromodeoxyuridine (BrdU). Ionizing radiation (IR) was generated using a Faxitron X-ray system. UV irradiation (at a dose of 40 J/m$^2$) was performed in a UV-Stratalinker 1800 equipped with a 254 nm UV lamp (Stratagene). Immediately after exposure to radiation, cells were placed back to incubator and incubated for various periods of time as indicated. For cell cycle analyses, ethanol-fixed cells were stained with propidium iodide (20 μg/ml; Molecular Probes) and subjected to flow cytometry in a Becton Dickinson cell sorter.

### RNA interference

To knock down MRE11 expression in human cells, we employed short-hairpin (sh) RNA technology. The oligonucleotides shRNA-MRE11-top (5′-gatccccacaggagaagagatcaactttcaagagaagttgatctcttctcctgtttttggaaa-3′) and shRNA-MRE11-bottom 5′-agcttttccaaaaaacaggagaagagatcaacttctcttgaaagttgatctcttctcctgtggg-3′) were annealed and ligated into the pSUPER vector (Oligoengine) digested with HindIII and BglII (regions homologous to the MRE11 sequence are underlined in each oligonucleotide). For control RNAi experiments, the oligonucleotides shRNA-C-top (5′-gatccccagacgtgtacacaactagtttcaagagaactagttgtgtacacgtctttttggaaa-3′) and shRNA-C-bottom (5′-agcttttccaaaaaagacgtgtacacaactagttctcttgaaactagttgtgtacacgtctggg-3′) were annealed and processed as above. These oligonucleotides were designed by scrambling of the shRNA-MRE11 sequence within the MRE11 homology region. The resulting plasmid constructs were further modified by introducing a puromycin resistance marker. To do so, the 1.4 kb BamHI/PvuI fragment of pPUR (Clontech) was ligated into the BamHI and SmaI sites of the pSUPER derivatives. The shRNA plasmids were introduced into U2OS cells by liposomal transfection with Metafectene (Biontex) that was carried out essentially according to the manufacturer instructions. At 24 h posttransfection, cell cultures were supplemented with puromycin (2 μg/ml) to enhance the fraction of shRNA-expressing clones. Cells were usually harvested 3 days after addition of puromycin and analyzed as described below.

The nucleotide sequences of CtIP and control (Ctrl) siRNAs and siRNA transfection method were described previously (24).

### Immunofluorescence staining and analyses

Cells grown on cover slips were fixed in methanol for 30 min at −20°C, which was followed by incubation in acetone for 30 s. After blocking in PBS supplemented with 2% FCS (blocking solution), cover slips were incubated overnight at 4°C with appropriate primary antibodies [rabbit polyclonal anti-RECQ5 (1:1000) in combination with either mouse monoclonal anti-RAD50 (1:200) or mouse monoclonal anti-γ-H2AX (1:200); all antibodies were diluted in blocking solution]. After washing with PBS, the cells were incubated with FITC-conjugated sheep anti-rabbit (Sigma; dilution of 1:700) and Texas Red-conjugated donkey anti-mouse (Abcam; dilution of 1:200) secondary antibodies for 1 h at room temperature. The cover slips were then mounted with Vectashield (Vector Labs) and sealed. Images were taken on an Olympus IX81 fluorescence microscope and acquired with a CCD camera (Orca AG, Hamamatsu) using cellR software (Olympus). At least 150 nuclei were analyzed in each experiment.

### Immunoprecipitation assay

Cells grown in a 10-cm dish were subjected to trypsinization, harvested by centrifugation and suspended in 0.5 ml of lysis buffer [50 mM Tris HCl (pH 8.0), 120 mM NaCl, 20 mM NaF, 15 mM sodium pyrophosphate, 0.5 mM sodium orthovanadate and 0.5% (v/v) NP-40] supplemented with a protease inhibitor cocktail (Complete, Mini; Roche). After a 30-min incubation on ice, the lysate was treated with 50 U of RNase-free DNase I (Roche) at 25°C for 30 min, and clarified by centrifugation. Cell extracts (1 mg) were incubated overnight at 4°C with purified rabbit anti-RECQ5 IgGs (1 μg) or with IgGs purified from pre-immune serum (1 μg). Immune complexes were subsequently incubated with protein A/G-agarose beads (20 μl, Santa Cruz Biotechnology) for 1 h at 4°C. After extensive washing with lysis buffer, beads were boiled in SDS PAGE loading buffer (25 μl) for 10 min to release bound proteins. Immunoprecipitates were analyzed by western blotting. For mass spectrometry (MS) analysis, the immunoprecipitation protocol was scaled up to include 10 mg of total protein. The eluates from protein A/G agarose beads were concentrated using a speed-vac before loading on a 7.5% (w/v) SDS-polyacrylamide gel.

### Liquid chromatography-MS/MS analysis

SDS PAGE gel was stained with Coomassie Brilliant Blue and sample lanes were cut into 10 slices. Each slice was further diced into smaller cubes (1 mm) and subjected to two cycles of rehydration in 50 mM ammonium bicarbonate ($NH_4HCO_3$) and dehydration in 80% (v/v) acetonitrile. Gel pieces were then incubated with 37 mM DTT solution at 50°C for 30 min. After two additional rounds of dehydration in 80% (v/v) acetonitrile, gel pieces were incubated with 20 mM iodoacetamide for 15 min in dark for protein alkylation. After another three rounds of rehydration in 50 mM $NH_4HCO_3$ and shrinking in 80% (v/v) acetonitrile, the gel pieces were incubated with freshly

diluted trypsin solution (12.5 ng/μl) at 37°C for 4 h and then at 25°C overnight. Digested peptides were finally extracted by 0.1% formic acid (one time) and 80% (v/v) acetonitrile (three times) after which extracts were dried under vacuum. The tryptic peptides were analyzed on a Finnigan LCQ Deca (ThermoFisher, Basel Switzerland). Prior to MS analysis, peptides were separated by an online high-pressure liquid chromatograph (Agilent, Palo Alto, CA) on a $C_{18}$ reverse phase column using acetonitrile/water system. MS/MS spectra were searched against the human portion (taxonomy ID: 9606) of the UniProt database (http://www.uniprot.org). The peptides identified were interrogated using the Mascot search algorithm (28). Mascot protein score of >45 was considered significant. Individual ions scores >41 indicate identity or extensive homology ($P < 0.05$).

### CBD pull-down assay

CBD-tagged RECQ5 was produced in *E. coli* BL21-CodonPlus(DE3)-RIL cells (Stratagene) as previously described (11). Cells harvested from a 10-ml culture were resuspended in 1 ml of NET-150 buffer [10 mM Tris (pH 8.0), 1 mM EDTA, 150 mM NaCl, 10% (v/v) glycerol and 0.1% (v/v) Triton X-100] supplemented with a protease inhibitor cocktail (Complete, Mini; Roche) and disrupted by sonication followed by centrifugation at 20 000*g* for 45 min. Clarified cell extract (typically 50 μl) was incubated with 20 μl of chitin beads (NEB) in a total volume of 400 μl of NET-150 buffer for 2 h at 4°C. After extensive washing with NET-150 buffer, beads were incubated with recombinant MRN proteins (1 μg) in 400 μl of NET-150 buffer supplemented with ethidium bromide (50 μg/ml) for 2 h at 4°C. Bound proteins were analyzed by western blotting.

### Strand exchange assay

Strand exchange assays with RECQ5 were performed essentially as described previously (12). Briefly, reactions were carried at 37°C in buffer containing 20 mM Tris acetate (pH 7.9), 50 mM KOAc, 10 mM $Mg(OAc)_2$, 1 mM DTT and 50 μg/ml BSA. 1 nM DNA substrates (60-mer/30-mer partial duplex and complementary 60-mer oligonucleotide, of which the former 60-mer oligonucleotide was radiolabeled at 5′ end) were preincubated with 40 nM RECQ5 for 10 min to form a forked duplex. RECQ5-mediated strand exchange between the arms of the fork was initiated by addition of ATP (2 mM). Where required, the annealing mixture was preincubated with 40 nM MRN complex for 5 min prior to addition of ATP. Aliquots (5 μl) from different reaction time points were subjected to electrophoresis in 10% nondenaturing polyacrylamide gel (acrylamide/bis-acrylamide 19:1) run in 1xTBE buffer at 140 V. Gels were dried and subjected to phosphor-imaging analysis using a Typhoon 9400 scanner.

### Nuclease assay

The 3′→5′ exonuclease activity of the MR(N) complex was measured using a 5′-tailed oligoduplex prepared by annealing of a 30-mer oligonucleotide (5′-ggagtaaagt actaggtatgtcgacattga-3′) to the 3′-half of a 60-mer oligonucleotide (5′-gaggtcactccagtgaattcgagctcgcagtcaatgtcgac atacctagtactttactcc-3′). The 30-mer oligonucleotide was radiolabeled at the 5′-end prior to annealing. Reactions were conducted at 37°C in buffer containing 30 mM MOPS (pH 7.0), 25 mM KCl, 1 mM DTT, 2 mM $MnCl_2$, 2 mM ATP and 50 μg/ml BSA. Reaction mixtures contained 1 nM DNA substrate, 40 nM MR(N) and varying concentrations of RECQ5 or *E. coli* RecQ, ranging from 0 to 80 nM. MR(N) and RECQ5 (or RecQ) were preincubated for 5 min on ice before adding to the DNA substrate. Reactions were terminated after 30 min by adding an equal volume of stop solution [80% (v/v) formamide, 10 mM EDTA, 0.1% (w/v) bromophenol blue and 0.1% (w/v) xylene cyanol] and heating at 95°C for 5 min. Reaction aliquots were subjected to electrophoresis in 15% (w/v) polyacrylamide gel containing 8 M urea (acrylamide/bis-acrylamide 19:1) run in 1xTBE buffer at 300 V. Gels were dried and subjected to phosphor-imaging analysis using a Typhoon 9400 scanner. DNA bands in the gel images were quantified using ImageQuant software (Molecular Dynamics).

## RESULTS

### Physical interaction between RECQ5 and the MRN complex

To identify proteins associated with RECQ5 *in vivo*, we performed large-scale immunoprecipitation combined with mass spectrometric analysis. Using affinity-purified rabbit polyclonal anti-RECQ5 antibody, we immunoprecipitated RECQ5 from whole cell extract of HEK 293T cells containing 10 mg of protein. IgG purified from pre-immune serum was used as the negative control. The immunoprecipitated proteins were separated by SDS PAGE and visualized by Coomassie Blue staining (Figure S1). The lane containing RECQ5 immunoprecipitate was cut into 10 slices and proteins in each slice were identified by MS as described in Materials and Methods section. This analysis revealed a number of potential RECQ5 interactors involved in DNA metabolism (Figure S1 and Table 1). Our attention was in particular drawn to the MRN complex, a nuclease that plays a pivotal role in the recognition and repair of DSBs (20,21).

To verify the MS data, the RECQ5 immunoprecipitate from 293T cells was subjected to western blot analysis using antibodies against the individual MRN subunits. We found that this immunoprecipitate contained a large fraction of the endogenous MRN proteins, whereas the control immunoprecipitate obtained with IgG isolated from a pre-immune rabbit serum was devoid of these proteins (Figure 1A, compare lanes 1 3). The amount of MRN detected in RECQ5 immunoprecipitates from cell lysates pre-treated with DNaseI or ethidium bromide was comparable with that detected in RECQ5 immunoprecipitate from nontreated lysate, indicating that the observed association of RECQ5 with MRN proteins is DNA independent (Figure 1A; compare lanes 3, 4 and 5). We also

**Table 1.** A selection of proteins identified by mass spectrometric analysis of the RECQ5 immunoprecipitate from 293T cells

| Protein | Swiss-Prot entry | Sequence coverage (%) | Number of peptides | Mascot protein score[a] |
|---|---|---|---|---|
| RECQ5[b] | O94762 | 18.0 | 57 | 347 |
| MRE11[b] | P49959 | 13.7 | 43 | 257 |
| RAD50[b] | Q92878 | 20.1 | 120 | 253 |
| NBS1[b] | O60934 | 6.1 | 18 | 157 |
| DNA-dependent protein kinase catalytic subunit (DNA-PKcs)[b] | P78527 | 15.5 | 160 | 1354 |
| RECQ4[b] | O94761 | 5.2 | 26 | 111 |
| MCM7[b] | P33993 | 20.4 | 44 | 251 |
| RNA polymerase II largest subunit RPB1[b] | P24928 | 25.6 | 240 | 1602 |
| RNA polymerase II subunit 2 (RPB2) | P30876 | 12.7 | 43 | 315 |
| Nucleolin | P19338 | 11.4 | 13 | 109 |
| E3 ubiquitin–protein ligase EDD1 (UBR5) | O95071 | 3 | 25 | 370 |

[a]Mascot protein score of >45 was considered significant.
[b]Confirmed by immunoblotting (IB).
The full list is available upon request.

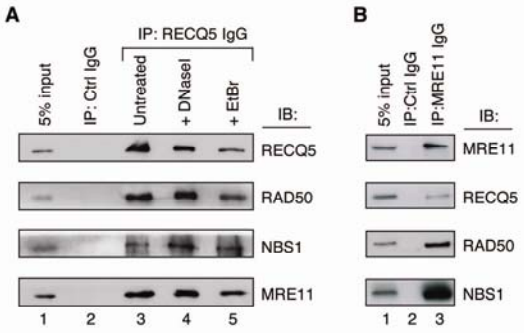


**Figure 1.** RECQ5 associates with the MRN complex *in vivo*. (**A**) Co-immunoprecipitation of the MRE11, RAD50 and NBS1 proteins with RECQ5 from total extract of 293T cells (1 mg of protein). Lane 1, 5% of the input material; lane 2, immunoprecipitation using IgG (1 μg) isolated from a preimmune serum; lane 3, immunoprecipitation with affinity-purified rabbit anti-RECQ5 antibody (1 μg); lane 4, the same as lane 3, but the extract was pretreated with DNase I (50 U) for 30 min at 25°C; lane 5, the same as lane 3, but extract was supplemented with ethidium bromide (50 μg/ml). (**B**) Co-immunoprecipitation of RECQ5 with the MRE11 protein from total extract of HeLa cells. Lane 1, 5% of the input material; lane 2, immunoprecipitation using IgG (1 μg) isolated from a preimmune serum; lane 3, immunoprecipitation using mouse monoclonal anti-MRE11 antibody (1 μg). (**A** and **B**) Immunoprecipitated proteins were analyzed by SDS–PAGE followed by IB using antibodies described in Materials and Methods section.

performed a reciprocal co-immunoprecipitation experiment using anti-MRE11 antibody. We found that MRE11 immunoprecipitate from HeLa cells contained a significant amount of RECQ5 (Figure 1B). Collectively, these data indicate that a fraction of the MRN complex stably associates with RECQ5 *in vivo*.

Next, we compared the levels of the MRE11 protein in RECQ5 immunoprecipitates from cells exposed with various genotoxic agents including HU, IR and CDDP. This experiment revealed that the cellular level of the RECQ5–MRN complex is not significantly affected by DNA damage, suggesting that DNA damage does neither induce nor prevent the formation of the RECQ5–MRN complex *in vivo* (Figure S2A, compare lanes 2–4 with lane 1). We also examined the levels of RECQ5–MRN complex at different stages of the cell cycle. To do so, U2OS cells were synchronized at G1/S transition by HU treatment and then released into drug-free medium. Cells were collected at different time points after the removal of HU and subjected to immunoprecipitation with anti-RECQ5 antibody. In a parallel experiment, cell populations from the individual time points were subjected to FACS analysis to determine the stage of the cell cycle (Figure S2C). We found that the level of the RECQ5–MRN complex remained constant throughout the cell cycle, suggesting a constitutive association (Figure S2B).

To determine whether RECQ5 and MRN interact directly, we performed affinity pull-down assays with purified recombinant proteins. RECQ5 was expressed in bacteria as a fusion with a CBD tag and bound to chitin beads. The beads were subsequently incubated with purified MRN and MR complexes, respectively, that were produced in insect cells by means of baculovirus system. We found that both complexes were avidly bound to RECQ5 beads, but not to control beads coated with CBD, suggesting that the interaction between RECQ5 and MRN observed *in vivo* is direct and independent of NBS1 (Figure 2A).

In an attempt to further define the interaction site for RECQ5 on the MRN complex, we tested individually purified MRN subunits for binding to RECQ5–CBD beads. Interestingly, we found that both MRE11 and NBS1, but not RAD50, were bound to RECQ5, suggesting that the interaction between RECQ5 and the MRN complex is mediated not only by MRE11 but also by NBS1 (Figure 2B). To substantiate these findings, we performed immunoprecipitation experiments with total cell extracts from NBS and ATLD1 cells carrying hypomorphic mutations in the *NBS1* and *MRE11* genes, respectively. We found that the RECQ5 immunoprecipitate from NBS cells contained both MRE11 and RAD50 proteins in similar concentrations as the RECQ5 immunoprecipitate

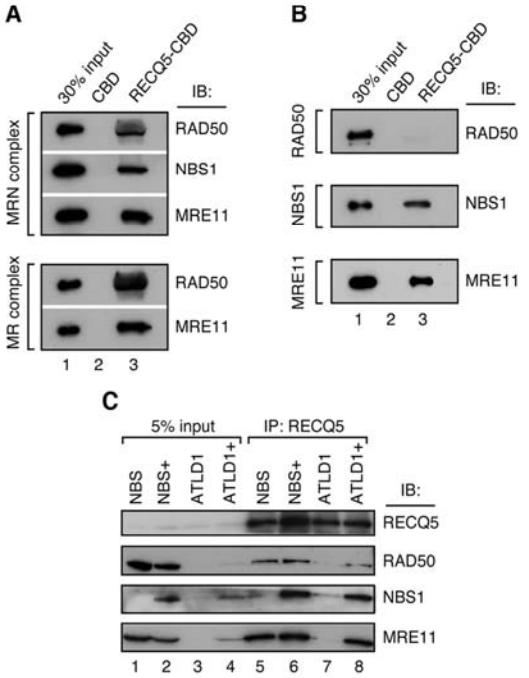


**Figure 2.** RECQ5 and the MRN complex interact directly. (**A**) Binding of purified MRN ('top panel') and MR ('bottom panel') complexes to chitin beads coated with RECQ5–CBD fusion. (**B**) Binding of individually purified RAD50 ('top panel'), NBS1 ('middle panel') and MRE11 ('bottom panel') proteins to chitin beads coated with RECQ5–CBD fusion. For (**A**) and (**B**): lane 1, 30% of input material; lane 2, chitin beads coated with CBD; lane 3, chitin beads coated with RECQ5–CBD fusion protein. Binding reactions were carried out as described in Materials and Methods section. (**C**) Western blot analysis of RECQ5 immunoprecipitates from total extracts of the following cells: NBS (NBS1 deficiency), NBS1+ (NBS complemented by stable transfection of the NBS1 cDNA), ATLD1 (MRE11 deficiency) and ATLD1+ (ATLD1 complemented by stable transfection of the MRE11 cDNA). Lanes 1–4, 5% of the input material as indicated, lanes 5–8, RECQ5 immunoprecipitates from total extracts (1 mg of protein) of the indicated cells. Blots were probed for the presence of RECQ5, MRE11, RAD50 and NBS1 using antibodies described in Materials and Methods section.

from NBS cells complemented with the wild-type NBS1 cDNA, confirming that RECQ5 binds to the MR complex in a manner independent of NBS1 (Figure 2C, lanes 1, 2, 5 and 6). In ATLD1 cells, the levels of NBS1 and RAD50 proteins were dramatically reduced as previously reported (29). However, a small amount of NBS1 could still be detected in the RECQ5 immunoprecipitate from these cells, indicating that NBS1 can interact with RECQ5 in absence of MRE11 (Figure 2C, lane 7). In MRE11-complemented ATLD1 cells, expression of all three subunits of the MRN complex could again be readily detected by western blot (Figure 2C, lane 4). Accordingly, the RECQ5 immunoprecipitate from total extract of these cells was found to contain substantial amounts of all three MRN proteins (Figure 2C, lane 8).

### RECQ5 inhibits the 3′→5′ exonuclease activity of MRN complex

Next, we investigated whether the interaction between RECQ5 and the MRN complex affects the biochemical activities of these proteins. The SDS–PAGE profile of the purified proteins used in this study is shown in Figure S3. First, we tested the effect of MRN on the helicase activity of RECQ5. Previous studies demonstrated that RECQ5 displays a poor 3′→5′ helicase activity on oligonucleotide-based partial duplexes due to a strong strand-annealing activity residing in the C-terminal half of RECQ5 (11). However, RECQ5 could efficiently displace the lagging-strand oligonucleotide from synthetic forked structures with homologous arms where reannealing of this oligonucleotide is prevented by annealing of the parental strands (12). Thus, we evaluated the effect of the MRN complex on this strand-exchange reaction. We found that the rate of RECQ5-mediated strand-exchange was not altered upon addition of the MRN complex, suggesting that the MRN complex does not modulate the helicase activity of RECQ5 (Figure S4).

Since the MRN complex has been shown to possess 3′→5′ exonuclease activity (15), we tested the effect of RECQ5 on MRN-mediated exonucleolytic processing of a 30-bp duplex with a 5′-ssDNA tail containing 30 nt. Our initial experiments showed that the MRN complex required manganese and ATP as cofactors to exhibit efficient 3′→5′ exonuclease activity on this DNA substrate (data not shown), which is consistent with previously published data (18,30). Addition of RECQ5 to this reaction resulted in a significant decrease in the exonuclease activity of MRN (Figure 3A, lanes 3–7, and 3C). We did not observe the same effect with the *E. coli* RecQ helicase, excluding the possibility that the inhibition of the MRE11 nuclease by RECQ5 results from competition between these proteins for the DNA substrate (Figure 3B, lanes 3–7, and 3C).

To investigate whether the inhibition of exonuclease activity of MRN by RECQ5 is dependent on the presence of the NBS1 protein, we evaluated the effect of RECQ5 on the exonuclease activity of the MR complex. The MR complex displayed a similar exonuclease activity as the MRN complex (Figure 3A and B, compare lanes 3 and 8, and C). Most importantly, RECQ5, but not RecQ, was found to inhibit the MR-mediated exonucleolytic processing (Figure 3A and B, lanes 8–12, and C).

Collectively, these data indicate that RECQ5 inhibits the exonuclease activity of MRN most likely as a result of its binding to MRE11.

### RECQ5 and the MRN complex colocalize at sites of DNA damage

To explore a potential role for RECQ5–MRN interaction in the maintenance of genomic stability, we analyzed the spatial relationship of these proteins in the nucleus of U2OS cells in response to various types of DNA damage including stalled replication forks, DNA adducts and DSBs. After individual DNA-damaging treatments, cell were fixed with methanol, co-immunostained with anti-RECQ5 and anti-RAD50 antibodies and analyzed

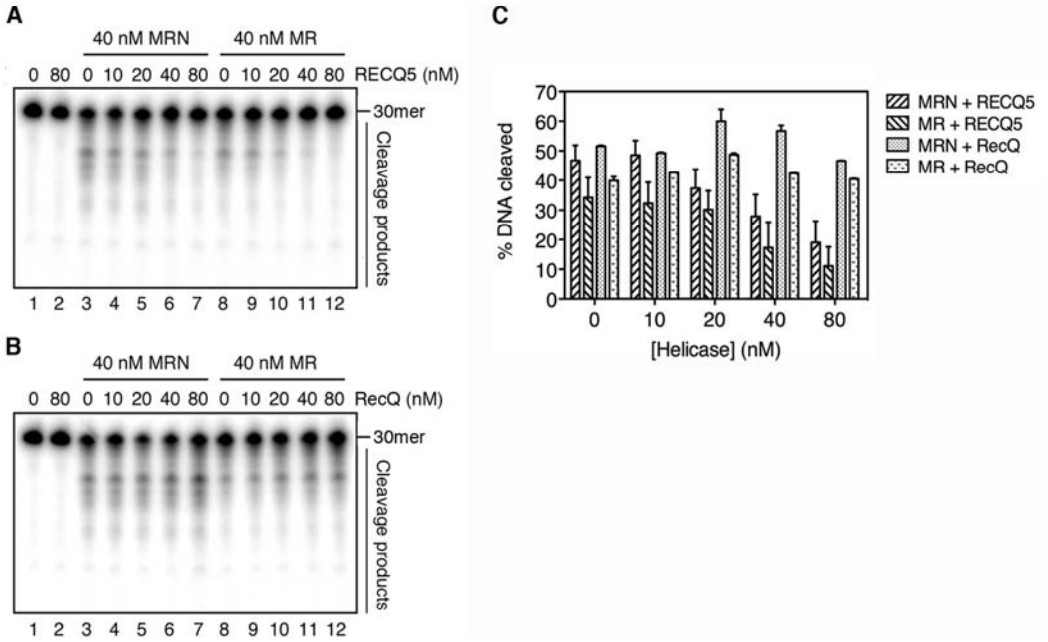


**Figure 3.** RECQ5 inhibits the 3′→5′ exonuclease activity of MR(N). (**A**) Effect of RECQ5 on the 3′→5′ exonuclease activity of MRN (lanes 3–7) and MR (lanes 8–12). (**B**) Effect of *E. coli* RecQ on the 3′→5′ exonuclease activity of MRN (lanes 3–7) and MR (lanes 8–12). In (**A**) and (**B**), reaction mixtures were incubated at 37°C for 30 min, and contained 1 nM 5′-tailed oligoduplex substrates (60-mer/30-mer with a 5′-$^{32}$P label on the shorter strand), 40 nM MRN or MR and various concentrations of RECQ5 or RecQ as indicated. Reaction products were analyzed by denaturing PAGE followed by phosphorimaging as described in Materials and Methods section. (**C**) Quantification of the gels shown in (**A**) and (**B**). Intensity of the DNA substrate band in each lane was measured using ImageQuant software. The obtained values were used to calculate the percentage of cleaved DNA. The values obtained for the reactions carried out in the absence of MR(N) were taken as 100% in these calculations. The data points represent the mean of three independent experiments.

by fluorescence microscopy. As expected, in majority of unperturbed cells, both RECQ5 and RAD50 were uniformly distributed in the nucleus (Figure 4A, top row). After HU treatment, which results in replication arrest due to depletion of deoxyribonucleotides, both RECQ5 and RAD50 formed bright nuclear foci that extensively colocalized in >70% of cells (Figure 4A, middle row). Moreover, RECQ5 and RAD50 partially colocalized after exposure of cells to UVC light (40 J/m$^2$) that can stall the progression of replication forks through induction of bulky DNA lesions (Figure 4A, bottom row). Thus, it is possible that RECQ5 and the MRN complex cooperate in the processing of stalled replication forks.

To generate DSBs, U2OS cells were presensitized by incorporation of BrdU into genomic DNA and then locally exposed to UVA light (355 nm) using micro-laser technology, which results in linear tracks of DSBs across each irradiated nucleus (31). These tracks can be detected by immunofluorescence imaging of phosphorylated histone H2AX (γ-H2AX) that is rapidly generated in the DSB-flanking chromatin by the ATM kinase (32). We found that RECQ5 started to accumulate at DSB tracks as early as 15 min after irradiation, reaching maximal levels at about 30 min after irradiation, and persisted at those sites as long as 1 h after irradiation (Figure 4B, top panel). Double staining for RECQ5 and RAD50 further confirmed these findings (Figure 4B, bottom panel).

Like MRN, RECQ5 was found to accumulate at microirradiated areas essentially in all γ-H2AX-positive cells (150 cells evaluated), suggesting that the recruitment of RECQ5 to DSBs is not restricted to any particular phase of the cell cycle. To confirm this assumption, microirradiated cells were doubly stained for RECQ5 and cyclin B1. We found that RECQ5 accumulated in the microirradiated nuclear regions in cyclin B1-positive cells (cells in S and G2) as well as in cells lacking any detectable amount of cyclin B1 (cells in G1) (Figure 4C). These data indicate that RECQ5 accumulates at DSBs throughout the interphase.

### The MRN complex is required for the recruitment of RECQ5 to sites of replication arrest

As the MRN complex is well known to function as a DNA damage sensor, we tested the possibility that it mediates the recruitment of RECQ5 to sites of DNA damage. First, we evaluated the effect of MRE11 deficiency on the focal distribution of RECQ5 after HU treatment. To do so, we silenced the expression of the *MRE11* gene in U2OS cells

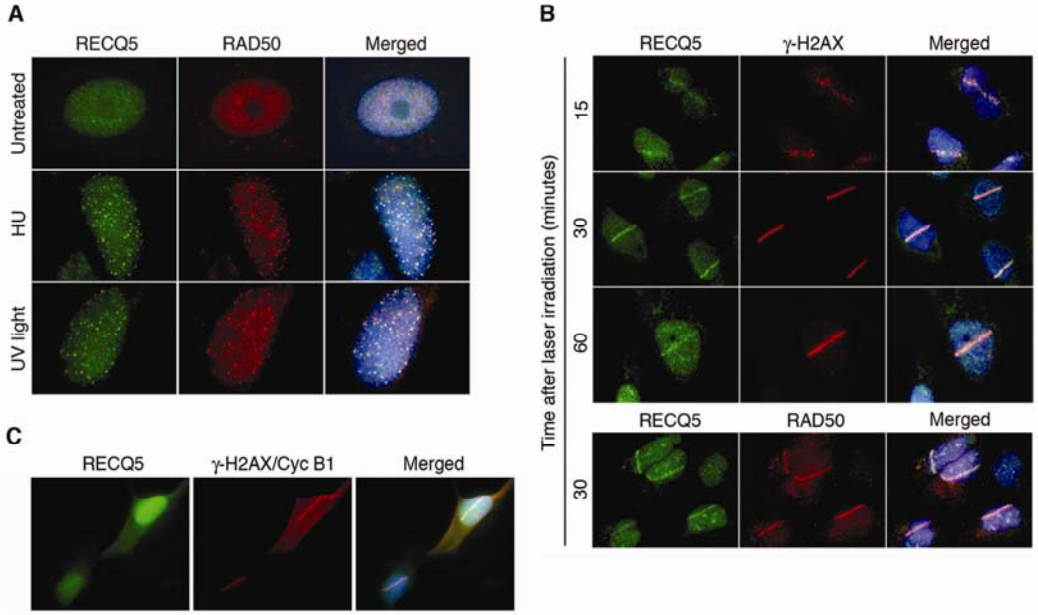


**Figure 4.** RECQ5 and RAD50 colocalize at sites of DNA damage. (**A**) Indirect immunofluorescence imaging of RECQ5 and RAD50 in U2OS cells prior to and after DNA replication arrest. Cells were either left untreated or incubated in the presence of HU for 16 h or exposed to UV light at a dose of 40 J/m$^2$ followed by incubation for 6 h. After genotoxic treatments, cells were fixed with methanol and triply stained for RECQ5 (green), RAD50 (red) and DNA (blue) as described in Materials and Methods section. Overlap between the green and red signals in merged images appears yellow. (**B**) RECQ5 and RAD50 accumulate at laser-induced DNA DSBs. U2OS cells were sensitized with BrdU (10 μM; incubation for 24 h) and subjected to microirradiation with pulsed UVA laser (λ = 355 nm) to generate linear tracks of DSBs. At indicated time points after irradiation, cells were fixed with methanol and co-immunostained either with anti-RECQ5 (green) and anti-γ-H2AX (red) antibodies or with anti-RECQ5 (green) and anti-RAD50 (red) antibodies as indicated. DAPI (blue) was used to stain nuclei. (**C**) U2OS cells were treated as in (**B**) and 30 min postirradiation, co-immunostained with antibodies against RECQ5, γ-H2AX (to detect microirradiated tracks) and cyclin B1 (to reveal cells in S/G2). γ-H2AX and cyclin B1 are displayed in the same channel (red). DAPI (blue) was used to stain nuclei.

using shRNA. We observed a dramatic reduction in the cellular level of MRE11 protein following puromycin selection for cells expressing anti-MRE11 shRNA construct, whereas no reduction in MRE11 levels was observed in cells harboring the control construct expressing a scrambled shRNA (Figure 5A). Depletion of MRE11 by shRNA also dramatically reduced the cellular level of RAD50, which is consistent with low levels of RAD50 found in ATLD1 cells, but it did not affect the level of RECQ5 (Figure 5A, lane 2 and Figure 2C, lane 3). Importantly, we found that shRNA-mediated depletion of MRE11 in U2OS cells completely abolished the formation of RECQ5 foci after HU treatment (Figure 5B, top panel). In contrast, HU-treated U2OS cells expressing the control shRNA contained both RECQ5 and RAD50 foci that showed extensive colocalization (Figure 5B, bottom panel, top row). Essentially the same results were obtained with ATLD1 and ATLD1-MRE11 cells (Figure 5C).

Further, the MRE11-proficient and MRE11-deficient cells were doubly stained for RECQ5 and γ-H2AX. Histone H2AX is phosphorylated in response to replication arrest in ATR-dependent manner and forms nuclear foci that colocalize with PCNA and hence can serve as markers for stalled replication forks (33,34). As expected, in 70% of MRE11-proficient cells treated with HU, RECQ5 extensively colocalized with γ-H2AX at bright nuclear foci (Figure 5B and C, bottom panels, bottom rows). MRE11-deficient cells also displayed γ-H2AX foci in response to HU treatment (Figure 5B and C, top panels, bottom rows). However, RECQ5 foci were not seen in these cells.

### The MRN complex is required for the recruitment of RECQ5 to DSBs

To evaluate whether MRE11 is required for the recruitment of RECQ5 to DSBs, we microirradiated ATLD1 cells with UVA laser and stained them for RECQ5 and γ-H2AX at 30 min after irradiation. We found that none of γ-H2AX-positive ATLD1 cells contained RECQ5 tracks (Figure 6, top panel). In contrast, accumulation of RECQ5 at irradiated areas was seen in ATLD1-McRE11 cells (Figure 6, top panel). Collectively, these data indicate that the recruitment of RECQ5 to DSBs is dependent on a functional MRN complex.

The MRN complex has multiple functions in the cellular response to DSBs. Following activation of the ATM kinase by MRN bound to DNA ends, more MRN accumulates in large chromatin domains flanking DSBs, which

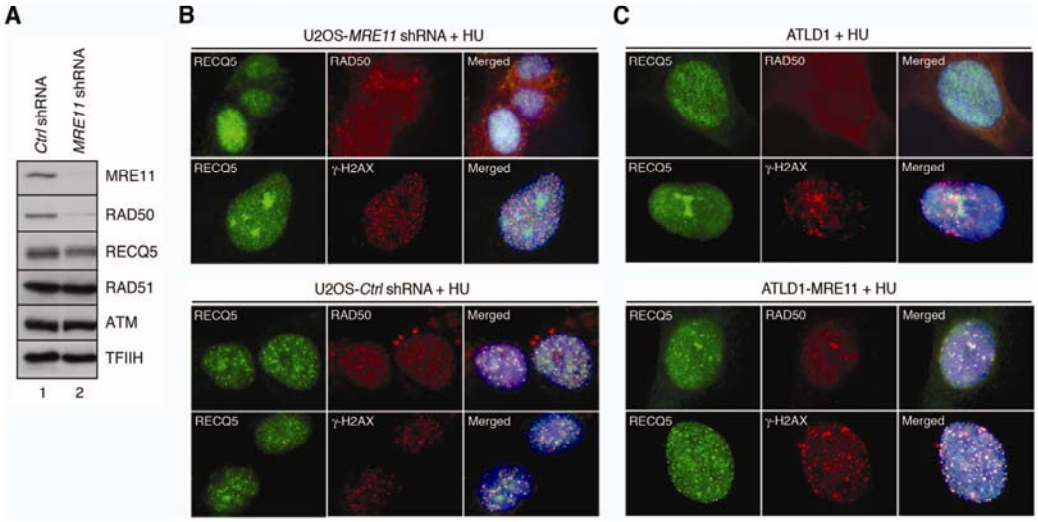


**Figure 5.** MRE11 is required for the recruitment of RECQ5 to arrested replication forks. (**A**) Western blot analysis of extracts of U2OS cells expressing indicated shRNAs. Cells were transfected with appropriate shRNA vector and subjected to puromycin selection for 3 days to enrich the population of transfected cells. Blots were probed for MRE11, RAD50, RECQ5, RAD51, ATM and TFIIH (loading control) using antibodies described in Materials and Methods section. Lane 1, extract from cells expressing control shRNA (*Ctrl* shRNA); lane 2, extract from cells expressing shRNA targeting the MRE11 transcript (*MRE11* shRNA). (**B**) Effect of shRNA-mediated depletion of MRE11 in U2OS cells on nuclear distribution of RECQ5 in response to HU. Cells were transfected either with the plasmid expressing *Ctrl* shRNA ('bottom panel') or the plasmid expressing *MRE11* shRNA ('top panel'), followed by puromycin selection. Two days after addition of puromycin, HU was added to a final concentration of 2 mM. After 16 h, cells were fixed and co-immunostained either for RECQ5 (green) and RAD50 (red) or for RECQ5 (green) and γ-H2AX (red) as indicated. (**C**) Nuclear distribution of RECQ5 in ATLD1 ('top panel') and ATLD1-MRE11 ('bottom panel') cells after replication arrest by HU. Exponentially growing cells were treated with 2 mM HU for 16 h and then fixed and co-immunostained either for RECQ5 (green) and RAD50 (red) or for RECQ5 (green) and γ-H2AX (red) as indicated.

is likely to enhance the DSB-induced signal by means of a positive feedback loop (32). Recruitment of MRN to DSB-flanking chromatin is critically dependent on MDC1 that forms a complex with MRN in a manner dependent on CK2 phosphorylation and directly interacts with γ-H2AX in the damaged chromatin (35–38). To address whether MDC1 is required for the recruitment of RECQ5 to sites of DSBs, we compared DSB-induced nuclear trafficking of RECQ5 in $MDC1^{+/+}$ and $MDC1^{-/-}$ MEFs. We found that MDC1 deficiency had no effect on the recruitment of RECQ5 to laser-induced DSB tracks (Figure 6, middle panel). Although this finding does not exclude the possibility that a fraction of the RECQ5 protein associate with DSB-flanking chromatin as a part of the MRN–MDC1 complex, it argues that MRN recruits RECQ5 to broken DNA ends. In both MDC1-proficient and MDC1-deficient MEFs, >97% of irradiated nuclei (out of at least 100 nuclei) contained RECQ5-positive tracks, further supporting the notion that RECQ5 associates with DSBs in a cell-cycle independent manner (data not shown).

MRN, in conjunction with CtIP, promotes resection of DSBs that arise during S/G2 phases of the cell cycle, generating 3′-ssDNA tails for HR repair (24). To address the question whether the recruitment of RECQ5 to DSBs occurs as a consequence of DSB resection, we depleted CtIP from U2OS cell by means of RNA interference (Figure S5A). Cells were fixed at 30 min after laser microirradiation and stained with anti-RECQ5 in combination with either anti-γ-H2AX or anti-RPA antibodies. We found that CtIP depletion had no effect on accumulation of RECQ5 at DSB tracks (Figure 6, bottom panel). In contrast, accumulation of RPA at microirradiated areas was completely abolished upon CtIP depletion (Figure S5B) as previously reported (24). These data indicate that the observed MRE11-dependent accumulation of RECQ5 at DSB sites is not dependent on DSB resection.

## DISCUSSION

HR provides the most accurate mechanism for the repair of DSBs and ssDNA gaps which frequently occur in the cell as a result of collision of the DNA replication machinery with DNA lesions and other obstacles or as a result of processing of DNA lesions by DNA repair enzymes (39,40). In mitotic cells, most recombination intermediates are processed through pathways such as synthesis-dependent strand annealing (SDSA) or double-Holliday junction (dHJ) dissolution that do not result in crossovers. These mechanisms are important for avoidance of potentially deleterious chromosomal rearrangements that can arise if the homologous sequence used for HR-mediated repair is located at different chromosomal locus. A key step in HR is the formation of a RAD51-ssDNA filament

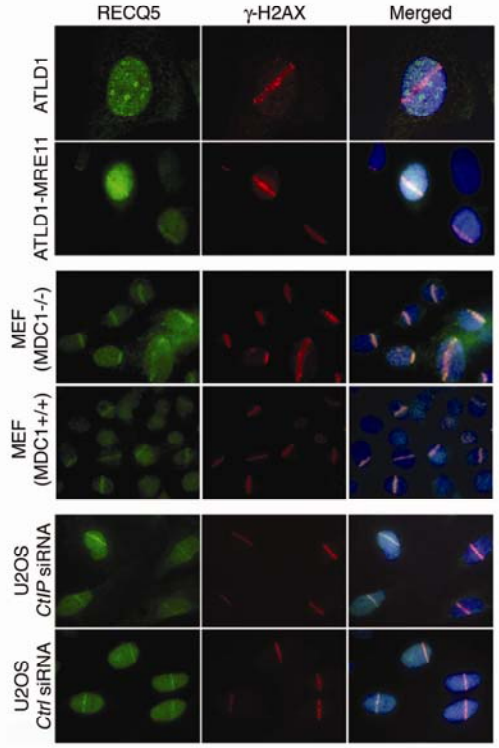


**Figure 6.** MRE11, but not MDC1 and CtIP, is required for the recruitment of RECQ5 to laser-induced DSBs. Indicated cell lines were irradiated with UVA laser at 24 h following addition of BrdU (10 μM), fixed at 30 min after the irradiation and co-immunostained to visualize RECQ5 (green) and γ-H2AX (red). DAPI (blue) was used to stain nuclei. For U2OS cell cultures, BrdU was added 2 days after transfection of *CtIP* or control (*Ctrl*) siRNA.

that mediates the search for sequence homology and associates with the donor sequence forming the so-called D-loop structure (39). Recent studies indicated that the RECQ5 DNA helicase counteracts the formation of crossovers during HR (13,14). Moreover, it has been shown that RECQ5 has the ability to disrupt RAD51 nucleoprotein filaments *in vitro* (13). However, the importance of this activity in the regulation of HR *in vivo* still remains to be explored. Furthermore, it is not clear by now how RECQ5 is recruited to the sites of HR.

Here we show that RECQ5 interacts with the MRN complex, a key player in the repair of DNA damage by HR. Our results suggest that this interaction is mediated through MRE11 and NBS1. At the biochemical level, RECQ5 specifically inhibited the 3′→5′ exonuclease activity of the MRN and MR complexes, suggesting that RECQ5 interacts with the nuclease or DNA-binding domains of MRE11 thereby impairing the access of MRE11 to the DNA substrate. At the cellular level, MRE11 was required for the accumulation of RECQ5 at sites of arrested replication forks and sites of DSBs. Interestingly, recruitment of RECQ5 to DSBs was not dependent on MDC1, which mediates chromatin retention of MRN at sites of DNA damage (35,36). Moreover, RECQ5 accumulation at DSBs was not affected upon depletion of CtIP, indicating that it is not dependent on the DNA-end resection of DSBs in S/G2 generating 3′-ssDNA tails to initiate repair by HR (24). Instead, our data argue that RECQ5 migrates to and acts at broken DNA ends as a part of the MRN complex.

In the budding yeast *Saccharomyces cerevisiae*, the formation of crossovers during HR is counteracted mainly by the Srs2 DNA helicase, which has no obvious sequence homologs in higher eukaryotes (41,42). Like RECQ5, Srs2 has the capacity to disrupt Rad51 filaments formed on ssDNA (43,44). Srs2 also shows preference for unwinding of D-loop structures, and its helicase activity is stimulated by Rad51 filaments on dsDNA, supporting the proposed role for Srs2 in promoting SDSA (45). Strikingly, Srs2 has been shown to physically interact with the DNA-binding domain of Mre11 (46). This, together with our finding of a physical interaction between RECQ5 and the MRN complex in human cells, lends further support to the hypothesis that RECQ5 is a functional ortholog of Srs2 (13). Moreover, our data might explain how these anti-recombinases are delivered to sites of DNA repair. However, the precise role of the MRN complex in the function of these proteins during HR still remains to be addressed.

Interestingly, we have found that RECQ5 accumulates at DSBs throughout the interphase. A recent study demonstrated that RAD51 accumulates at laser-induced damage sites not only in S/G2 phase, where DSBs are repaired by HR, but also in G1 phase where HR repair is suppressed (47). Thus, it is possible that one function of RECQ5 is to prevent RAD51-mediated HR events in G1 cells that could lead to detrimental chromosomal rearrangements because of the lack of an undamaged sister chromatid.

We found that MRE11 was required for the RECQ5 focus formation in response to replication arrest by HU. Given the role for MRN as a DSB sensor, one can assume that these foci represent broken replication forks undergoing HR repair. However, HU-induced DNA DSBs become apparent only after 24 h of continuous HU treatment (48). In contrast, RECQ5 foci could readily be observed at 16 h following addition of HU, suggesting that they rather represent sites of stalled replication forks. Previous studies indicated that the MRN complex is associated with replication forks throughout S-phase via phosphorylation-dependent interaction with RPA (49–51). It was also shown that the MRN complex colocalizes with RPA in response to replication arrest by HU (48,52). Thus, it is possible that the MRN complex tethers RECQ5 to ssDNA regions generated at stalled replication forks to prevent formation of RAD51 filaments and subsequent DNA recombination. Such a 'fork clearing' function was proposed for the *E. coli* UvrD DNA helicase, a bacterial ortholog of Srs2, based on finding that the lethality conferred by *uvr*D deletion to certain replication mutants is suppressed by inactivation of the genes involved in the RecFOR pathway of HR (53,54). There is also evidence suggesting that Srs2 prevents

recombination events at stalled replication forks favoring lesion bypass by translesion polymerases or through template-switching mechanism (55,56).

The BLM helicase also suppresses crossover events during HR as evidenced by elevated rate of sister chromatid exchanges (SCEs) and increased incidence of loss of heterozygocity in BLM-deficient cells relative to normal cells (1). Recent studies demonstrated that, out of human RecQ helicases, only BLM could promote dHJ dissolution, suggesting that BLM is the human counterpart of the yeast Sgs1 helicase (3,4,41). Although there is also some evidence suggesting that BLM functions in the SDSA pathway of HR, genetic studies using mutant mouse cells clearly indicated that BLM and RECQ5 have nonredundant roles in suppression of crossovers, which is similar to the situation of Srs2 and Sgs1 in yeast (14,41,57).

A recent study suggested that the human F-box helicase 1 (FBH1), which is conserved in *Schizosaccharomyces pombe*, but not in *S. cerevisiae*, is a functional ortholog of Srs2. It was shown that FBH1 shares homology with Srs2 within the helicase domain and suppresses specific recombination defects of *S. cerevisiae* srs2 mutants (58). Although it remains to be determined whether FBH1 possesses the ability to displace RAD51 from ssDNA, the existence of both Fbh1 and Srs2 in *S. pombe* rather suggests that these two helicases use different mechanisms to suppress recombination. This is further supported by the synthetic lethality of mutations in these genes, which is suppressed by deletion of the recombination gene rhp57 (59). Fbh1 is also essential for viability in absence of Rqh1, the sole RecQ homolog of *S. pombe* (59). Simultaneous inactivation of the FBH1 and BLM homologs in chicken DT40 cells is not lethal, but it results in much higher frequency of SCE relative to SCE levels in the respective single mutants (59). Thus, it seems that BLM, RECQ5 and FBH1 act rather in a complementary fashion during processing of HR intermediates. Since FBH1 helicase can function as the substrate specificity subunit of an SCF ubiquitin ligase complex one can speculate that it regulates recombination by triggering proteolytic degradation of recombination factors (60).

RECQ5 is not the sole human RecQ helicase that interacts with the MRN complex. There is evidence for a functional link between MRN and BLM. Similar to Sgs1, BLM was found to coexist with MRN in a large complex containing proteins involved in the recognition and repair of aberrant DNA structures, although no evidence for a direct BLM MRN interaction was reported (61). It was also shown that BLM and MRN colocalize at nuclear foci in response to replication stress and that BLM is required for the relocalization of MRN to sites of replication arrest (61,62). Previous studies also demonstrated that the MRN complex physically interacts with WRN, which is required for the resolution of HR intermediates (63 65). Moreover, these studies revealed that the relocalization of WRN to sites of DNA damage is dependent on a functional MRN complex (63,64). However, WRN and RECQ5 differ in the mode of their interaction with MRN. The formation of WRN MRN complex *in vivo* is dependent on DNA damage (63,64), whereas, based on our data, RECQ5 appears to constitutively interact with MRN *in vivo*. The interaction between WRN and the MRN complex is solely mediated by NBS1 (63), while we show that RECQ5 can bind to both MRE11 and NBS1 and that the absence of NBS1 does not affect the association of RECQ5 with the MR complex. At the functional level, MRN dramatically stimulates the helicase activity of WRN (63), whereas it has no effect on the helicase activity of RECQ5. Further studies will definitely be needed to understand the molecular mechanisms underlying the cooperation between RecQ DNA helicases and the MRN complex in the biological processes that enforce genomic stability.

## SUPPLEMENTARY DATA

Supplementary Data is available at NAR Online.

## ACKNOWLEDGEMENTS

We thank Vilhelm Bohr for providing us with baculoviruses expressing MRN proteins, Torsten Kleffmann for help with mass spectrometry analysis, Manuel Stucki for helpful discussions and Christiane König for technical assistance.

## FUNDING

Swiss National Science Foundation (3100A0-102198, 3100A0-116008); UBS AG, Cancer League of the Canton of Zurich and Czech Science Foundation (GA204/09/0565). Funding for open access charge: Swiss National Science Foundation.

*Conflict of interest statement.* None declared.

## REFERENCES

1. Hanada,K. and Hickson,I.D. (2007) Molecular genetics of RecQ helicase disorders. *Cell Mol. Life Sci.*, **64**, 2306–2322.
2. Sharma,S., Doherty,K.M. and Brosh,R.M. Jr (2006) Mechanisms of RecQ helicases in pathways of DNA metabolism and maintenance of genomic stability. *Biochem. J.*, **398**, 319–337.
3. Wu,L. and Hickson,I.D. (2003) The Bloom's syndrome helicase suppresses crossing over during homologous recombination. *Nature*, **426**, 870–874.
4. Wu,L., Chan,K.L., Ralf,C., Bernstein,D.A., Garcia,P.L., Bohr,V.A., Vindigni,A., Janscak,P., Keck,J.L. and Hickson,I.D. (2005) The HRDC domain of BLM is required for the dissolution of double Holliday junctions. *EMBO J.*, **24**, 2679–2687.
5. Crabbe,L., Verdun,R.E., Haggblom,C.I. and Karlseder,J. (2004) Defective telomere lagging strand synthesis in cells lacking WRN helicase activity. *Science*, **306**, 1951–1953.
6. Crabbe,L., Jauch,A., Naeger,C.M., Holtgreve-Grez,H. and Karlseder,J. (2007) Telomere dysfunction as a cause of genomic instability in Werner syndrome. *Proc. Natl Acad. Sci. USA*, **104**, 2205–2210.
7. Sangrithi,M.N., Bernal,J.A., Madine,M., Philpott,A., Lee,J., Dunphy,W.G. and Venkitaraman,A.R. (2005) Initiation of DNA replication requires the RECQL4 protein mutated in Rothmund-Thomson syndrome. *Cell*, **121**, 887–898.
8. Matsuno,K., Kumano,M., Kubota,Y., Hashimoto,Y. and Takisawa,H. (2006) The N-terminal noncatalytic region of Xenopus RecQ4 is required for chromatin binding of DNA polymerase alpha in the initiation of DNA replication. *Mol. Cell Biol.*, **26**, 4843–4852.
9. Sekelsky,J.J., Brodsky,M.H., Rubin,G.M. and Hawley,R.S. (1999) Drosophila and human RecQ5 exist in different isoforms generated by alternative splicing. *Nucleic Acids Res.*, **27**, 3762–3769.

10. Shimamoto,A., Nishikawa,K., Kitao,S. and Furuichi,Y. (2000) Human RecQ5beta, a large isomer of RecQ5 DNA helicase, localizes in the nucleoplasm and interacts with topoisomerases 3alpha and 3beta. *Nucleic Acids Res.*, **28**, 1647–1655.
11. Garcia,P.L., Liu,Y., Jiricny,J., West,S.C. and Janscak,P. (2004) Human RECQ5β, a protein with DNA helicase and strand-annealing activities in a single polypeptide. *EMBO J.*, **23**, 2882–2891.
12. Kanagaraj,R., Saydam,N., Garcia,P.L., Zheng,L. and Janscak,P. (2006) Human RECQ5β helicase promotes strand exchange on synthetic DNA structures resembling a stalled replication fork. *Nucleic Acids Res.*, **34**, 5217–5231.
13. Hu,Y., Raynard,S., Sehorn,M.G., Lu,X., Bussen,W., Zheng,L., Stark,J.M., Barnes,E.L., Chi,P., Janscak,P. *et al.* (2007) RECQL5/Recql5 helicase regulates homologous recombination and suppresses tumor formation via disruption of Rad51 presynaptic filaments. *Genes Dev.*, **21**, 3073–3084.
14. Hu,Y., Lu,X., Barnes,E., Yan,M., Lou,H. and Luo,G. (2005) Recql5 and Blm RecQ DNA helicases have nonredundant roles in suppressing crossovers. *Mol. Cell Biol.*, **25**, 3431–3442.
15. D'Amours,D. and Jackson,S.P. (2002) The Mre11 complex: at the crossroads of DNA repair and checkpoint signalling. *Nat. Rev. Mol. Cell Biol.*, **3**, 317–327.
16. Assenmacher,N. and Hopfner,K.P. (2004) MRE11/RAD50/NBS1: complex activities. *Chromosoma*, **113**, 157–166.
17. de Jager,M., van Noort,J., van Gent,D.C., Dekker,C., Kanaar,R. and Wyman,C. (2001) Human Rad50/Mre11 is a flexible complex that can tether DNA ends. *Mol. Cell*, **8**, 1129–1135.
18. Paull,T.T. and Gellert,M. (1999) Nbs1 potentiates ATP-driven DNA unwinding and endonuclease cleavage by the Mre11/Rad50 complex. *Genes Dev.*, **13**, 1276–1288.
19. Stracker,T.H., Theunissen,J.W., Morales,M. and Petrini,J.H. (2004) The Mre11 complex and the metabolism of chromosome breaks: the importance of communicating and holding things together. *DNA Repair (Amst.)*, **3**, 845–854.
20. Lee,J.H. and Paull,T.T. (2007) Activation and regulation of ATM kinase activity in response to DNA double-strand breaks. *Oncogene*, **26**, 7741–7748.
21. Lavin,M.F. and Kozlov,S. (2007) ATM activation and DNA damage response. *Cell Cycle*, **6**, 931–942.
22. Bernstein,D.A. and Keck,J.L. (2003) Domain mapping of Escherichia coli RecQ defines the roles of conserved N- and C-terminal regions in the RecQ family. *Nucleic Acids Res.*, **31**, 2778–2785.
23. Williams,R.S., Williams,J.S. and Tainer,J.A. (2007) Mre11-Rad50-Nbs1 is a keystone complex connecting DNA repair machinery, double-strand break signaling, and the chromatin template. *Biochem. Cell Biol.*, **85**, 509–520.
24. Sartori,A.A., Lukas,C., Coates,J., Mistrik,M., Fu,S., Bartek,J., Baer,R., Lukas,J. and Jackson,S.P. (2007) Human CtIP promotes DNA end resection. *Nature*, **450**, 509–514.
25. Carson,C.T., Schwartz,R.A., Stracker,T.H., Lilley,C.E., Lee,D.V. and Weitzman,M.D. (2003) The Mre11 complex is required for ATM activation and the G2/M checkpoint. *EMBO J.*, **22**, 6610–6620.
26. Tauchi,H., Kobayashi,J., Morishima,K., Matsuura,S., Nakamura,A., Shiraishi,T., Ito,E., Masnada,D., Delia,D. and Komatsu,K. (2001) The forkhead-associated domain of NBS1 is essential for nuclear foci formation after irradiation but not essential for hRAD50.hMRE11.NBS1 complex DNA repair activity. *J. Biol. Chem.*, **276**, 12–15.
27. Lou,Z., Minter-Dykhouse,K., Franco,S., Gostissa,M., Rivera,M.A., Celeste,A., Manis,J.P., van Deursen,J., Nussenzweig,A., Paull,T.T. *et al.* (2006) MDC1 maintains genomic stability by participating in the amplification of ATM-dependent DNA damage signals. *Mol. Cell*, **21**, 187–200.
28. Perkins,D.N., Pappin,D.J., Creasy,D.M. and Cottrell,J.S. (1999) Probability-based protein identification by searching sequence databases using mass spectrometry data. *Electrophoresis*, **20**, 3551–3567.
29. Stewart,G.S., Maser,R.S., Stankovic,T., Bressan,D.A., Kaplan,M.I., Jaspers,N.G., Raams,A., Byrd,P.J., Petrini,J.H. and Taylor,A.M. (1999) The DNA double-strand break repair gene hMRE11 is mutated in individuals with an ataxia-telangiectasia-like disorder. *Cell*, **99**, 577–587.
30. Paull,T.T. and Gellert,M. (1998) The 3′ to 5′ exonuclease activity of Mre 11 facilitates repair of DNA double-strand breaks. *Mol. Cell*, **1**, 969–979.
31. Lukas,C., Bartek,J. and Lukas,J. (2005) Imaging of protein movement induced by chromosomal breakage: tiny 'local' lesions pose great 'global' challenges. *Chromosoma*, **114**, 146–154.
32. Bekker-Jensen,S., Lukas,C., Kitagawa,R., Melander,F., Kastan,M.B., Bartek,J. and Lukas,J. (2006) Spatial organization of the mammalian genome surveillance machinery in response to DNA strand breaks. *J. Cell Biol.*, **173**, 195–206.
33. Ward,I.M. and Chen,J. (2001) Histone H2AX is phosphorylated in an ATR-dependent manner in response to replicational stress. *J. Biol. Chem.*, **276**, 47759–47762.
34. Limoli,C.L., Giedzinski,E., Bonner,W.M. and Cleaver,J.E. (2002) UV-induced replication arrest in the xeroderma pigmentosum variant leads to DNA double-strand breaks, γ-H2AX formation, and Mre11 relocalization. *Proc. Natl Acad. Sci. USA*, **99**, 233–238.
35. Lukas,C., Melander,F., Stucki,M., Falck,J., Bekker-Jensen,S., Goldberg,M., Lerenthal,Y., Jackson,S.P., Bartek,J. and Lukas,J. (2004) Mdc1 couples DNA double-strand break recognition by Nbs1 with its H2AX-dependent chromatin retention. *EMBO J.*, **23**, 2674–2683.
36. Stucki,M., Clapperton,J.A., Mohammad,D., Yaffe,M.B., Smerdon,S.J. and Jackson,S.P. (2005) MDC1 directly binds phosphorylated histone H2AX to regulate cellular responses to DNA double-strand breaks. *Cell*, **123**, 1213–1226.
37. Spycher,C., Miller,E.S., Townsend,K., Pavic,L., Morrice,N.A., Janscak,P., Stewart,G.S. and Stucki,M. (2008) Constitutive phosphorylation of MDC1 physically links the MRE11-RAD50-NBS1 complex to damaged chromatin. *J. Cell Biol.*, **181**, 227–240.
38. Melander,F., Bekker-Jensen,S., Falck,J., Bartek,J., Mailand,N. and Lukas,J. (2008) Phosphorylation of SDT repeats in the MDC1 N terminus triggers retention of NBS1 at the DNA damage-modified chromatin. *J. Cell Biol.*, **181**, 213–226.
39. Krogh,B.O. and Symington,L.S. (2004) Recombination proteins in yeast. *Annu. Rev. Genet.*, **38**, 233–271.
40. Li,X. and Heyer,W.D. (2008) Homologous recombination in DNA repair and DNA damage tolerance. *Cell Res.*, **18**, 99–113.
41. Ira,G., Malkova,A., Liberi,G., Foiani,M. and Haber,J.E. (2003) Srs2 and Sgs1-Top3 suppress crossovers during double-strand break repair in yeast. *Cell*, **115**, 401–411.
42. Robert,T., Dervins,D., Fabre,F. and Gangloff,S. (2006) Mrc1 and Srs2 are major actors in the regulation of spontaneous crossover. *EMBO J.*, **25**, 2837–2846.
43. Krejci,L., Van Komen,S., Li,Y., Villemain,J., Reddy,M.S., Klein,H., Ellenberger,T. and Sung,P. (2003) DNA helicase Srs2 disrupts the Rad51 presynaptic filament. *Nature*, **423**, 305–309.
44. Veaute,X., Jeusset,J., Soustelle,C., Kowalczykowski,S.C., Le Cam,E. and Fabre,F. (2003) The Srs2 helicase prevents recombination by disrupting Rad51 nucleoprotein filaments. *Nature*, **423**, 309–312.
45. Dupaigne,P., Le Breton,C., Fabre,F., Gangloff,S., Le Cam,E. and Veaute,X. (2008) The Srs2 helicase activity is stimulated by Rad51 filaments on dsDNA: implications for crossover incidence during mitotic recombination. *Mol. Cell*, **29**, 243–254.
46. Chiolo,I., Carotenuto,W., Maffioletti,G., Petrini,J.H., Foiani,M. and Liberi,G. (2005) Srs2 and Sgs1 DNA helicases associate with Mre11 in different subcomplexes following checkpoint activation and CDK1-mediated Srs2 phosphorylation. *Mol. Cell Biol.*, **25**, 5738–5751.
47. Kim,J.S., Krasieva,T.B., Kurumizaka,H., Chen,D.J., Taylor,A.M. and Yokomori,K. (2005) Independent and sequential recruitment of NHEJ and HR factors to DNA damage sites in mammalian cells. *J. Cell Biol.*, **170**, 341–347.
48. Robison,J.G., Lu,L., Dixon,K. and Bissler,J.J. (2005) DNA lesion-specific co-localization of the Mre11/Rad50/Nbs1 (MRN) complex and replication protein A (RPA) to repair foci. *J. Biol. Chem.*, **280**, 12927–12934.
49. Maser,R.S., Mirzoeva,O.K., Wells,J., Olivares,H., Williams,B.R., Zinkel,R.A., Farnham,P.J. and Petrini,J.H. (2001) Mre11 complex

and DNA replication: linkage to E2F and sites of DNA synthesis. *Mol. Cell Biol.*, **21**, 6006–6016.
50. Mirzoeva,O.K. and Petrini,J.H. (2003) DNA replication-dependent nuclear dynamics of the Mre11 complex. *Mol. Cancer Res.*, **1**, 207–218.
51. Olson,E., Nievera,C.J., Liu,E., Lee,A.Y., Chen,L. and Wu,X. (2007) The Mre11 complex mediates the S-phase checkpoint through an interaction with replication protein A. *Mol. Cell Biol.*, **27**, 6053–6067.
52. Robison,J.G., Elliott,J., Dixon,K. and Oakley,G.G. (2004) Replication protein A and the Mre11.Rad50.Nbs1 complex co-localize and interact at sites of stalled replication forks. *J. Biol. Chem.*, **279**, 34802–34810.
53. Veaute,X., Delmas,S., Selva,M., Jeusset,J., Le Cam,E., Matic,I., Fabre,F. and Petit,M.A. (2005) UvrD helicase, unlike Rep helicase, dismantles RecA nucleoprotein filaments in Escherichia coli. *EMBO J.*, **24**, 180–189.
54. Flores,M.J., Sanchez,N. and Michel,B. (2005) A fork-clearing role for UvrD. *Mol. Microbiol.*, **57**, 1664–1675.
55. Papouli,E., Chen,S., Davies,A.A., Huttner,D., Krejci,L., Sung,P. and Ulrich,H.D. (2005) Crosstalk between SUMO and ubiquitin on PCNA is mediated by recruitment of the helicase Srs2p. *Mol. Cell*, **19**, 123–133.
56. Pfander,B., Moldovan,G.L., Sacher,M., Hoege,C. and Jentsch,S. (2005) SUMO-modified PCNA recruits Srs2 to prevent recombination during S phase. *Nature*, **436**, 428–433.
57. Bugreev,D.V., Yu,X., Egelman,E.H. and Mazin,A.V. (2007) Novel pro- and anti-recombination activities of the Bloom's syndrome helicase. *Genes Dev.*, **21**, 3085–3094.
58. Chiolo,I., Saponaro,M., Baryshnikova,A., Kim,J.H., Seo,Y.S. and Liberi,G. (2007) The human F-Box DNA helicase FBH1 faces *Saccharomyces cerevisiae* Srs2 and postreplication repair pathway roles. *Mol. Cell Biol.*, **27**, 7439–7450.
59. Morishita,T., Furukawa,F., Sakaguchi,C., Toda,T., Carr,A.M., Iwasaki,H. and Shinagawa,H. (2005) Role of the *Schizosaccharomyces pombe* F-box DNA helicase in processing recombination intermediates. *Mol. Cell Biol.*, **25**, 8074–8083.
60. Kim,J.H., Kim,J., Kim,D.H., Ryu,G.H., Bae,S.H. and Seo,Y.S. (2004) SCFhFBH1 can act as helicase and E3 ubiquitin ligase. *Nucleic Acids Res.*, **32**, 2287–2297.
61. Wang,Y., Cortez,D., Yazdi,P., Neff,N., Elledge,S.J. and Qin,J. (2000) BASC, a super complex of BRCA1-associated proteins involved in the recognition and repair of aberrant DNA structures. *Genes Dev.*, **14**, 927–939.
62. Franchitto,A. and Pichierri,P. (2002) Bloom's syndrome protein is required for correct relocalization of RAD50/MRE11/NBS1 complex after replication fork arrest. *J. Cell Biol.*, **157**, 19–30.
63. Cheng,W.H., von Kobbe,C., Opresko,P.L., Arthur,L.M., Komatsu,K., Seidman,M.M., Carney,J.P. and Bohr,V.A. (2004) Linkage between Werner syndrome protein and the Mre11 complex via Nbs1. *J. Biol. Chem.*, **279**, 21169–21176.
64. Franchitto,A. and Pichierri,P. (2004) Werner syndrome protein and the MRE11 complex are involved in a common pathway of replication fork recovery. *Cell Cycle*, **3**, 1331–1339.
65. Saintigny,Y., Makienko,K., Swanson,C., Emond,M.J. and Monnat,R.J. Jr (2002) Homologous recombination resolution defect in Werner syndrome. *Mol. Cell Biol.*, **22**, 6971–6978.

## 4 Conclusion and Perspective

The role of human RECQ5 protein in the cell is not well understood. Although a human disease associated with deficiency of RECQ5 has not been found, RECQ5 knockout mice were shown to be cancer prone and highly genetically instable (Results 3.4) (Hu, Raynard et al. 2007). Identification of new protein partners of RECQ5 and study of these protein-protein interactions are vital to understand the role of RECQ5 the maintenance of genomic stability.

RECQ5 was found to directly interact with PCNA and associated with DNA replication machinery during S phase. RECQ5 was also shown to persist at the sites of stalled replication forks after exposure of cells to UV irradiation. At biochemical level, RECQ5 was shown to promote strand exchange between arms of synthetic forked DNA structures resembling a stalled replication fork (Results 3.3). The proposed fork regression activity of RECQ5 at stalled replication forks could well explain the elevated level of crossovers in RECQ5-deficient cells.

RECQ5 was also shown to be able to disrupt RAD51 presynaptic filament, suggesting another mechanism for how RECQ5 controls homologous recombination in the cell (Results 3.4) (Hu, Raynard et al. 2007). Further characterization of the interaction between RECQ5 and RAD51 will involve mutation studies to generate a RECQ5 mutant that lacks the RAD51 binding site. The ultimate goal will be to check whether the mutant is able to displace RAD51 from ssDNA *in vitro* and correct the hyper-recombination phenotype of RECQ5 knockout cells *in vivo*.

RECQ5 was found to interact with the MRN complex *in vivo* and *in vitro*. In majority of unperturbed cells, both RECQ5 and MRN were uniformly distributed in the nucleus. In response to DNA double-strand breaks and stalled replication fork, RECQ5 was found to relocate to the sites of DNA

damage, and this relocation was dependent on the MRN complex (Results 3.5). In future studies, a RECQ5 peptide, which abolishes the interaction between RECQ5 and MRN, could be over-produced in human cells to prove that the recruitment of RECQ5 to sites of DNA damage is dependent on a direct protein-protein interaction with MRN. Moreover, the effect of MRN on the ability of RECQ5 to displace RAD51 from ssDNA could be investigated.

A major interaction partner of RECQ5 identified in our yeast two-hybrid screen was SKP1, a scaffold component of SCF ubiquitin ligases (Cardozo and Pagano 2004). A direct interaction between RECQ5 and SKP1 was confirmed using recombinant proteins (data not shown). Experiments towards reconstitution of a $SCF^{RECQ5}$ complex using recombinant proteins would address the possibility of RECQ5 functioning as an F-box protein, which determines the substrate specificity of SCF complexes. It would also be interesting to check the levels of RECQ5 at different stages of the cell cycle and after different types of DNA damage to see if RECQ5 is subjected to proteolytic degradation. It should be noted that our yeast two-hybrid screening revealed that RECQ5 interacts with the F-box protein FBW7, which forms $SCF^{FBW7}$ and is responsible for degradation of several proto-oncogenes that function in cellular growth and division pathways, including MYC, cyclin E and JUN (Welcker and Clurman 2008).

The association between RECQ5 and RPB1, the largest subunit of RNA polymerase II (RNAPII) was identified both in our yeast two-hybrid screen and in the mass spectrometry experiments. The interaction was confirmed by Western blot analysis of RECQ5 immunoprecipitates from various cell lines, and RPB1 was shown to extensively colocalize with RECQ5 in the nucleus following UVC irradiation (Radhakrishnan Kanagaraj, unpublished data). In addition, the mass spectrometry experiments revealed interaction between RECQ5 and the RPB2 (the second largest subunit of RNAPII). Given the fact that RPB1 and RPB2 constitute the catalytic core of the enzyme (Svejstrup

2007) (Hartzog 2003), it would be very interesting to find out weather RECQ5 has any effect on RNA transcription *in vivo* and *in vitro*. Further characterization of this interaction will involve mapping the interaction domains in the RECQ5-RNAPII complex; examining the role of RECQ5 in transcription-coupled repair; testing the ability of RECQ5 to disrupt stalled RNAPII complexes.

# REFERENCES


Ababou, M., S. Dutertre, et al. (2000). "ATM-dependent phosphorylation and accumulation of endogenous BLM protein in response to ionizing radiation." Oncogene **19**(52): 5955-5963.

Aebersold, R. and M. Mann (2003). "Mass spectrometry-based proteomics." Nature **422**(6928): 198-207.

Assenmacher, N. and K. P. Hopfner (2004). "MRE11/RAD50/NBS1: complex activities." Chromosoma **113**(4): 157-66.

Bachrati, C. Z. and I. D. Hickson (2003). "RecQ helicases: suppressors of tumorigenesis and premature aging." Biochem. J. **374**(3): 577-606.

Bekker-Jensen, S., C. Lukas, et al. (2006). "Spatial organization of the mammalian genome surveillance machinery in response to DNA strand breaks." J Cell Biol **173**(2): 195-206.

Bennett, R. J. and J. L. Keck (2004). "Structure and Function of RecQ DNA Helicases." Critical Reviews in Biochemistry and Molecular Biology **39**(2): 79-97.

Bennett, R. J., M.-F. Noirot-Gros, et al. (2000). "Interaction between Yeast Sgs1 Helicase and DNA Topoisomerase III." Journal of Biological Chemistry **275**(35): 26898-26905.

Bennett, R. J., J. A. Sharp, et al. (1998). "Purification and Characterization of the Sgs1 DNA Helicase Activity of Saccharomyces cerevisiae." Journal of Biological Chemistry **273**(16): 9644-9650.

Bernstein, D. A. and J. L. Keck (2003). "Domain mapping of Escherichia coli RecQ defines the roles of conserved N- and C-terminal regions in the RecQ family." Nucleic Acids Research **31**(11): 2778-2785.

Bernstein, D. A. and J. L. Keck (2005). "Conferring Substrate Specificity to DNA Helicases: Role of the RecQ HRDC Domain." Structure **13**(8): 1173-1182.

Bernstein, D. A., M. C. Zittel, et al. (2003). "High-resolution structure of the E.coli RecQ helicase catalytic core." EMBO J. **22**(19): 4910-4921.

Bishop, D. K. and D. Zickler (2004). "Early Decision: Meiotic Crossover Interference prior to Stable Strand Exchange and Synapsis." Cell **117**(1): 9-15.

Brown, G. S. a. R. (2002). "'Expert Reviews in Molecular Medicine' Found at URL: http://www.expertreviews.org/."

Bussen, W., S. Raynard, et al. (2007). "Holliday Junction Processing Activity of the BLM-Topo III{alpha}-BLAP75 Complex." Journal of Biological Chemistry **282**(43): 31484-31492.

Cannavo, E. (2006). The role of Human MutL Proteins in DNA Repair. Zurich, University of Zurich. **PhD:** 112.

Cardozo, T. and M. Pagano (2004). "The SCF ubiquitin ligase: insights into a molecular machine." Nat Rev Mol Cell Biol **5**(9): 739-751.

Carney, J. P., R. S. Maser, et al. (1998). "The hMre11/hRad50 protein complex and Nijmegen breakage syndrome: linkage of double-strand break repair to the cellular DNA damage response." Cell **93**(3): 477-86.

Carson, C. T., R. A. Schwartz, et al. (2003). "The Mre11 complex is required for ATM activation and the G2/M checkpoint." Embo J **22**(24): 6610-20.

Cheng, W. H., C. von Kobbe, et al. (2004). "Linkage between Werner syndrome protein and the Mre11 complex via Nbs1." J Biol Chem **279**(20): 21169-76.

Christmann, M., M. T. Tomicic, et al. (2003). "Mechanisms of human DNA repair: an update." Toxicology **193**(1-2): 3-34.

Costanzo, V., K. Robertson, et al. (2001). "Mre11 protein complex prevents double-strand break accumulation during chromosomal DNA replication." Mol Cell **8**(1): 137-47.

Courcelle, J., C. Carswell-Crumpton, et al. (1997). "recF and recR are required for the resumption of replication at DNA replication forks in Escherichia coli." Proceedings of the National Academy of Sciences **94**(8): 3714-3719.

Courcelle, J. and P. C. Hanawalt (2001). "Participation of recombination proteins in rescue of arrested replication forks in UV-irradiated Escherichia coli need not involve recombination." Proceedings of the National Academy of Sciences **98**(15): 8196-8202.

Courcelle, J. and P. C. Hanawalt (2003). "RECA-DEPENDENT RECOVERY OF ARRESTED DNA REPLICATION FORKS." Annual Review of Genetics **37**(1): 611-646.

Crabbe, L., A. Jauch, et al. (2007). "Telomere dysfunction as a cause of genomic instability in Werner syndrome." Proc Natl Acad Sci U S A **104**(7): 2205-10.

Crabbe, L., R. E. Verdun, et al. (2004). "Defective telomere lagging strand synthesis in cells lacking WRN helicase activity." Science **306**(5703): 1951-3.

Critchlow, S. E. and S. P. Jackson (1998). "DNA end-joining: from yeast to man." Trends in Biochemical Sciences **23**(10): 394-398.

Cromie, G. A., J. C. Connelly, et al. (2001). "Recombination at Double-Strand Breaks and DNA Ends: Conserved Mechanisms from Phage to Humans." Molecular Cell **8**(6): 1163-1174.

D'Amours, D. and S. P. Jackson (2002). "The Mre11 complex: at the crossroads of dna repair and checkpoint signalling." Nat Rev Mol Cell Biol **3**(5): 317-27.

D'Amours, D. and S. P. Jackson (2002). "The MRE11 complex: at the crossroads of DNA repair and checkpoint signalling." Nat Rev Mol Cell Biol **3**(5): 317-327.

de Jager, M., J. van Noort, et al. (2001). "Human Rad50/Mre11 is a flexible complex that can tether DNA ends." Mol Cell **8**(5): 1129-35.

Ellis, N. A. (1997). "DNA helicases in inherited human disorders." Current Opinion in Genetics & Development **7**(3): 354-363.

Enomoto, T. (2001). "Functions of RecQ Family Helicases: Possible Involvement of Bloom's and Werner's Syndrome Gene Products in Guarding Genome Integrity during DNA Replication." J Biochem (Tokyo) **129**(4): 501-507.

Fields, S. and O.-k. Song (1989). "A novel genetic system to detect protein¬ñprotein interactions." Nature **340**(6230): 245-246.

Foucault, F., C. Vaury, et al. (1997). "Characterization of a new BLM mutation associated with a topoisomerase II alpha defect in a patient with Bloom's syndrome." Human Molecular Genetics **6**(9): 1427-1434.

Franchitto, A. and P. Pichierri (2002). "Bloom's syndrome protein is required for correct relocalization of RAD50/MRE11/NBS1 complex after replication fork arrest." J Cell Biol **157**(1): 19-30.

Franchitto, A. and P. Pichierri (2004). "Werner syndrome protein and the MRE11 complex are involved in a common pathway of replication fork recovery." Cell Cycle **3**(10): 1331-9.

Frei, C. and S. M. Gasser (2000). "The yeast Sgs1p helicase acts upstream of Rad53p in the DNA replication checkpoint and colocalizes with Rad53p in S-phase-specific foci." Genes and Development **14**(1): 81-96.

Fricke, W. M., V. Kaliraman, et al. (2001). "Mapping the DNA Topoisomerase III Binding Domain of the Sgs1 DNA Helicase." Journal of Biological Chemistry **276**(12): 8848-8855.

Friedberg, E. C. (1995). "Out of the shadows and into the light: the emergence of DNA repair." Trends in Biochemical Sciences **20**(10): 381.

Friedberg, E. C. (2001). "How nucleotide excision repair protects against cancer." Nat Rev Cancer **1**(1): 22-33.

Gangloff, S., J. P. McDonald, et al. (1994). "The yeast type I topoisomerase Top3 interacts with Sgs1, a DNA helicase homolog: a potential eukaryotic reverse gyrase." Molecular and Cellular Biology **14**(12): 8391-8398.

Garcia, P. L., Y. Liu, et al. (2004). "Human RECQ5beta, a protein with DNA helicase and strand-annealing activities in a single polypeptide." Embo J **23**(14): 2882-91.

Garcia, P. L., Y. Liu, et al. (2004). "Human RECQ5beta, a protein with DNA helicase and strand-annealing activities in a single polypeptide." The EMBO Journal **23**: 2882-2891.

Gietz, R. D., B. Triggs-Raine, et al. (1997). "Identification of proteins that interact with a protein of interest: Applications of the yeast two-hybrid system." Molecular and Cellular Biochemistry **172**(1): 67-79.

Gietz, R. D. a. R. A. W. (2002). "TRANSFORMATION OF YEAST BY THE Liac/SS CARRIER DNA/PEG METHOD." Methods in Enzymology **350**: 87-96.

Hanada, K. and I. D. Hickson (2007). "Molecular genetics of RecQ helicase disorders." Cell Mol Life Sci **64**(17): 2306-22.

Hanada, K., T. Ukita, et al. (1997). "RecQ DNA helicase is a suppressor of illegitimate recombination in Escherichia coli." Proceedings of the National Academy of Sciences **94**(8): 3860-3865.

Harmon, F. G., R. J. DiGate, et al. (1999). "RecQ Helicase and Topoisomerase III Comprise a Novel DNA Strand Passage Function: A Conserved Mechanism for Control of DNA Recombination." Molecular Cell **3**(5): 611-620.

Harmon, F. G. and S. C. Kowalczykowski (1998). "RecQ helicase, in concert with RecA and SSB proteins, initiates and disrupts DNA recombination." Genes and Development **12**(8): 1134-1144.

Harmon, F. G. and S. C. Kowalczykowski (2001). "Biochemical Characterization of the DNA Helicase Activity of the Escherichia coli RecQ Helicase." Journal of Biological Chemistry **276**(1): 232-243.

Hartzog, G. A. (2003). "Transcription elongation by RNA polymerase II." Current Opinion in Genetics & Development **13**(2): 119-126.

Hellman, U., C. Wernstedt, et al. (1995). "Improvement of an "In-Gel" Digestion Procedure for the Micropreparation of Internal Protein Fragments for Amino Acid Sequencing." Analytical Biochemistry **224**(1): 451-455.

Heyer, W.-D. (2004). "Damage Signaling: RecQ Sends an SOS to You." Current Biology **14**(20): R895-R897.

Hickson, I. D. (2003). "RecQ helicases: caretakers of the genome." Nat Rev Cancer **3**(3): 169-178.

Hickson, L. W. a. I. D. (2003). "The Bloom's syndrome helicase suppresses crossing over during homologous recombination." Nature **426**: 870-874.

Hishida, T., Y.-W. Han, et al. (2004). "Role of the Escherichia coli RecQ DNA helicase in SOS signaling and genome stabilization at stalled replication forks." Genes and Development **18**(15): 1886-1897.

Hoeijmakers, J. H. J. (2001). "Genome maintenance mechanisms for preventing cancer." Nature **411**(6835): 366-374.

Hu, P., S. Beresten, et al. (2001). "Evidence for BLM and Topoisomerase III{{alpha}} interaction in genomic stability." Hum. Mol. Genet. **10**(12): 1287-1298.

Hu, Y., X. Lu, et al. (2005). "Recql5 and Blm RecQ DNA Helicases Have Nonredundant Roles in Suppressing Crossovers." Mol. Cell. Biol. **25**(9): 3431-3442.

Hu, Y., X. Lu, et al. (2005). "Recql5 and Blm RecQ DNA helicases have nonredundant roles in suppressing crossovers." Mol Cell Biol **25**(9): 3431-42.

Hu, Y., S. Raynard, et al. (2007). "RECQL5/Recql5 helicase regulates homologous recombination and suppresses tumor formation via disruption of Rad51 presynaptic filaments." Genes and Development **21**(23): 3073-3084.

Hu, Y., S. Raynard, et al. (2007). "RECQL5/Recql5 helicase regulates homologous recombination and suppresses tumor formation via disruption of Rad51 presynaptic filaments." Genes Dev **21**(23): 3073-84.

Ira, G., A. Malkova, et al. (2003). "Srs2 and Sgs1-Top3 Suppress Crossovers during Double-Strand Break Repair in Yeast." Cell **115**(4): 401-411.

Jackson, K. K. K. S. P. (2001). "DNA double-strand breaks: signaling, repair and the cancer connection." Nature Genetics **27**: 247-254.

Jackson, S. P. (2002). "Sensing and repairing DNA double-strand breaks." Carcinogenesis **23**(5): 687-696.

Jeong SM, K. K., Juni N, Shibata T. (2000). "Identification of Drosophila melanogaster RECQE as a member of a new family of RecQ homologues that is preferentially expressed in early embryos." Mol Gen Genet **263**(2): 183-93.

Kaliraman, V., J. R. Mullen, et al. (2001). "Functional overlap between Sgs1-Top3 and the Mms4-Mus81 endonuclease." Genes and Development **15**(20): 2730-2740.

Kanagaraj, R., N. Saydam, et al. (2006). "Human RECQ5beta helicase promotes strand exchange on synthetic DNA structures resembling a stalled replication fork." Nucleic Acids Res **34**(18): 5217-31.

Kanagaraj, R., N. Saydam, et al. (2006). "Human RECQ5 β helicase promotes strand exchange on synthetic DNA structures resembling a stalled replication fork." Nucleic Acids Research **34**(18): 5217-5231.

Karow, J. K., L. Wu, et al. (2000). "RecQ family helicases: roles in cancer and aging." Current Opinion in Genetics & Development **10**(1): 32-38.

Kawasaki, K., S. Maruyama, et al. (2002). "Drosophila melanogaster RECQ5/QE DNA helicase: stimulation by GTP binding." Nucl. Acids Res. **30**(17): 3682-3691.

Khakhar, R. R., J. A. Cobb, et al. (2003). "RecQ helicases: multiple roles in genome maintenance." Trends in Cell Biology **13**(9): 493-501.

Kitao, S., I. Ohsugi, et al. (1998). "Cloning of Two New Human Helicase Genes of the RecQ Family: Biological Significance of Multiple Species in Higher Eukaryotes." Genomics **54**(3): 443-452.

Kolodner, R. D. and G. T. Marsischky (1999). "Eukaryotic DNA mismatch repair." Current Opinion in Genetics & Development **9**(1): 89-96.

Kowalczykowski, S. C., D. A. Dixon, et al. (1994). "Biochemistry of homologous recombination in Escherichia coli." Microbiology and Molecular Biology Reviews **58**(3): 401-465.

Kunkel, T. A. and D. A. Erie (2005). "DNA MISMATCH REPAIR*." Annual Review of Biochemistry **74**(1): 681-710.

Lavin, M. F. and S. Kozlov (2007). "ATM activation and DNA damage response." Cell Cycle **6**(8): 931-42.

Lee, J. H. and T. T. Paull (2007). "Activation and regulation of ATM kinase activity in response to DNA double-strand breaks." Oncogene **26**(56): 7741-8.

Lee, J. Y., M. Kozak, et al. (2007). "Evidence That a RecQ Helicase Slows Senescence by Resolving Recombining Telomeres." PLoS Biology **5**(6): e160.

Lee, S.-K., R. E. Johnson, et al. (1999). "Requirement of Yeast SGS1 and SRS2 Genes for Replication and Transcription." Science **286**(5448): 2339-2342.

Li, G.-M. (2008). "Mechanisms and functions of DNA mismatch repair." Cell Res **18**(1): 85-98.

Lieber, M. R. (1999). "The biochemistry and biological significance of nonhomologous DNA end joining: an essential repair process in multicellular eukaryotes." Genes to Cells **4**(2): 77-85.

Limoli, C. L., E. Giedzinski, et al. (2002). "UV-induced replication arrest in the xeroderma pigmentosum variant leads to DNA double-strand breaks, gamma - H2AX formation, and Mre11 relocalization." Proc Natl Acad Sci U S A **99**(1): 233-8.

Lindahl, T. (1993). "Instability and decay of the primary structure of DNA." Nature **362**(6422): 709-715.

Lu, J., J. R. Mullen, et al. (1996). "Human homologues of yeast helicase." Nature **383**(6602): 678-679.

Lukas, C., J. Bartek, et al. (2005). "Imaging of protein movement induced by chromosomal breakage: tiny 'local' lesions pose great 'global' challenges." Chromosoma **114**(3): 146-54.

Luo, G., M. S. Yao, et al. (1999). "Disruption of mRad50 causes embryonic stem cell lethality, abnormal embryonic development, and sensitivity to ionizing radiation." Proc Natl Acad Sci U S A **96**(13): 7376-81.

Machwe, A., L. Xiao, et al. (2005). "RecQ Family Members Combine Strand Pairing and Unwinding Activities to Catalyze Strand Exchange." Journal of Biological Chemistry **280**(24): 23397-23407.

Magner, D. B., M. D. Blankschien, et al. (2007). "RecQ Promotes Toxic Recombination in Cells Lacking Recombination Intermediate-Removal Proteins." Molecular Cell **26**(2): 273-286.

Mankouri, H. W. and I. D. Hickson (2007). "The RecQ helicase-topoisomerase III-Rmi1 complex: a DNA structure-specific `dissolvasome'?" Trends in Biochemical Sciences **In Press, Corrected Proof**.

Maser, R. S., O. K. Mirzoeva, et al. (2001). "Mre11 complex and DNA replication: linkage to E2F and sites of DNA synthesis." Mol Cell Biol **21**(17): 6006-16.

Matsuura, S., H. Tauchi, et al. (1998). "Positional cloning of the gene for Nijmegen breakage syndrome." Nat Genet **19**(2): 179-81.

McCulloch, S. D., L. Gu, et al. (2003). "Bi-directional Processing of DNA Loops by Mismatch Repair-dependent and -independent Pathways in Human Cells." Journal of Biological Chemistry **278**(6): 3891-3896.

Meetei, A. R., S. Sechi, et al. (2003). "A Multiprotein Nuclear Complex Connects Fanconi Anemia and Bloom Syndrome." Mol. Cell. Biol. **23**(10): 3417-3426.

Mirzoeva, O. K. and J. H. Petrini (2003). "DNA replication-dependent nuclear dynamics of the Mre11 complex." Mol Cancer Res **1**(3): 207-18.

Miyajima, A., M. Seki, et al. (2000). "Sgs1 Helicase Activity Is Required for Mitotic but Apparently Not for Meiotic Functions." Molecular and Cellular Biology **20**(17): 6399-6409.

Modrich, P. (2006). "Mechanisms in Eukaryotic Mismatch Repair." Journal of Biological Chemistry **281**(41): 30305-30309.

MolecularStation (2007). "'DNA' Found at URL:http://bccd.cs.uni.edu/mediawiki/index.php/Introduction_to_DNA."

Morozov, V., A. R. Mushegian, et al. (1997). "A putative nucleic acid-binding domain in Bloom's and Werner's syndrome helicases." Trends in Biochemical Sciences **22**(11): 417-418.

Mullen, J. R., F. S. Nallaseth, et al. (2005). "Yeast Rmi1/Nce4 Controls Genome Stability as a Subunit of the Sgs1-Top3 Complex." Molecular and Cellular Biology **25**(11): 4476-4487.

Nakayama, H., K. Nakayama, et al. (1984). "Isolation and genetic characterization of a thymineless death-resistant mutant of Escherichia coli K12: Identification of a new mutation (recQ1) that blocks the RecF recombination pathway." Molecular and General Genetics MGG **195**(3): 474-480.

Nakayama, K., N. Irino, et al. (1985). "The recQ gene of Escherichia coli K12: molecular cloning and isolation of insertion mutants." Molecular and General Genetics MGG **200**(2): 266-271.

Nakayama, M., K. Kawasaki, et al. (2004). "The possible roles of the DNA helicase and C-terminal domains in RECQ5/QE: complementation study in yeast." DNA Repair **3**(4): 369-378.

Nakayama, M., S. Maruyama, et al. (2006). "Relationships of Drosophila melanogaster RECQ5/QE to cell-cycle progression and DNA damage." FEBS Letters **580**(30): 6938-6942.

Oh, S. D., J. P. Lao, et al. (2007). "BLM Ortholog, Sgs1, Prevents Aberrant Crossing-over by Suppressing Formation of Multichromatid Joint Molecules." Cell **130**(2): 259-272.

Ohhata, T., R. Araki, et al. (2001). "Cloning, genomic structure and chromosomal localization of the gene encoding mouse DNA helicase RECQL5[beta]." Gene **280**(1-2): 59-66.

Olson, E., C. J. Nievera, et al. (2007). "The Mre11 complex mediates the S-phase checkpoint through an interaction with replication protein A." Mol Cell Biol **27**(17): 6053-67.

Ozsoy, A. Z., H. M. Ragonese, et al. (2003). "Analysis of helicase activity and substrate specificity of Drosophila RECQ5." Nucl. Acids Res. **31**(5): 1554-1564.

Ozsoy, A. Z., J. J. Sekelsky, et al. (2001). "Biochemical characterization of the small isoform of Drosophila melanogaster RECQ5 helicase." Nucl. Acids Res. **29**(14): 2986-2993.

Paull, T. T. and M. Gellert (1998). "The 3' to 5' exonuclease activity of Mre 11 facilitates repair of DNA double-strand breaks." Mol Cell **1**(7): 969-79.

Paull, T. T. and M. Gellert (1999). "Nbs1 potentiates ATP-driven DNA unwinding and endonuclease cleavage by the Mre11/Rad50 complex." Genes Dev **13**(10): 1276-88.

Pedrazzi, G., C. Perrera, et al. (2001). "Direct association of Bloom's syndrome gene product with the human mismatch repair protein MLH1." Nucl. Acids Res. **29**(21): 4378-4386.

Perkins, D. N. and D. M. C. Darryl J. C. Pappin, John S. Cottrell (1999). "Probability-based protein identification by searching sequence databases using mass spectrometry data." Electrophoresis **20**(18): 3551-3567.

Pinto, L. A., C. G. R. d. Silva, et al. (2003). "Escherichia coli as a model system to study DNA repair genes of eukaryotic organisms." Genetics and Molecular Research **2**(1): 77-91.

Raynard, S., W. Bussen, et al. (2006). "A Double Holliday Junction Dissolvasome Comprising BLM, Topoisomerase III{alpha}, and BLAP75." J. Biol. Chem. **281**(20): 13861-13864.

Rosenfeld, J., J. Capdevielle, et al. (1992). "In-gel digestion of proteins for internal sequence analysis after one- or two-dimensional gel electrophoresis." Analytical Biochemistry **203**(1): 173-179.

Rouse, J. and S. P. Jackson (2002). "Interfaces Between the Detection, Signaling, and Repair of DNA Damage." Science **297**(5581): 547-551.

Sancar, A. (1996). "DNA Excision Repair." Annual Review of Biochemistry **65**(1): 43-81.

Sancar, A., L. A. Lindsey-Boltz, et al. (2004). "MOLECULAR MECHANISMS OF MAMMALIAN DNA REPAIR AND THE DNA DAMAGE CHECKPOINTS." Annual Review of Biochemistry **73**(1): 39-85.

Sangrithi, M. N., J. A. Bernal, et al. (2005). "Initiation of DNA replication requires the RECQL4 protein mutated in Rothmund-Thomson syndrome." Cell **121**(6): 887-98.

Sartori, A. A., C. Lukas, et al. (2007). "Human CtIP promotes DNA end resection." Nature **450**(7169): 509-14.

Sekelsky, J. J., M. H. Brodsky, et al. (1999). "Drosophila and human RecQ5 exist in different isoforms generated by alternative splicing." Nucleic Acids Res **27**(18): 3762-9.

Sekelsky, J. J., M. H. Brodsky, et al. (1999). "Drosophila and human RecQ5 exist in different isoforms generated by alternative splicing." Nucl. Acids Res. **27**(18): 3762-3769.

Seki, M., T. Nakagawa, et al. (2006). "Bloom Helicase and DNA Topoisomerase III{alpha} Are Involved in the Dissolution of Sister Chromatids." Mol. Cell. Biol. **26**(16): 6299-6307.

Sharma, S., K. M. Doherty, et al. (2006). "Mechanisms of RecQ helicases in pathways of DNA metabolism and maintenance of genomic stability." Biochemical Journal **398**(3): 319-337.

Sharma, S., K. M. Doherty, et al. (2006). "Mechanisms of RecQ helicases in pathways of DNA metabolism and maintenance of genomic stability." Biochem J **398**(3): 319-37.

Shimamoto, A., K. Nishikawa, et al. (2000). "Human RecQ5{beta}, a large isomer of RecQ5 DNA helicase, localizes in the nucleoplasm and interacts with topoisomerases 3{alpha} and 3{beta}." Nucl. Acids Res. **28**(7): 1647-1655.

Shimamoto, A., K. Nishikawa, et al. (2000). "Human RecQ5beta, a large isomer of RecQ5 DNA helicase, localizes in the nucleoplasm and interacts with topoisomerases 3alpha and 3beta." Nucleic Acids Res **28**(7): 1647-55.

Sinclair, D. A., K. Mills, et al. (1997). "Accelerated Aging and Nucleolar Fragmentation in Yeast sgs1 Mutants." Science **277**(5330): 1313-1316.

Smith, G. C. M. and S. P. Jackson (1999). "The DNA-dependent protein kinase." Genes and Development **13**(8): 916-934.

Stewart, G. S., R. S. Maser, et al. (1999). "The DNA double-strand break repair gene hMRE11 is mutated in individuals with an ataxia-telangiectasia-like disorder." Cell **99**(6): 577-87.

Svejstrup, J. Q. (2007). "Contending with transcriptional arrest during RNAPII transcript elongation." Trends in Biochemical Sciences **32**(4): 165-171.

Tauchi, H., J. Kobayashi, et al. (2001). "The forkhead-associated domain of NBS1 is essential for nuclear foci formation after irradiation but not essential for hRAD50[middle dot]hMRE11[middle dot]NBS1 complex DNA repair activity." J Biol Chem **276**(1): 12-5.

Trenz, K., E. Smith, et al. (2006). "ATM and ATR promote Mre11 dependent restart of collapsed replication forks and prevent accumulation of DNA breaks." Embo J **25**(8): 1764-74.

Trujillo, K. M. and P. Sung (2001). "DNA structure-specific nuclease activities in the Saccharomyces cerevisiae Rad50*Mre11 complex." J Biol Chem **276**(38): 35458-64.

Ui, A., Y. Satoh, et al. (2001). "The N-terminal region of Sgs1, which interacts with Top3, is required for complementation of MMS sensitivity and suppression of hyper-recombination in sgs1 disruptants." Molecular Genetics and Genomics **265**(5): 837-850.

Umezu, K., K. Nakayama, et al. (1990). "Escherichia coli RecQ Protein is a DNA Helicase." Proceedings of the National Academy of Sciences **87**(14): 5363-5367.

van Gent, D. C., J. H. J. Hoeijmakers, et al. (2001). "Chromosomal stability and the DNA double-stranded break connection." Nat Rev Genet **2**(3): 196-206.

Ward, I. M. and J. Chen (2001). "Histone H2AX is phosphorylated in an ATR-dependent manner in response to replicational stress." J Biol Chem **276**(51): 47759-62.

Watt, P., E. Louis, et al. (1995). "Sgs1: a eukaryotic homolog of E. coli RecQ that interacts with topoisomerase II in vivo and is required for faithful chromosome segregation." Cell **81**(2): 253-260.

Welcker, M. and B. E. Clurman (2008). "FBW7 ubiquitin ligase: a tumour suppressor at the crossroads of cell division, growth and differentiation." Nat Rev Cancer **8**(2): 83-93.

Wood, R. D. (1997). "Nucleotide Excision Repair in Mammalian Cells." Journal of Biological Chemistry **272**(38): 23465-23468.

Wu, L., K. L. Chan, et al. (2005). "The HRDC domain of BLM is required for the dissolution of double Holliday junctions." Embo J **24**(14): 2679-87.

Wu, L. and I. D. Hickson (2003). "The Bloom's syndrome helicase suppresses crossing over during homologous recombination." Nature **426**(6968): 870-4.

Wu, L. and I. D. Hickson (2006). "DNA Helicases Required for Homologous Recombination and Repair of Damaged Replication Forks." Annual Review of Genetics **40**(1): 279-306.

Yamaguchi-Iwai, Y., E. Sonoda, et al. (1999). "Mre11 is essential for the maintenance of chromosomal DNA in vertebrate cells." Embo J **18**(23): 6619-29.

Yin, J., A. Sobeck, et al. (2005). "BLAP75, an essential component of Bloom's syndrome protein complexes that maintain genome integrity." The EMBO Journal.

Young, K. H. (1998). "Yeast two-hybrid: so many interactions, (in) so little time." Biology of Reproduction **58**(2): 302-311.

Zhou, B.-B. S. and S. J. Elledge (2000). "The DNA damage response: putting checkpoints in perspective." Nature **408**(6811): 433-439.

Zhu, J., S. Petersen, et al. (2001). "Targeted disruption of the Nijmegen breakage syndrome gene NBS1 leads to early embryonic lethality in mice." Curr Biol **11**(2): 105-9.

# CURRICULUM VITAE

Name: Lu ZHENG

Date of Birth: 20.07.1979

Nationality: CHINA

Email: zheng@imcr.uzh.ch

**Education:**

2003.11-Present PhD candidate, biochemistry, Institute of Molecular Cancer Research (IMCR), University of Zurich, Switzerland

2000.12-2003.7 M.S., biochemistry, Faculty of Medicine, National University of Singapore, Singapore

Thesis: Characterization and Localization of CD38 protein in murine testis

1996.9-2000.7 B.S., biochemistry, Faculty of Life Science, Nanjing University, P.R. CHINA

1993.9-1996.7 High school, Shangrao No. 1 high school, Shangrao, Jiangxi, P.R.CHINA